NAVAL POSTGRADUATE SCHOOL
Monterey, California

THESIS

ANALYSIS OF A MAGNETIC THREE-AXIS STABILIZED ATTITUDE CONTROL SYSTEM FOR THE NPSAT1 SPACECRAFT

by

Todd A. Zirkle

September 2001

Thesis Advisor: Michael Spencer
Second Reader: Barry Leonard

Approved for public release; distribution is unlimited.

Report Documentation Page

Report Date	Report Type	Dates Covered (from... to)
30 Sep 2001	N/A	-

Title and Subtitle Analysis of a Magnetic Three-Axis Stabilized Attitude Control System for the NPSAT1 Satellite	**Contract Number**
	Grant Number
	Program Element Number
Author(s) Zirkle, Todd A.	**Project Number**
	Task Number
	Work Unit Number
Performing Organization Name(s) and Address(es) Research Office Naval Postgraduate School Monterey Ca. 93943-5138	**Performing Organization Report Number**
Sponsoring/Monitoring Agency Name(s) and Address(es)	**Sponsor/Monitor's Acronym(s)**
	Sponsor/Monitor's Report Number(s)
Distribution/Availability Statement Approved for public release, distribution unlimited	
Supplementary Notes	
Abstract	
Subject Terms	
Report Classification unclassified	**Classification of this page** unclassified
Classification of Abstract unclassified	**Limitation of Abstract** UU
Number of Pages 110	

REPORT DOCUMENTATION PAGE			Form Approved OMB No. 0704-0188
Public reporting burden for this collection of information is estimated to average 1 hour per response, including the time for reviewing instruction, searching existing data sources, gathering and maintaining the data needed, and completing and reviewing the collection of information. Send comments regarding this burden estimate or any other aspect of this collection of information, including suggestions for reducing this burden, to Washington headquarters Services, Directorate for Information Operations and Reports, 1215 Jefferson Davis Highway, Suite 1204, Arlington, VA 22202-4302, and to the Office of Management and Budget, Paperwork Reduction Project (0704-0188) Washington DC 20503.			
1. AGENCY USE ONLY *(Leave blank)*	**2. REPORT DATE** September 2001	**3. REPORT TYPE AND DATES COVERED** Master's Thesis	
4. TITLE AND SUBTITLE: Analysis of a Magnetic Three-Axis Stabilized Attitude Control System for the NPSAT1 Satellite			**5. FUNDING NUMBERS**
6. AUTHOR(S) Zirkle, Todd A.			
7. PERFORMING ORGANIZATION NAME(S) AND ADDRESS(ES) Naval Postgraduate School Monterey, CA 93943-5000			**8. PERFORMING ORGANIZATION REPORT NUMBER**
9. SPONSORING / MONITORING AGENCY NAME(S) AND ADDRESS(ES) N/A			**10. SPONSORING / MONITORING AGENCY REPORT NUMBER**
11. SUPPLEMENTARY NOTES The views expressed in this thesis are those of the author and do not reflect the official policy or position of the Department of Defense or the U.S. Government.			
12a. DISTRIBUTION / AVAILABILITY STATEMENT Approved for public release; distribution is unlimited			**12b. DISTRIBUTION CODE**

13. ABSTRACT ***(maximum 200 words)***

The NPSAT1 satellite uses an active magnetic torque rod system, with a magnetometer for attitude determination, to maintain 3-axis stabilization, with a slightly gravity gradient friendly structure.

This thesis will examine the performance of three combinations of programs and simulation models for the NPSAT1 satellite attitude control system. The models include a magnetic control law with a reduced order estimator to generate torque commands to achieve spacecraft nadir pointing and a magnetic rate (Bdot) control law to reduce spacecraft angular rates. The performances of two Bdot mode switching designs are compared. Also, a case is made for the benefits of priming the system's reduced estimator prior to mode switching.

All of the control methods analyzed appear to be valid control methods to achieve three-axis attitude stabilization using only magnetic torquers for active control. The most efficient control method analyzed incorporates a hand-off method from a magnetic rate (Bdot) control loop to a magnetic control loop. The results of this analysis indicates that the best use of this method is to perform the Bdot hand-off following the achievement of a predetermined combined angular rate.

14. SUBJECT TERMS Attitude Control System, Magnetic, 3-Axis Stabilized, Bdot Control Law			**15. NUMBER OF PAGES** 110
			16. PRICE CODE
17. SECURITY CLASSIFICATION OF REPORT Unclassified	**18. SECURITY CLASSIFICATION OF THIS PAGE** Unclassified	**19. SECURITY CLASSIFICATION OF ABSTRACT** Unclassified	**20. LIMITATION OF ABSTRACT** UL

NSN 7540-01-280-5500 Standard Form 298 (Rev. 2-89)
Prescribed by ANSI Std. 239-18

THIS PAGE INTENTIONALLY LEFT BLANK

Approved for public release; distribution is unlimited.

ANALYSIS OF A THREE-AXIS STABILIZED ATTITUDE CONTROL SYSTEM FOR THE NPSAT1 SPACECRAFT

Todd A. Zirkle
Lieutenant, United States Navy
B.S., United States Naval Academy, 1994

Submitted in partial fulfillment of the
requirements for the degree of

MASTER OF SCIENCE IN SPACE SYSTEMS OPERATIONS

from the

NAVAL POSTGRADUATE SCHOOL
SEPTEMBER 2001

Author: _____
Todd A. Zirkle

Approved by: _____
Michael Spencer, Thesis Advisor

_____
Barry Leonard, Second Reader

_____
Rudy Panholzer, Dean
Graduate School of Engineering & Applied Sciences

THIS PAGE INTENTIONALLY LEFT BLANK

ABSTRACT

The NPSAT1 satellite uses an active magnetic torque rod system, with a magnetometer for attitude determination, to maintain 3-axis stabilization, with a slightly gravity gradient friendly structure.

This thesis will examine the performance of three combinations of programs and simulation models for the NPSAT1 satellite attitude control system. The models include a magnetic control law with a reduced order estimator to generate torque commands to achieve spacecraft nadir pointing and a magnetic rate (Bdot) control law to reduce spacecraft angular rates. The performances of two Bdot mode switching designs are compared. Also, a case is made for the benefits of priming the system's reduced estimator prior to mode switching.

All of the control methods analyzed appear to be valid control methods to achieve three-axis attitude stabilization using only magnetic torquers for active control. The most efficient control method analyzed incorporates a hand-off method from a magnetic rate (Bdot) control loop to a magnetic control loop. The results of this analysis indicates that the best use of this method is to perform the Bdot hand-off following the achievement of a predetermined combined angular rate.

THIS PAGE INTENTIONALLY LEFT BLANK

TABLE OF CONTENTS

THIS PAGE INTENTIONALLY LEFT BLANK

LIST OF FIGURES

LIST OF TABLES

THIS PAGE INTENTIONALLY LEFT BLANK

ACKNOWLEDGMENTS

The testing and validating of the NPSAT1 attitude control system has been the most challenging and rewarding time I've spent at the Naval Postgraduate School. My thesis advisor Dr. Michael Spencer cheerfully gave of his time and expertise. His interest and knowledge of spacecraft attitude control systems and his willingness to indulge my ideas and ineptitude were a great source of inspiration and guidance throughout this analysis.

Many thanks to Dan Sakoda, Jim Horning, Ron Phelps, and David Rigmaiden for providing the experience and technical knowledge sufficient to convince me there were too many possible thesis topics and too little time. Their contagious enthusiasm for the spacecraft they build provided a positive atmosphere and a never-ending source of motivation for my efforts.

A special thanks to Barry Leonard for providing his unmatched expertise in control systems and for giving me permission to play with and tear apart his programs and simulations. His fresh ideas and confidence have been a continuous source of inspiration.

I would like to thank Rudy Panholzer for graciously giving me free reign to choose any NPSAT1 subsystem to research that I wanted. His commitment to the space program at the Naval Postgraduate School has provided me the opportunity to receive an excellent education, while thoroughly enjoying myself.

THIS PAGE INTENTIONALLY LEFT BLANK

EXECUTIVE SUMMARY

The development of the attitude control system (ACS) for the NPSAT1 satellite was driven primarily by one object, namely, student learning through analysis and design of an actual spacecraft. Another concern driving the NPSAT1 satellite's development effort was the motivation to produce a small inexpensive research satellite composed of COTS (Commercial Off The Shelf) components and space flight experiments. This naturally led toward a system that was sensitive to the anticipated low power budget.

During the effort to keep the above-mentioned concerns in the forefront of the attitude control system's design process, the design team elected a control system that was to maintain three-axis stabilization using only magnetic torquers and magnetometers. Barry Leonard (Naval Postgraduate School Adjunct Professor) produced two potential system models. Both models use a magnetic control law and a reduced estimator to determine the spacecraft states and achieve three-axis stabilized nadir pointing using magnetic torque rods and a magnetometer. The second model also uses an added magnetic rate (Bdot) control law as suggested by the Naval Research Laboratory for initial de-tumbling of the spacecraft after deployment. [Ref. 1]

This thesis examines the performance of the two systems as stand-alone models and when used in conjunction with the Bdot control program. One application of the Bdot control loop hands off attitude control after a predetermined time interval and a second application after a predetermined combined angular rate has been achieved. After assigning initial conditions and establishing a test strategy, the models and programs were modified to include data capture, storage and plotting algorithms. Due to the need to find the lowest ACS power budget possible, in order to allow greater power availability for research payloads, this analysis is sensitive to the trade-offs between system power consumption and time to achieve three-axis attitude control after launch and deployment or after a loss of attitude control due to disturbance forces. The ACS needs to achieve and maintain stability within operational requirements (currently nadir pointing +/- 10 degrees), yet still maintain the robustness and capability to recover from a loss of attitude. The results from each of three combinations of control techniques is

summarized and plotted. Nine sets of initial conditions were tested with all three model and program combinations.

All of the control methods analyzed appear to be valid control methods to achieve three-axis attitude stabilization using only magnetic torquers and magnetometers. The most efficient control method analyzed appeared to be the model that incorporates a hand-off method from a Bdot control loop to an estimator control loop. The analysis results indicate that the best use of this method is to perform the Bdot hand-off following the achievement of a predetermined combined angular rate.

I. INTRODUCTION

The attitude of a satellite can be controlled by the interaction between the earth's magnetic field and a magnetic moment produced within the spacecraft. Many attitude control systems have been designed using magnetic torquers to supplement other active or passive attitude control methods.

The purpose of the NPSAT1 ACS is to prove a satellite's attitude can be maintained solely with magnetic torquers and a 3-axis magnetometer. Magnetic torquers rarely fail on orbit and multitudes of satellites have magnetic torque rods supplementing their control systems. The attitude control capability of the magnetic torquers, however, has limited effectiveness (+/- several degrees of pointing accuracy). One possibility for this capability is a low-power, non-complex safe mode for a more complex ACS. This research is helpful though to find the limits of technology necessary to make this a viable alternative method. The possibility of a low cost solution to attitude control that could salvage a mission after complex mechanical failures occur would be a substantial motivation for research to find such a method.

The NPSAT1 satellite will use an active magnetic torque rod system with a three-axis magnetometer for attitude determination to maintain 3-axis stabilization with a slightly gravity gradient friendly structure. This thesis will examine the performance of three combinations of programs and simulation models that may help start providing the evidence that such a system is feasible and viable for the NPSAT1 satellite. Graphs and tables will be included to augment the presentation of the analysis data in this thesis.

THIS PAGE INTENTIONALLY LEFT BLANK

II. BACKGROUND AND HISTORICAL PERSPECTIVE

NPSat1 is the second satellite in the Naval Postgraduate School's Small Satellite Design Program. The purpose of the Small Satellite Design Program is twofold. First, it provides hands-on education for officer students in the disciplines of satellite design, system integration, space systems operations, and software development. Second, it provides students with dedicated, on-orbit assets for experimentation and testing.

NPSat1 is an incremental improvement over the Postgraduate School's first small satellite, PANSAT. NPSat1 is a three-axis stabilized spacecraft equipped primarily with Commercial-Off-The-Shelf (COTS) hardware. Because of its three-axis stabilization, it is anticipated that the spacecraft could support a basic imaging capability with a COTS digital camera.

Several spacecraft components have already been acquired or built, and several experiments or payloads have already been envisioned for the mission. The solar cells and basic structure of the spacecraft were inherited from a cancelled Navy program at no cost to the Naval Postgraduate School. The primary spacecraft controller, a modified COTS 80386 PC-104 board, was already designed and built. The Digital Camera and its interface board had been purchased and tested with the PC-104 Central Processor. The Naval Research Laboratory has committed to flying their Coherent Electromagnetic Radio Tomography (CERTO) experiment onboard. Dr. Alan Ross, Navy TENCAP Chair in the Space Systems Academic Group, has indicated a desire to test his Triple Redundant Modular Computer experiment on board NPSAT1 as well.

The basic orbit profile for NPSAT1 was to be a circular Low Earth Orbit (LEO) between 400 and 800 kilometers, inclined at between 40 and 80 degrees with a mission life of 18 to 24 months.

The NPSat1 Attitude Determination and Control System (ADCS) was designed to provide three-axis stabilization. The spacecraft is gravity gradient friendly with the possibility of an optional telescoping boom for added stability. Active attitude control is achieved using three magnetic torque rods. Attitude determination software receives

inputs from a three-axis magnetometer to determine spacecraft attitude and rates. Figure 2.1 shows multiple views of the NPSAT1 spacecraft and the planned solar array layout. Three-axis stabilization provides a stable spacecraft to support the imagery and CERTO Missions on NPSat1. The cone is at the top of the spacecraft and the nadir pointing face is the bottom.

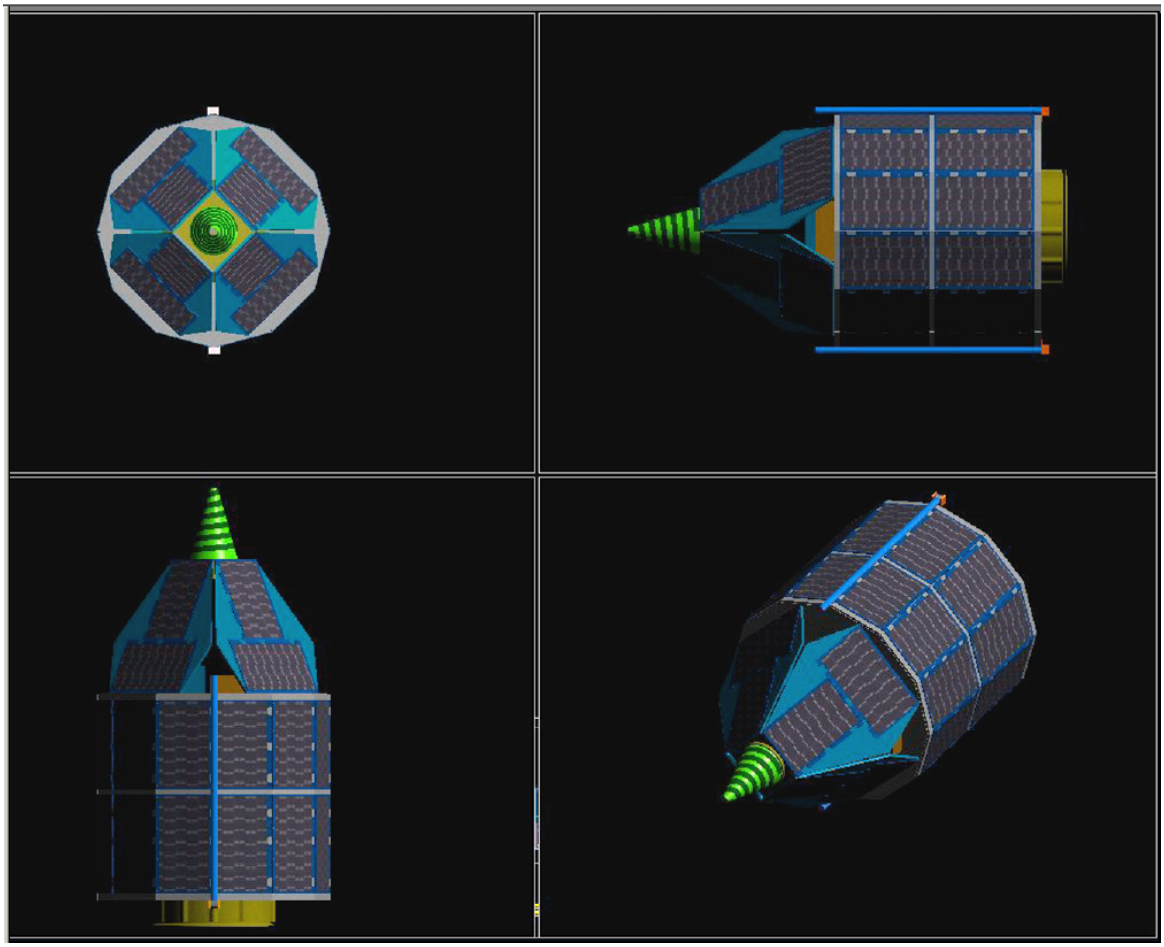

Figure 2.1. NPSAT1

The NPSAT1 spacecraft will be deployed from an Air Force Delta class expendable launch vehicle. The spacecraft will be deployed from an EELV secondary payload adapter (ESPA) ring. Figure 2.2 shows the NPSAT1 spacecraft as it will be configured on the ESPA ring.

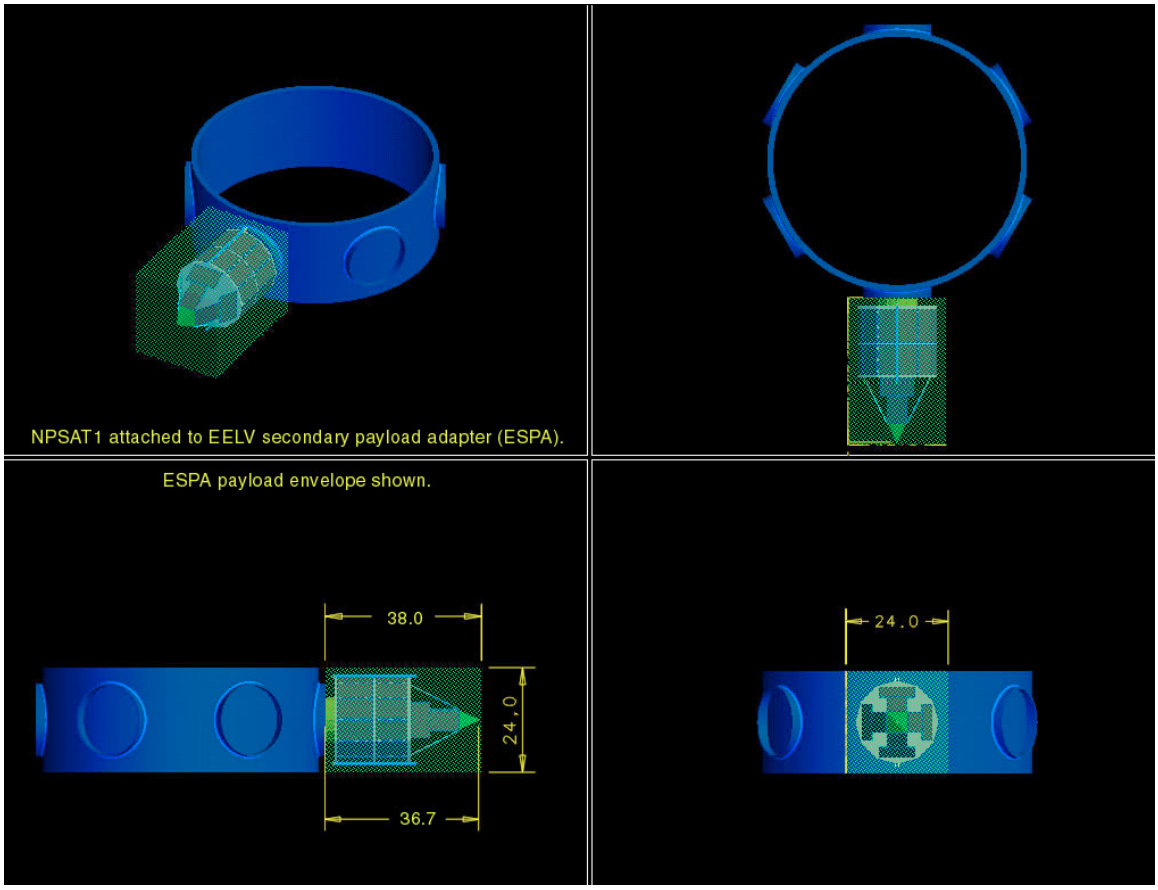

Figure 2.2. NPSAT1 attached to EELV payload adapter (ESPA)

THIS PAGE INTENTIONALLY LEFT BLANK

III. STATEMENT OF PURPOSE

A. OBJECTIVES OF RESEARCH

Initially, two objectives were sought, including sensitivity analysis of a magnetic control law program, and after a suggestion from the Naval Research Laboratory to try a magnetic rate (Bdot) control law [Ref. 1], a benefit analysis of including a magnetic rate control law for initial angular rate reduction of the NPSAT1 spacecraft. In the course of conducting the analysis, two secondary objectives were identified. Analysis was then to include the difference in system performance between switching from Bdot control to nadir-pointing control after a time interval or after acquisition of a specified reduced angular rate. The remaining secondary objective was to explore the benefits of mode switching before or after priming the systems reduced order estimator with historical data.

The analysis was conducted to determine the best configuration of the existing proposed attitude control systems for use on the NPSAT1 spacecraft. Two similar attitude control systems were examined in three different configurations. The first system consisted of two MATLAB programs and one SIMULINK model without a Bdot control loop. The second system consisted of one MATLAB program and one SIMULINK model with a timed hand-off from an integrated Bdot control loop. Additionally, the second system's reduced estimator received priming data prior to hand-off. The third configuration consisted of an independent Bdot control program which executed a control hand-off to the first SIMULINK model without priming the reduced estimator, after a predetermined, reduced, combined angular rate was achieved. Table 3.A.1 shows the programs included in each system configuration.

The research focused on three objectives. These included: initial condition sensitivity to all of the three program configurations, the difference between including the Bdot or no Bdot, and the difference between a timed Bdot hand-off or an angular rate based hand-off.

	SIMULINK model	MATLAB system programs
Configuration 1	LAB17.mdl	Lab15MOIData.m
"Lab17 model"		Lab16Data.m
Configuration 2	NPSAT1ACSINTRVW.mdl	NPSAT1ACSData.m
"Combo model"		
Configuration 3	Lab17.mdl	Lab15MOIData.m
"Lab17 hand-off model"		Lab16Data.m
		nps.m

Table 3.A.1. Configuration models and programs

B. APPROACH

Each of the two SIMULINK models was designed to generate control torque commands to three magnetic torque rods for active attitude control. Using initial spacecraft ephemeris data and a spherical harmonic model (8^{th} order), the systems estimate what the Earth's magnetic field should be at its current location. The system then computes the cross product of the expected magnetic field with the actual local magnetic field measured by a magnetometer. A cross product of the two magnetic vectors is used as an approximation of a magnetic control law to produce the first three system states (approximate euler angles). A reduced estimator is then used to approximate the other three system states (angular rates). These six states are fed to an actuator control law to generate torques.

The baseline model for the comparison was the SIMULINK model 'NPSATACSIntRvw.mdl' and its associated m-file, 'NPSAT1ACSDATA.m' which performed a timed Bdot control hand-off as previously described. [Ref. 2] This model is hereafter referred to as the "combo" model since the Bdot control loop is integrated within the SIMULINK model. The combo model, whose block diagram is shown in Figure 3.B.1, was used for the analysis baseline after analysis indicated that configuration exhibited the lowest power consumption of the three configurations. The three configurations of systems were evaluated for time response and power consumption.

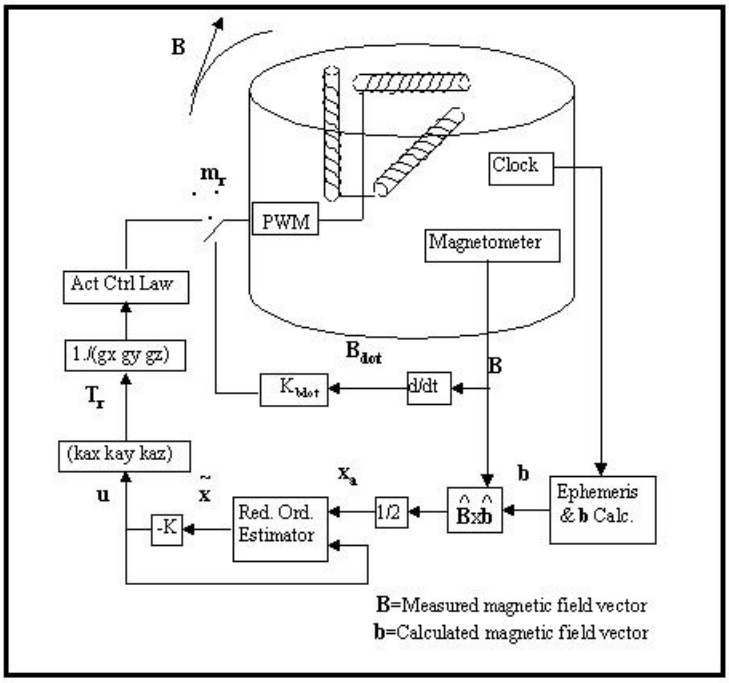

Figure 3.B.1. Block Diagram for "Combo" model

The programs and models for each of the three configurations are included in Appendix A.

THIS PAGE INTENTIONALLY LEFT BLANK

IV. PROGRAM SETUP AND PROCEDURE

A. INITIAL CONDITIONS AND ASSUMPTIONS

In order for the attitude control system for the NPSAT1 spacecraft to be viable, it must be able to handle the conditions immediately after deployment from the launch vehicle, and handle the maintenance of the spacecraft's operational pointing requirements. Initial conditions and assumptions were established. A representative number of test cases were run to establish the capability of the system to respond to those conditions. Each configuration was compared against the others to establish the best candidate for the final attitude control system. The primary measures of effectiveness were time to reach steady state and system power consumption.

The assumptions and initial conditions used during the simulations were chosen to approximate as closely as possible, the expected final characteristics of the satellite and its anticipated orbit. The minimum allowable altitude due to aerodynamic drag and aerodynamic disturbance torques for the spacecraft is 400km. The expected orbit is circular at 600km. As Figure 4.A.1 shows, the three 30 Am^2 torque rods can easily counter solar, gravity gradient, or aerodynamic torques encountered at 600km. The generated torques are greater than an order of magnitude more powerful than the anticipated disturbance forces.

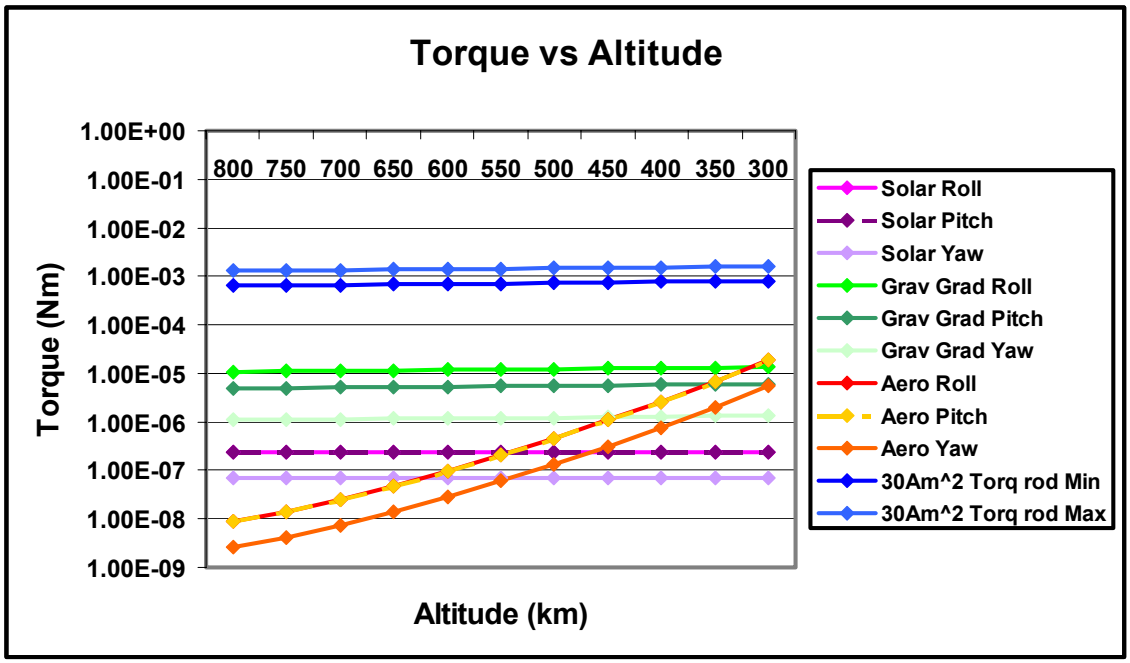

Figure 4.A.1. Torque vs. Altitude.

Initial satellite angular rates were based on the expected possible tip-off rates encountered by the launch vehicle at the moment of deployment. It was assumed that +/- 0.1 rad/sec was a conservative range of possible rates for spacecraft pitch and roll. Since the yaw rate induced by the launcher to the spacecraft is not expected to be as great as the pitch and roll rates, it was given a range of +/- 0.01 rad/sec. For simplification and standardization of initial conditions between tests, the initial pitch and roll rates were assigned either a "high rate" magnitude (+ 0.1 rad/sec or –0.1 rad/sec) or a "low rate" magnitude (+0.01 rad/sec or –0.01 rad/sec). The initial yaw rate was assigned a positive or negative "low rate" only. Considering all the possible combinations of the "high" and "low" angular rates resulted in 32 different, testable, initial angular rate combinations. For simplification of notation, the angular rates were assigned a three letter combination of either capital or lower case N's or P's, representing the magnitude of each rate as well as its sign (negative or positive). Example: nNp represents an initial pitch, roll and yaw rate of –0.01 rad/sec, -0.1 rad/sec and +0.01 rad/sec respectively.

Power consumption, as well as time response analysis of the various models to each of the selected test cases required the capture of data from 11 diferent program

variables. The variables included the output torques for each of the three torque rods, a sum of the absolute values of the three rods' output, the Euler angles ϕ, θ, and ψ, the angular rates $\dot{\phi}$, $\dot{\theta}$, and $\dot{\psi}$, and time.

B. EXPERIMENTAL PROCEDURE

1. Correlation Between Initial Conditions and Test Cases

The Bdot control law program 'nps.m' and the combo SIMULINK model were each evaluated for all 32 expected, representative, initial angular rate combinations. The programs' time responses represented the time each program required to reduce the angular rates to a combined rate of less than 1.5 degrees per second. The resulting time responses seemingly had no correlation with any particular aspect of the initial conditions. Table 4.B.1.1 shows the lack of apparent correlation between the time responses for the Bdot control law program 'nps.m' and the combo model and the initial conditions.

	Combo		Combo		Time req'd		Time req'd
Init Rates	Sim (sec)	Init Rates	Sim (sec)	Init Rates	Bdot (sec)	Init Rates	Bdot (sec)
pPp	20000	Pnp	100000	pPp	9200	Pnp	650
ppn	30000	npn	110000	ppn	20	npn	550
nnp	30000	npp	110000	nnp	3500	npp	640
NPp	30000	ppp	110000	NPp	6700	ppp	3700
NPn	30000	Npp	110000	NPn	6900	Npp	950
nPn	30000	PNn	110000	nPn	8900	PNn	14000
NNp	40000	nnn	120000	NNp	11000	nnn	32
Ppn	50000	PNp	120000	Ppn	3500	PNp	6700
Pnn	60000	pNp	120000	Pnn	1100	pNp	8700
Nnn	70000	PPp	120000	Nnn	3550	PPp	11000
Nnp	70000	pnp	140000	Nnp	3800	pnp	12
pPn	80000	nPp	150000	pPn	3500	nPp	8900
pNn	80000	nNp	170000	pNn	8700	nNp	9044
NNn	80000	nNn	170000	NNn	11000	nNn	9000
pnn	90000	PPn	180000	pnn	380	PPn	11200
Npn	90000	Ppp	270000	Npn	840	Ppp	3000

Table 4.B.1.1. Time to Achieve System Steady State.

Except where all of the initial rate magnitudes were "low" (0.01 rad/sec), in which case response times tended to also be relatively low, the data did not support linking higher initial angular rates with longer system settling times, as was expected.

Neither did the results suggest any correlation between sign order of the initial angular rates with a higher or lower system settling time. Instead, the resulting data seemed to suggest that the 'nps.m' program had certain initial positive or negative angular rate combinations that the program responded to poorly with respect to system settling times. Many combinations whose sign order matched, yet magnitudes varied, produced similar system steady state time responses, regardless of the difference in individual angular rate magnitudes.

The data did not favor a spread of test cases based on initial angular rate combinations as a means to guarantee a representative spread of system performance. Instead, using the data collected by running the combo model simulation (configuration 2), the 32 combinations of initial angular rates were sorted in order of their system steady state settling times. The combo model was chosen as the standard of performance to measure all other programs or combinations of programs against to determine the optimal system configuration for the full range of expected initial conditions. Two pieces of data of specific interest in the analysis was the total system torque rod output, used to calculate an energy index, and the time to reach the system steady state for each test case. Figure 4.B.1.1 shows an early plot of instantaneous and cumulative torque rod power. Note that the torque rods chosen for the NPSAT1 spacecraft are limited to +/- 30 Am^2

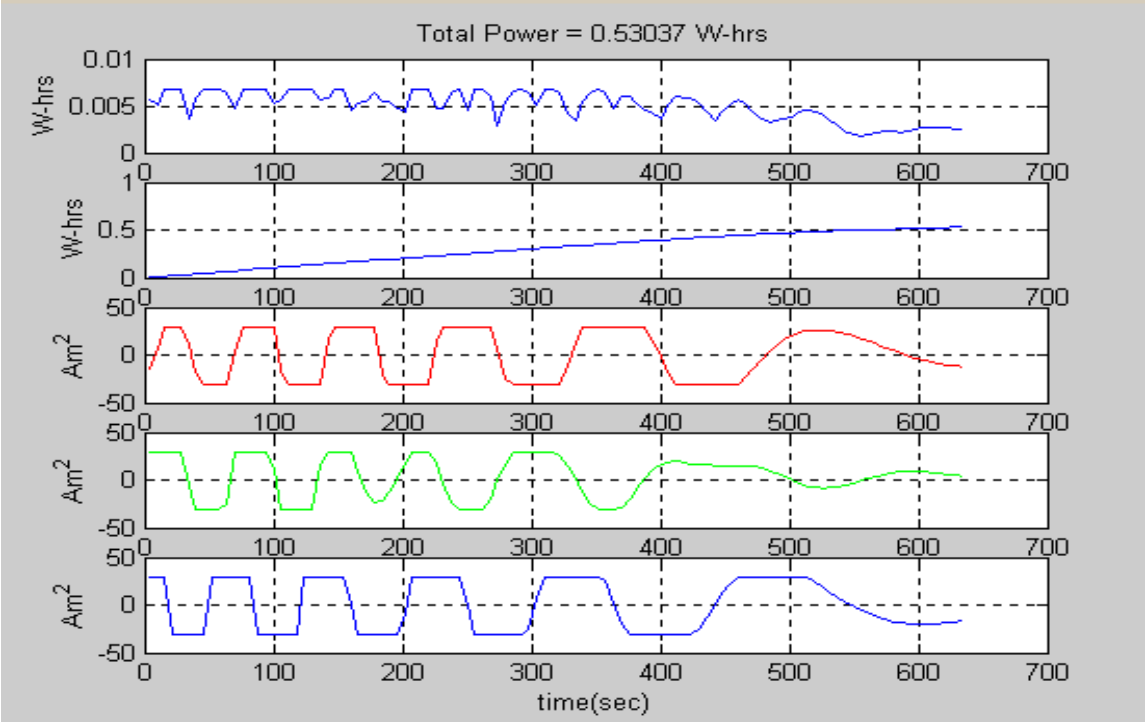

Figure 4.B.1.1. Three Torque Rod Output vs. Time.

Nine test cases were chosen to represent a spread of settling times demonstrated by the combo model, from the lowest demonstrated settling time to the highest. The nine sets of initial angular rates included “ppn,” “NPn,” “NNp,” “pPn,” “Pnp,” “nnn,” “pnp,” “nNp,” and “Ppp.”

2. Run Program, Capture Data

There were three configurations of programs and models that were run for each of the nine test cases. For each iteration, the data was recorded and analyzed to determine the power required by the system to reach the desired system steady state. The power required is represented in the form of an energy index. The torque rod output is measured in Am^2. If the output is integrated over the length of time to reach system steady state, the result is an “energy index” (Am^2 * sec) that was used for comparison against the other three programs and methods that were run with the same initial conditions.

In order to capture the data variables of interest from the simulations and program runs, the programs and simulation models were modified to include output blocks to

generate MATLAB '.mat' files which included the desired data, or the programs were modified to generate new variables which could be saved from the MATLAB work space. The programs 'nps.m' and the combo model were each run for all 32 combinations of initial angular rates.

The Bdot control law program 'nps.m' required modifications of the MATLAB source code to record the 11 variables from each program run. Additional data manipulation and plotting programs were created for further data analysis and to plot the analysis results. The program 'grabdataset.m' was written for execution following every different iteration of the 'nps.m' program to clear the MATLAB workspace after copying all desired variables into an 11 element matrix. Each of the variables was sampled at a pre-assigned change in time or dt (sec) until the simulation reached its chosen final combined rates goal. The value chosen for all of the simulations was dt = 2.0 seconds. The plotting programs 'plotresult2.m' and 'rodtotal_vs_time.m' were used to provide graphical representation of the data. The source code for the programs 'grabdataset.m,' 'plotresult2.m' and 'rodtotal_vs_time.m' are provided in Appendix A.

Both SIMULINK models were modified to capture the same 11 variables that were recorded from the 'nps.m' program runs. Each SIMULINK model was run with the same initial conditions used in the iterations that were run with the Bdot control law program. The output blocks added to the simulation models are shown in Figure 4.B.2.1.

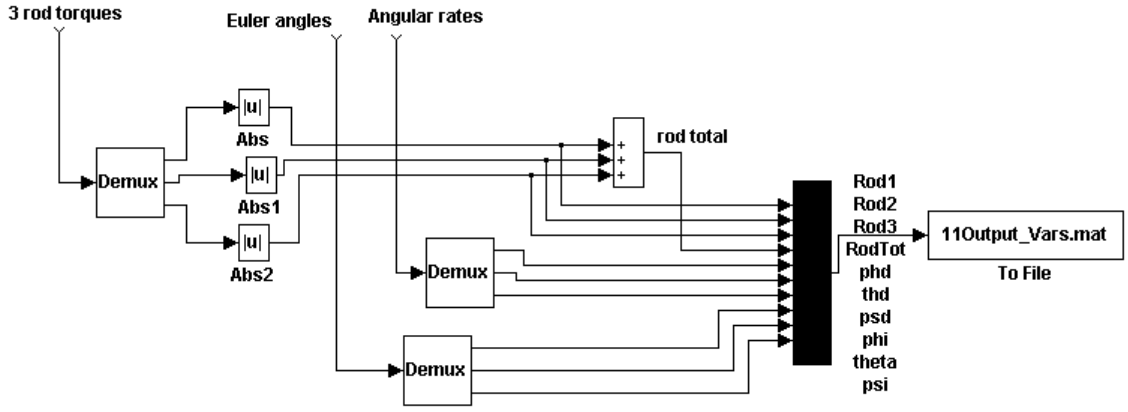

Figure 4.B.2.1. Simulink Output Data Capture Blocks.

The output '.mat' files were imported into the MATLAB work space for data analysis and plotting using the programs 'grabdataset.m,' 'create_variables.m,' 'rodtotal_vs_time.m' and 'plotresult2.m,' which are provided in Appendix A.

The program 'grabdataset.m' was written for manipulating data captured from a SIMULINK simulation run. The program measured and plotted the instantaneous and cumulative total of commanded rod torques and the time required to achieve a 3-axis steady state pointing accuracy of less than 10 degrees. This program also solved and plotted the area under the instantaneous rod torque total curve, producing an energy index for comparison with other runs using different initial conditions.

Eleven variables were recorded in a matrix as a '.mat file' from a simulation using one of two modified SIMULINK simulations. The program picked off the following desired variables: the torque rod outputs in Am^2 as 'rod1', 'rod2', and 'rod3.' The total commanded torque from the three rods combined was 'rodtot.' The angular rates were recorded as 'Phd,' 'Thd' and 'Psd,' and the Euler angles were recorded as 'Ph,' 'Th' and 'Ps.'

The Bdot MATLAB program output data and SIMULINK system models' output data needed to be merged into a common format for data analysis. The program 'create variables.m' was written for capturing data from the NRL program 'nps.m.' The program captured 11 variables for analysis and plotting purposes. Many of the data parameters were manually entered into the program code from the MATLAB workspace. Future analysis will benefit from the development of an automated data capture program that combines all of the steps used to manipulate the data for this analysis. The resulting data was saved from the MATLAB workspace to a data folder. The '.mat' file's name reflected the initial conditions used to produce the data.

EXAMPLE FILE NAME: 'bdot_pNp_case1.mat.' In this example, pNp stands for 'Phd' =.01 rad/s, 'Thd' =-.1 rad/s, 'Psd' =.01 rad/s.

The program 'Rodtotal_vs_Time.m' was written to plot simulated torque rod data for analysis of simulations supporting NPSSAT1. This program captured a row of data from a saved 11 row matrix. The matrix was produced from one of two modified

SIMULINK simulations. The program grabbed torque rod totals and plotted them vs. time.

3. Run Program Handoff Method, Capture Data

The program 'NPSSAT1TESTCASE.m' was written for manipulating data captured from MATLAB programs and SIMULINK runs that were run in the hand-off mode. Since each program ran independently, their data had to be combined for analysis.

This program computed and plotted the results of the two different simulations' data. The Bdot control law program 'nps.m' was used to arrest angular rotation rates to the predetermined rate goal (less than or equal to 1.5 degrees/sec). Then, the final states of that simulation were used for the initial conditions of the second program, which further arrested the rotation rates and achieved a predetermined three-axis nadir pointing accuracy. Data from the program 'nps.m,' was used to provide the initial conditions for each of two modified SIMULINK simulations. The data stored as a result of running one of the two follow-on simulations were loaded into the MATLAB work space, with the stored data from the Bdot program run. The 'NPSSAT1TESTCASE.m' program essentially combined two other programs, 'grabdataset.m' and 'create_variables.m.'

After loading the desired '.mat' files containing data matrices into the MATLAB workspace, the matrix sizes were used to edit the program's array sizes. The data are saved as a single '.mat' file.

The 'NPSSAT1TESTCASE.m' program captured torque rod total and time variables for analysis and plotting purposes. The program then measured and plotted the instantaneous and cumulative total of commanded rod torques and the time required to achieve a 3-axis steady state pointing accuracy of less than 10 degrees. This program computed and plotted the area under the instantaneous rod total curve to produce an energy index for comparison with other runs using different initial conditions.

4. Run Plotting Programs

Once the four programs or combinations of programs were run for each of the nine test cases, the ability to use and manipulate the data with calculations was relatively straight forward. In order to manipulate the data from both the independent Bdot program and its second handoff program, the data had to be merged together at the point

of handoff, which occurred at the instant the Bdot program reached its assigned combined angular rate threshold. The resultant data was then used as if it were merely the results of one of the individual programs.

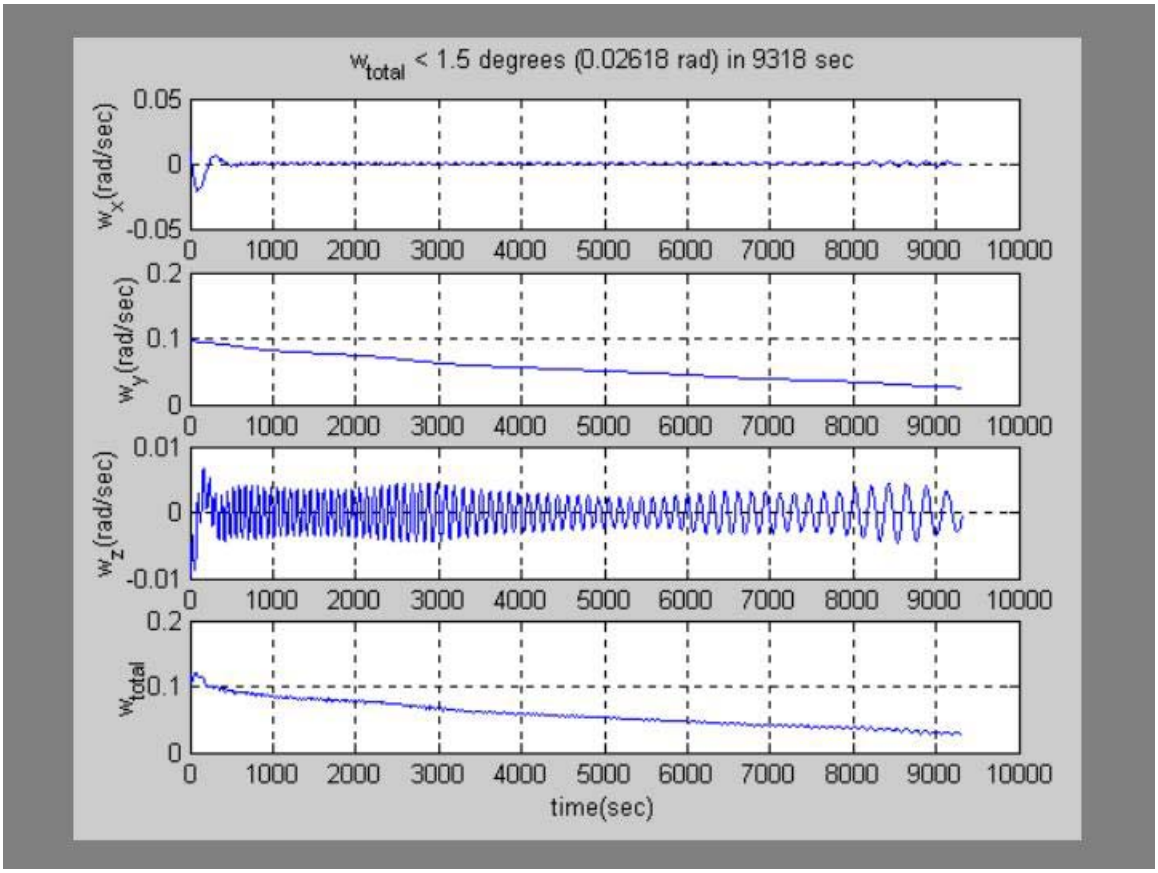

Figure 4.B.4.1. Angular Rates vs. Time (pPn).

An example of the plotting program 'plotresult2.m' is shown in Figure 4.B.4.1. The initial angular rates were ϕdot = +0.01 rad/sec, θdot = +0.1 rad/sec, and ψdot = -0.01 rad/sec (pPn). The program 'nps.m' was assigned a combined angular rate goal of 1.5 deg/sec. The program arrested the angular rates until the sum of the absolute values of the three angular rates dropped below the assigned threshold.

Figure 4.B.4.2 shows the results of configuration 3 (on the left side of the figure), the Bdot control handoff method to the 'Lab17.mdl' for the test cases "pPn" (ϕdot = +0.01 rad/sec, θdot = +0.1 rad/sec, and ψdot = -0.01 rad/sec) and "NNp." (ϕdot = -0.1

rad/sec, θdot = -0.1 rad/sec, and ψdot = +0.01 rad/sec). In this method, the SIMULINK model 'Lab17' has not been activated until the Bdot program 'nps.m' has finished arresting the angular rates.

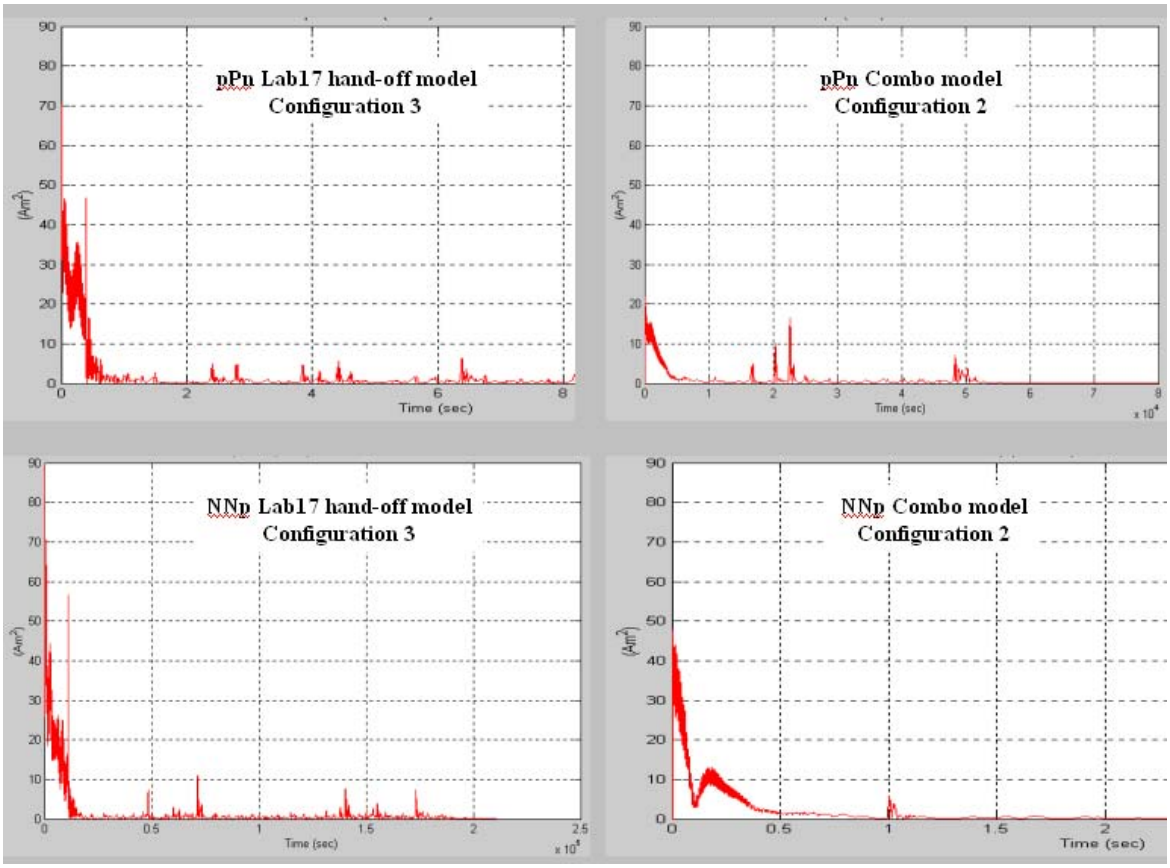

Figure 4.B.4.2. Bdot 'nps.m' handoff to 'Lab17.mdl'.

The point at which the handoff occurred is quite distinguishable in these cases, occurring at 5,000 seconds and 1,500 seconds respectively. The graphical representation of the data in this case was instrumental in recognizing a difference in the smoothness of transitions between different handoff models. Using the same initial conditions for configuration 2, the internal system Bdot control handoff to the estimator in the combo SIMULINK model shows a much smoother transition at the handoff point. As Figure 4.B.4.2 indicates, the sudden spike in required energy from the torque rods does not occur. This observation proved to be true for many of the handoff cases.

While attempting to explain why there was a difference between the configurations, several insights were gained into the operations of the models. The combo model, essentially, is a Bdot loop operating for a period of time within the model, then handing off the control to the reduced order estimator. The Kalman filter within the seemingly idle reduced order estimator loop of the model was in fact gathering magnetic field crossed with magnetometer information, while the Bdot loop was arresting the initial angular rates. Therefore, when the control was handed off by the Bdot loop to the reduced order estimator, the filter already had better knowledge than if the system started gathering magnetic field data at the handoff point. The right side of Figure 4.B.4.2 shows the handoff which includes the "better knowledge."

THIS PAGE INTENTIONALLY LEFT BLANK

V. RESULTS

A. OVERVIEW

The progression of analysis objectives began with sensitivity analysis of the existing ACS model, which had no Bdot control law. While that analysis was being conducted, Naval Research Laboratory personnel recommended using a magnetic rate (Bdot) control law to reduce the satellite angular rates to a lower "manageable" level prior to using the reduced estimator models. [Ref. 1] The objective of showing the difference in performance between systems with or without the Bdot control law was started. It was expected that the systems would acquire steady state nadir pointing faster if the initial angular rates were reduced faster. The Bdot program 'nps.m' was analyzed for 32 different sets of initial conditions and reduced the rates much faster than the reduced estimator control system without Bdot. The performance measurements were based on the time required for the system to achieve nadir poining accuracies of +/- 10 degrees.

After several evolutionary steps of the ACS system, the combo model was produced, which incorporated the Bdot control law within the system model. The power consumption results out-performed all previous system versions. The decision to use the combo model as a benchmark for performance was made. The combo model, configuration 2 was analyzed for all 32 initial test case combinations for time response. Curiously, the time responses for the combo model compared to the other configurations did not have the best performance. It was discovered that a difference in time response was achieved if the Bdot hand-off was conducted after a predetermined, reduced angular rate was achieved instead of after a predetermined time interval. The decision to conduct analysis in support of three objectives was then made. The three objectives included: initial condition sensitivity to all of three program configurations, the difference between Bdot and no Bdot, and the difference between timed Bdot hand-off and angular rate based Bdot hand-off.

B. BDOT RESULTS

The results of the Bdot program runs offered no insight into the correlation between initial conditions and system time response. Sorting the data by time required to reach the combined angular rate goal of <=1.5 degrees/sec, had no correlation with a similar sorting of any of the other systems' results. There is no doubt that the Bdot control law program, 'nps.m,' by itself, arrested the angular rates faster than any other program or model. (See Figure 5.B.1)

Init Rates	Time req'd Bdot (sec)	Init Rates	Time req'd Bdot (sec)
pPp	9200	Pnp	650
ppn	20	npn	550
nnp	3500	npp	640
NPp	6700	ppp	3700
NPn	6900	Npp	950
nPn	8900	PNn	14000
NNp	11000	nnn	32
Ppn	3500	PNp	6700
Pnn	1100	pNp	8700
Nnn	3550	PPp	11000
Nnp	3800	pnp	12
pPn	3500	nPp	8900
pNn	8700	nNp	9044
NNn	11000	nNn	9000
pnn	380	PPn	11200
Npn	840	Ppp	3000

Figure 5.B.1. Bdot Time to Reduce Rates to <= 1.5 deg/sec Combined.

Unfortunately the program does not offer any three-axis pointing capability. There was, however, substantial time-savings, often by a factor of ten or more over the ability of the other programs to achieve partial acquisition by angular rate reduction. This performance led to the decision to analyze the affect of using the Bdot program independently until a specified combined angular rate goal was achieved. The final conditions, including angular rates and Euler position angles were handed off to the original 'Lab17.mdl' as initial conditions. (configuration 3).

The Bdot control law more efficiently arrested the angular rates, compared to configuration 1, the system without the magnetic control law ('Lab17.mdl'). The Bdot

program also appeared to help the other systems most efficiently when the Bdot program was run to a specific rate goal, instead of for a specified time. Once the control was handed off to the other programs or models, the energy levels and commanded torques required to resume the control effort were minimal.

C. CONFIGURATION 1 RESULTS

After conducting the nine test cases, configuration 1 seemingly had the poorest performance of the three configurations. Compared to the other two configurations, to achieve pointing accuracies of +/- 10 degrees, configuration 1 appeared to only perform well in the middle ground between the extremes of initial conditions (using the combo model as a bench mark). The best cases and worst cases for configuration 2 (the extremes), however, nearly always corresponded to poor performance from this configuration.

The energy indexes for this configuration tended to exceed the worst performance of the other two methods. The gains selected for this model, however, have been designed to be adequate for the entire range of initial conditions. It is quite likely that if a Bdot control law was added to this model, and the Bdot program maintained its control until a minimal residual combined angular rate existed, then the gains for the 'Lab17.mdl' could be optimized to accommodate the low initial rate conditions. Table 5.C.1 shows the nine case studies conducted. The order of the initial conditions is in increasing system time order for the reference combo model. Figures 5.C.1 through 5.C.18 show the instantaneous and cumulative power consumption results for configuration 1.

	Lab17	Energy Index [(Am^2)*(sec)x1e4]
Init Rates	Simulink (sec)	Lab17
ppn	200000	119278
NPn	67000	169540
NNp	92000	5585031
pPn	60000	66757
Pnp	90000	2474116
nnn	30000	1
pnp	170000	98606
nNp	200000	2677909
Ppp	40000	153848

Table 5.C.1. Configuration 1 (‘Lab17.mdl’) test results.

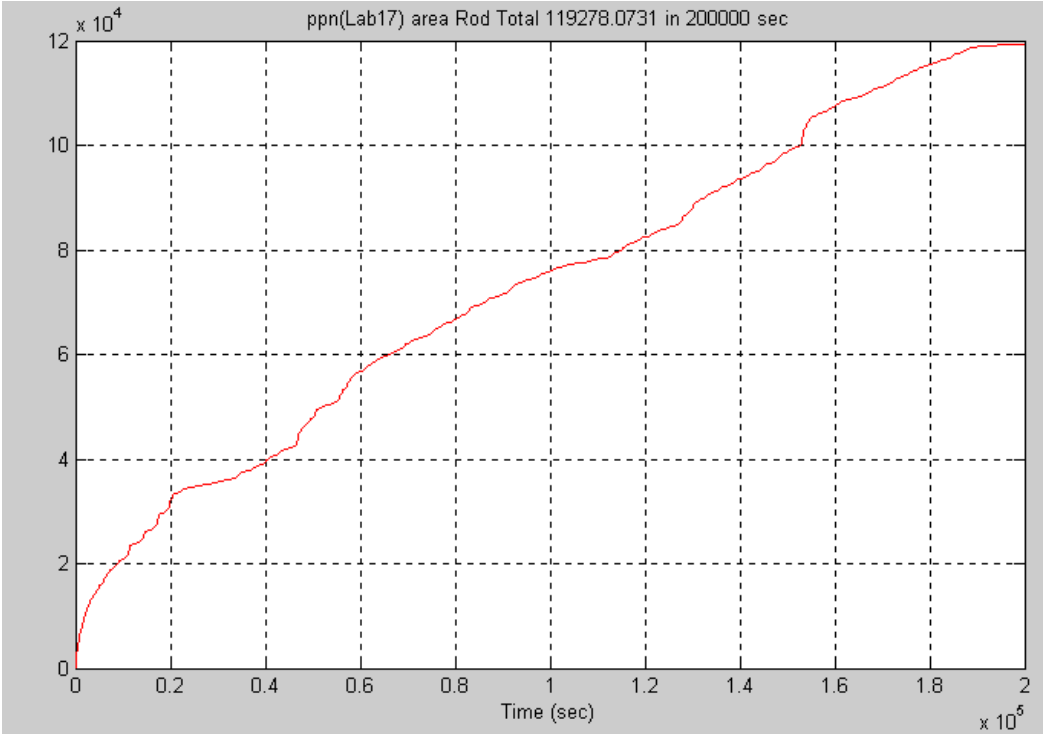

Figure 5.C.1. "ppn" Configuration 1: Cumulative Rod Total vs. Time

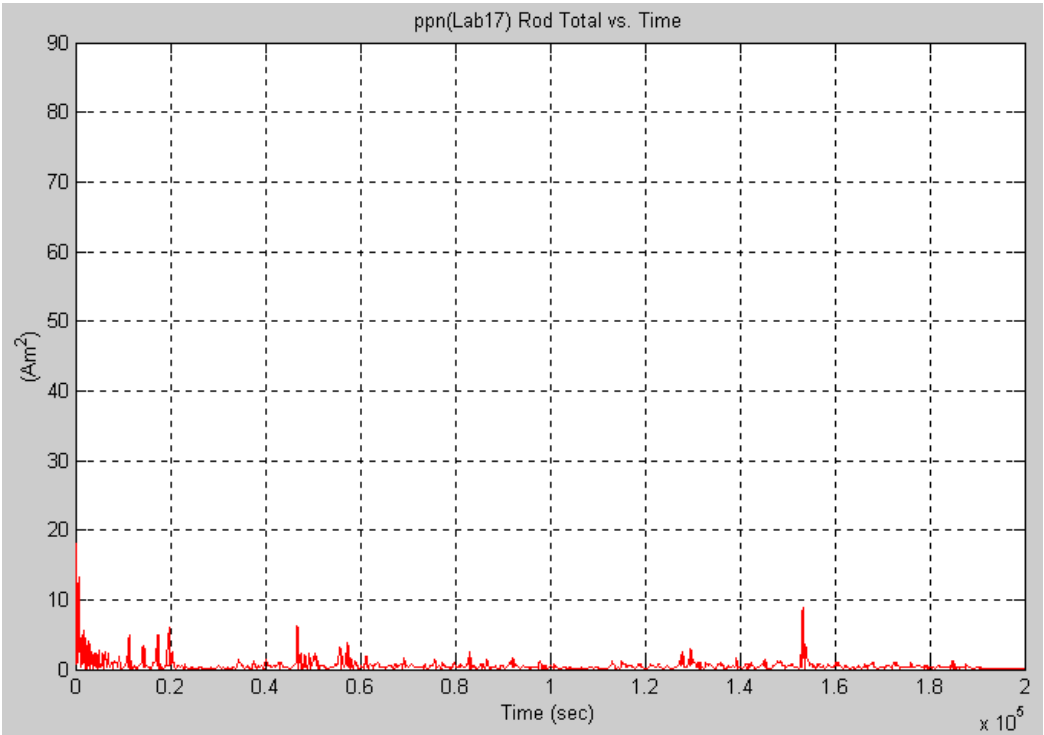

Figure 5.C.2. "ppn" Configuration 1: Instantaneous Rod Total vs. Time

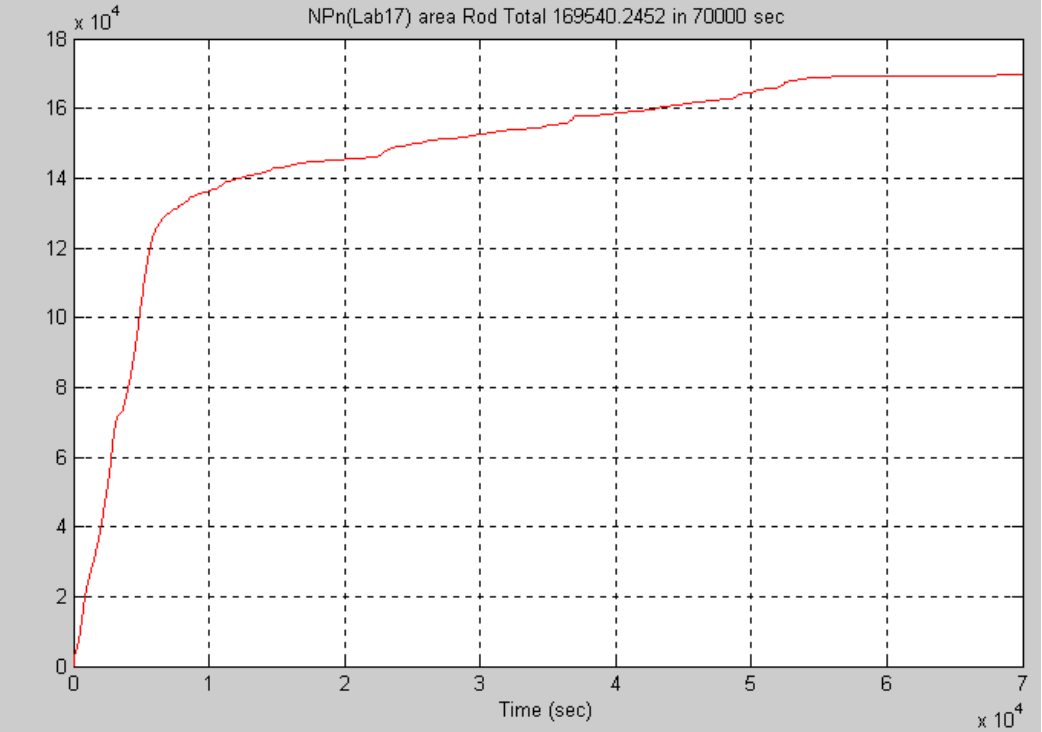

Figure 5.C.3. "NPn" Configuration 1: Cumulative Rod Total vs. Time

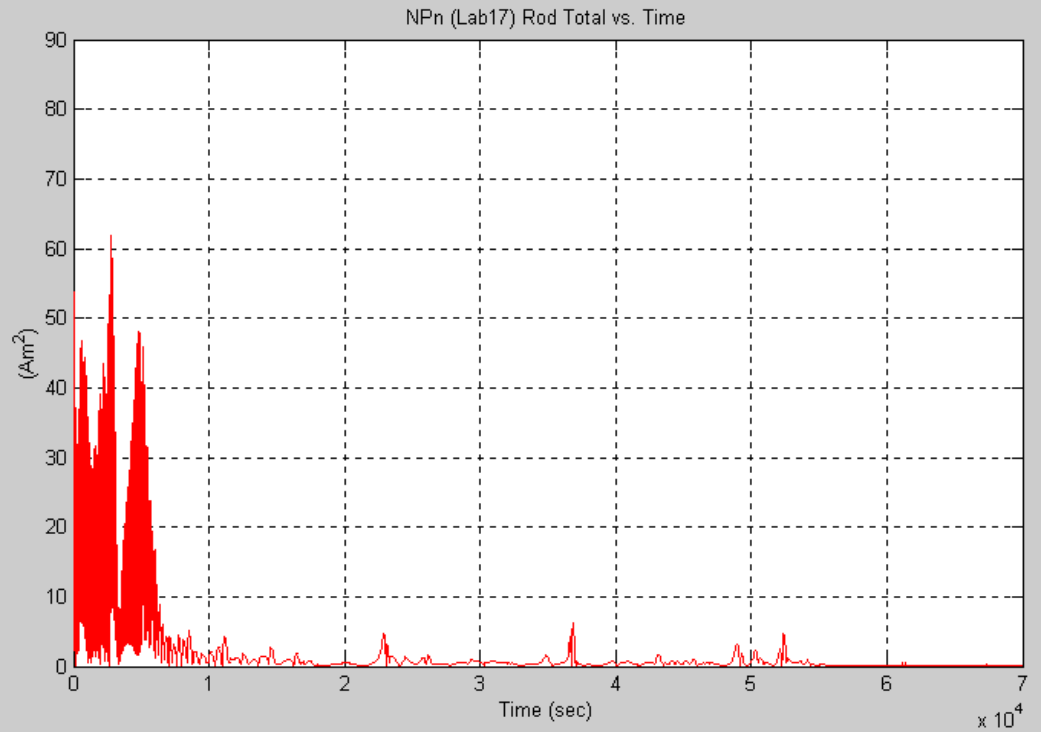

Figure 5.C.4. "NPn" Configuration 1: Instantaneous Rod Total vs. Time

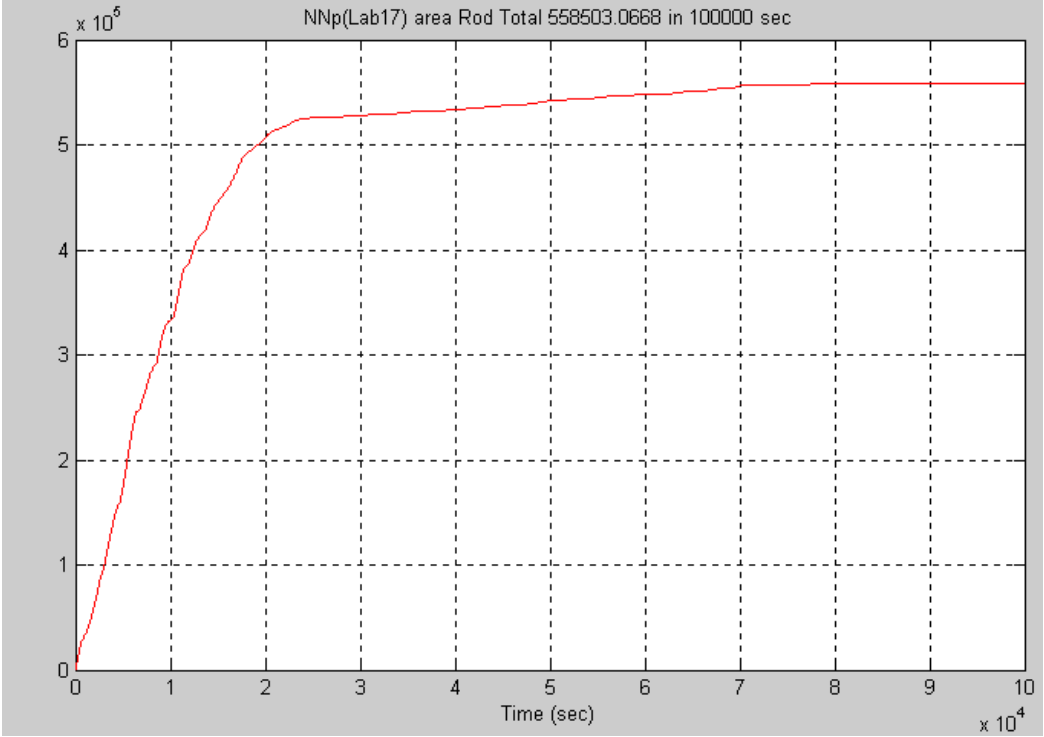

Figure 5.C.5. "NNp" Configuration 1: Cumulative Rod Total vs. Time

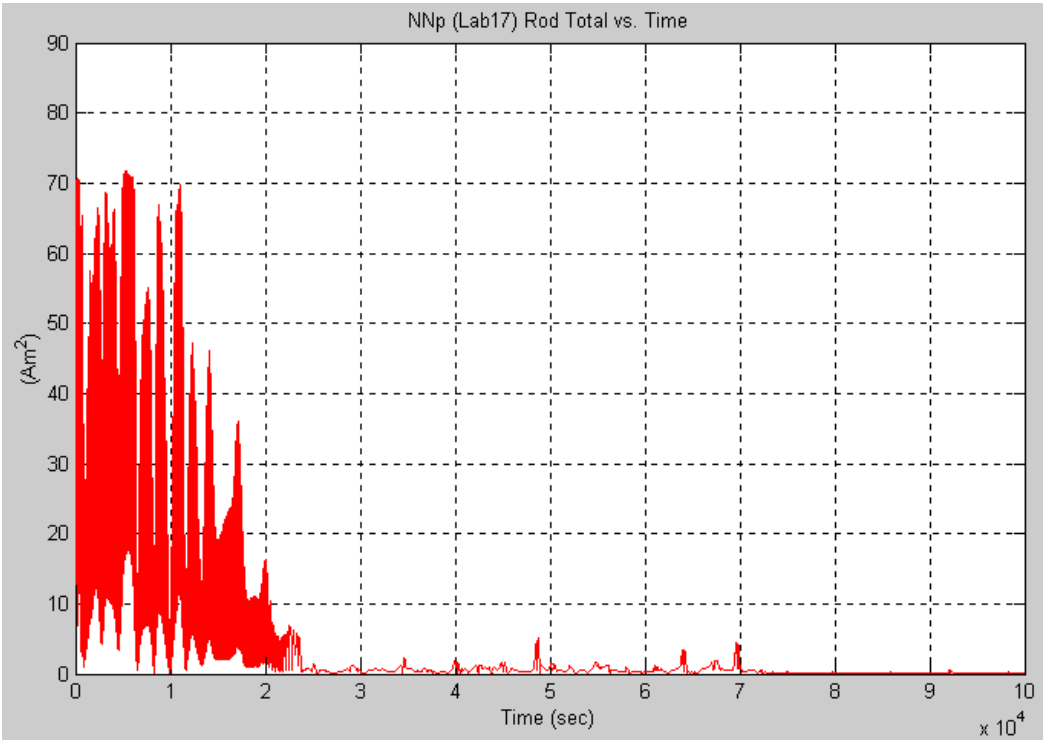

Figure 5.C.6. "NNp" Configuration 1: Instantaneous Rod Total vs. Time

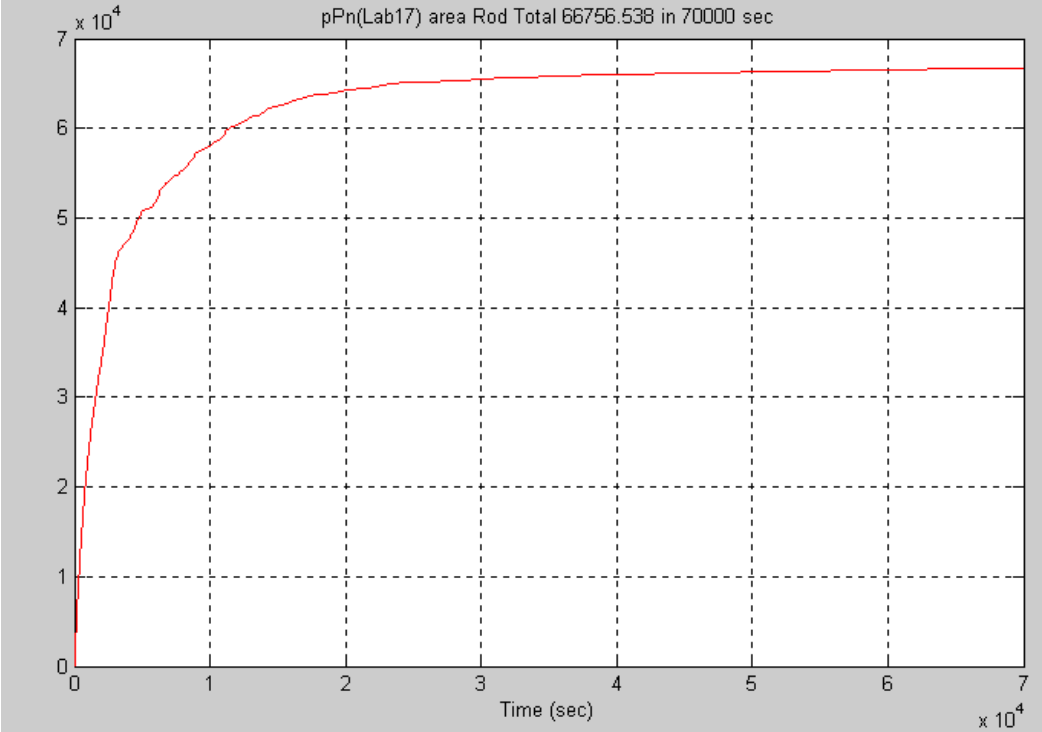

Figure 5.C.7. "pPn" Configuration 1: Cumulative Rod Total vs. Time

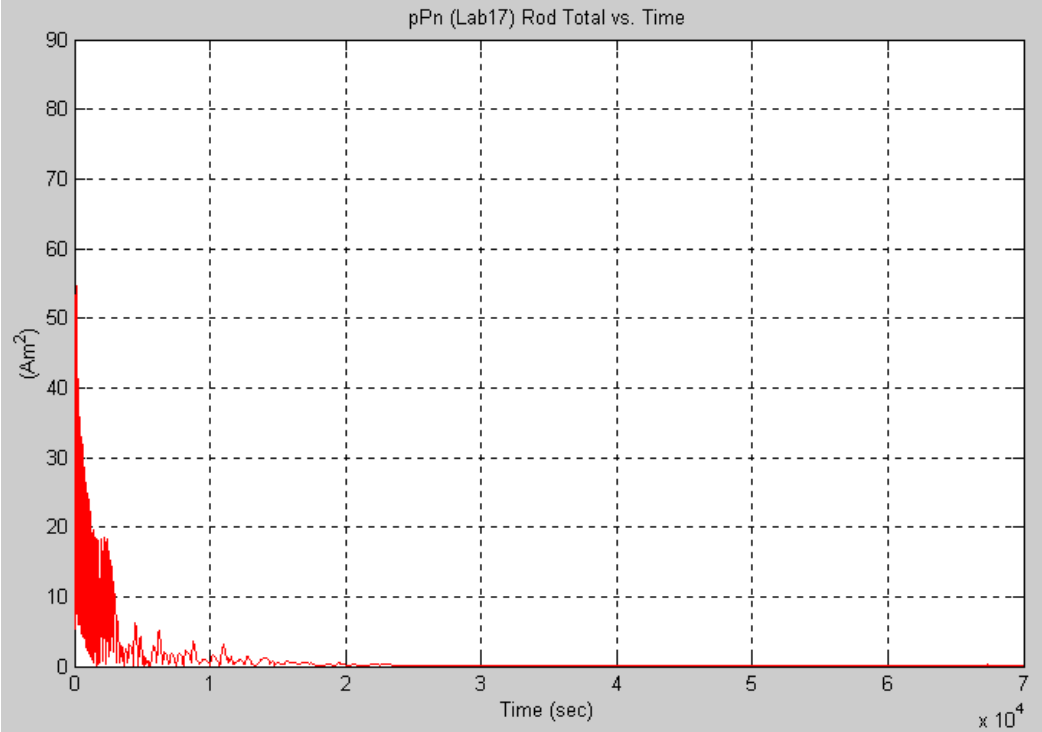

Figure 5.C.8. "pPn" Configuration 1: Instantaneous Rod Total vs. Time

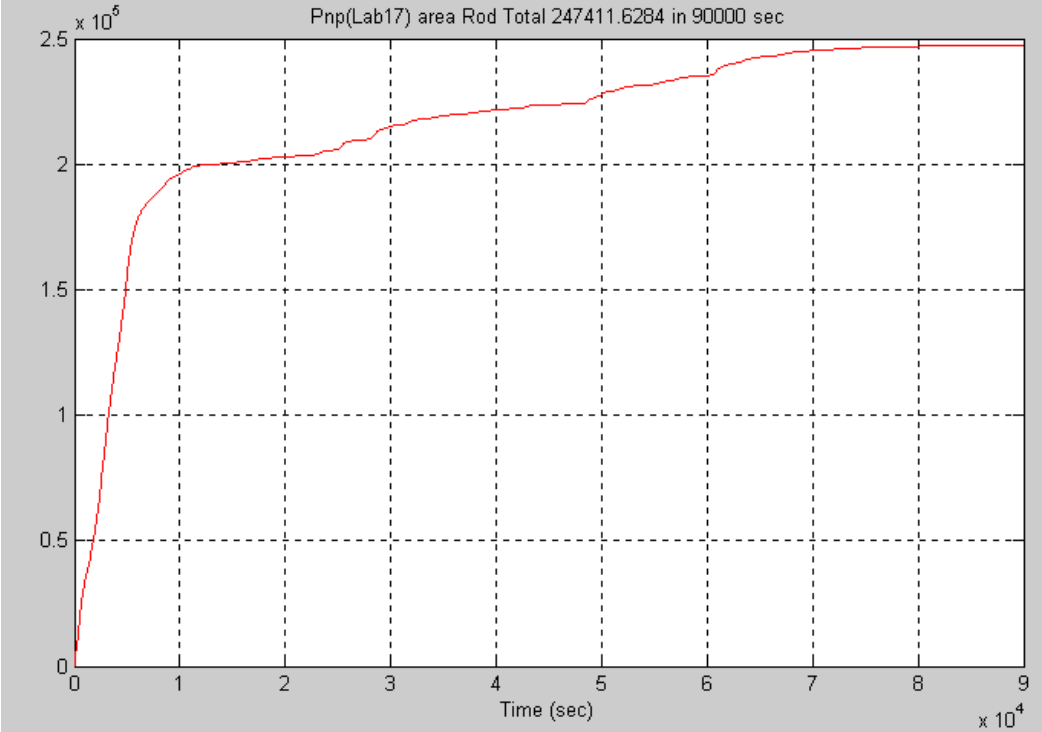

Figure 5.C.9. "Pnp" Configuration 1: Cumulative Rod Total vs. Time

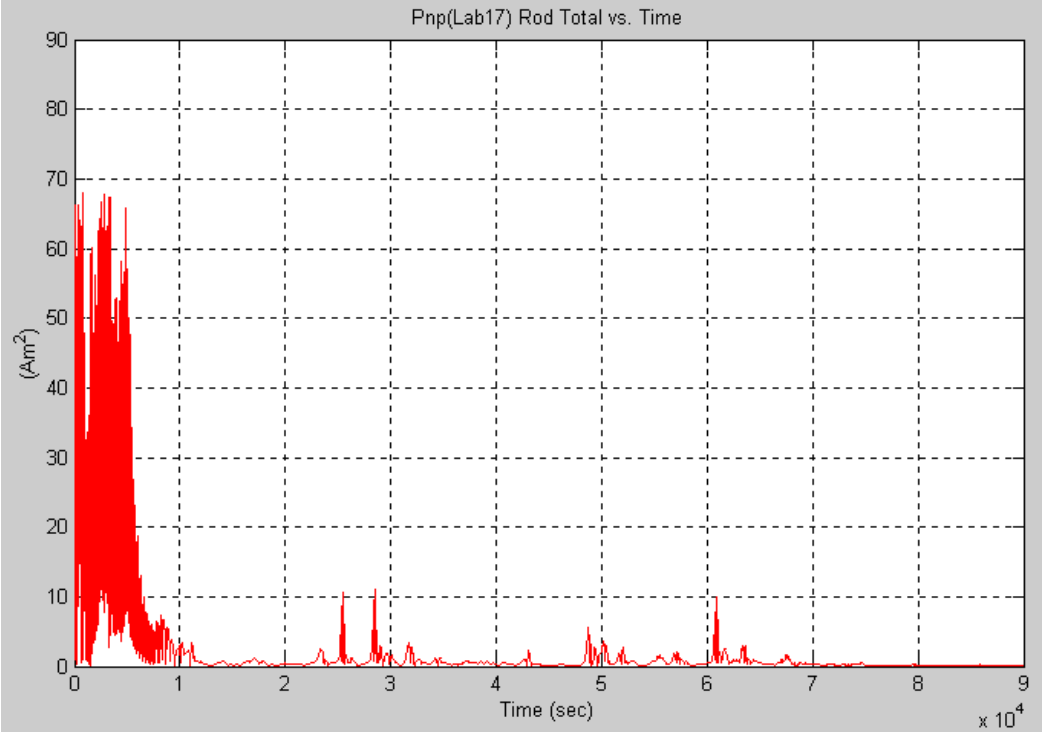

Figure 5.C.10. "Pnp" Configuration 1: Instantaneous Rod Total vs. Time

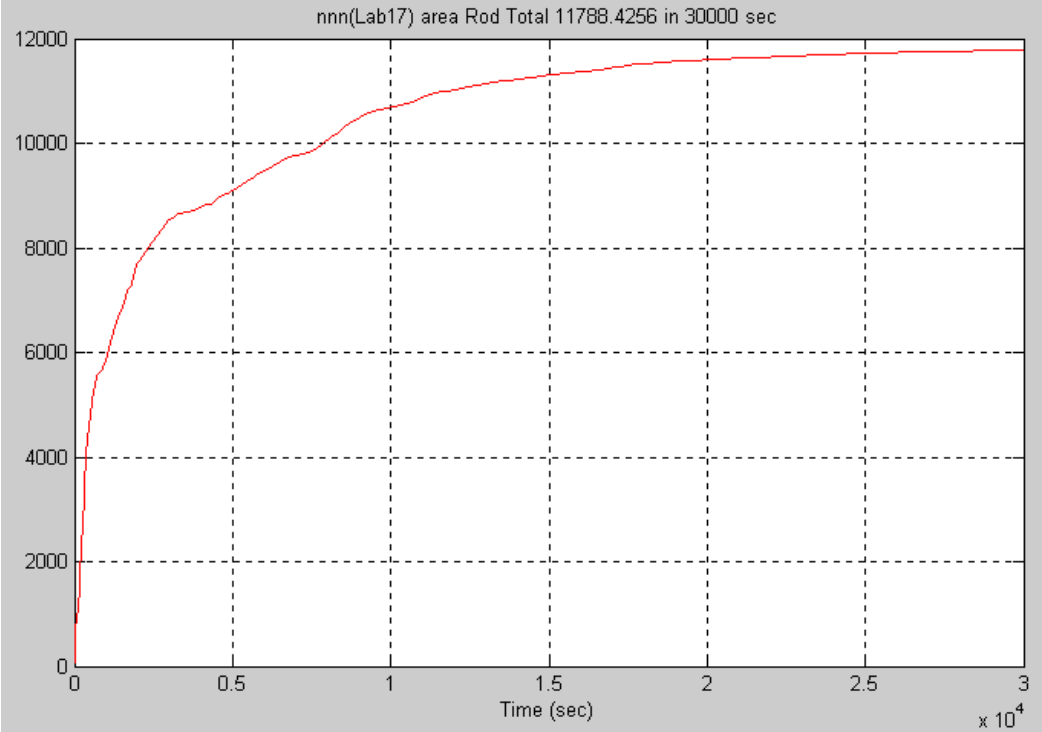

Figure 5.C.11. "nnn" Configuration 1: Cumulative Rod Total vs. Time

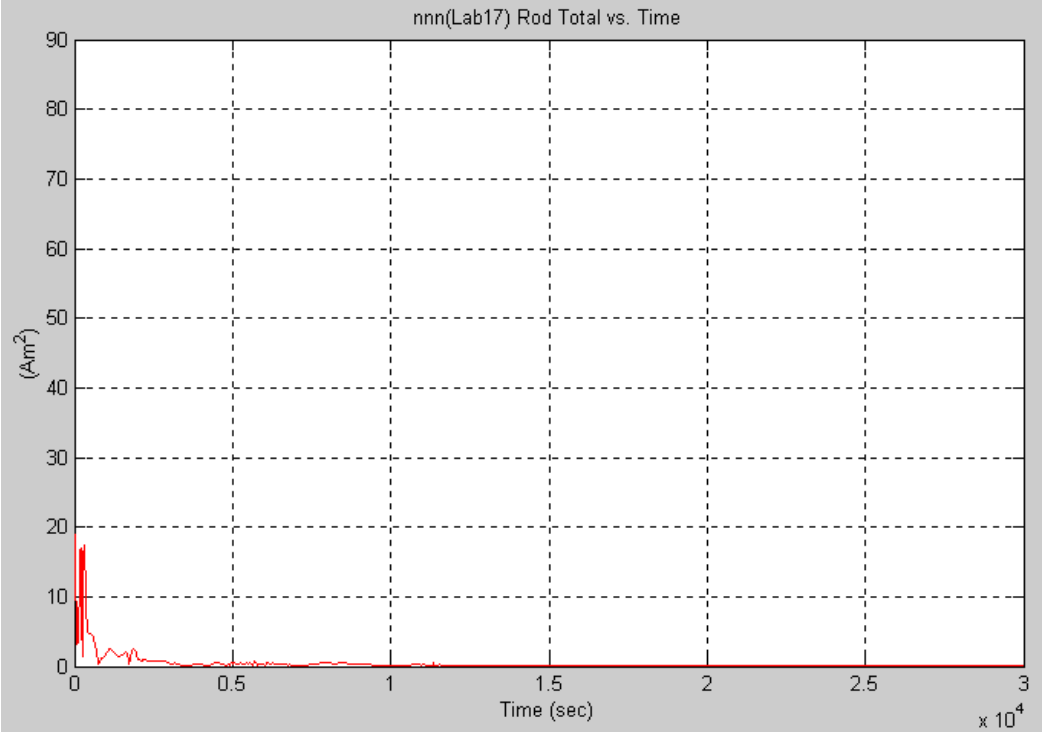

Figure 5.C.12. "nnn" Configuration 1: Instantaneous Rod Total vs. Time

Figure 5.C.13. "pnp" Configuration 1: Cumulative Rod Total vs. Time

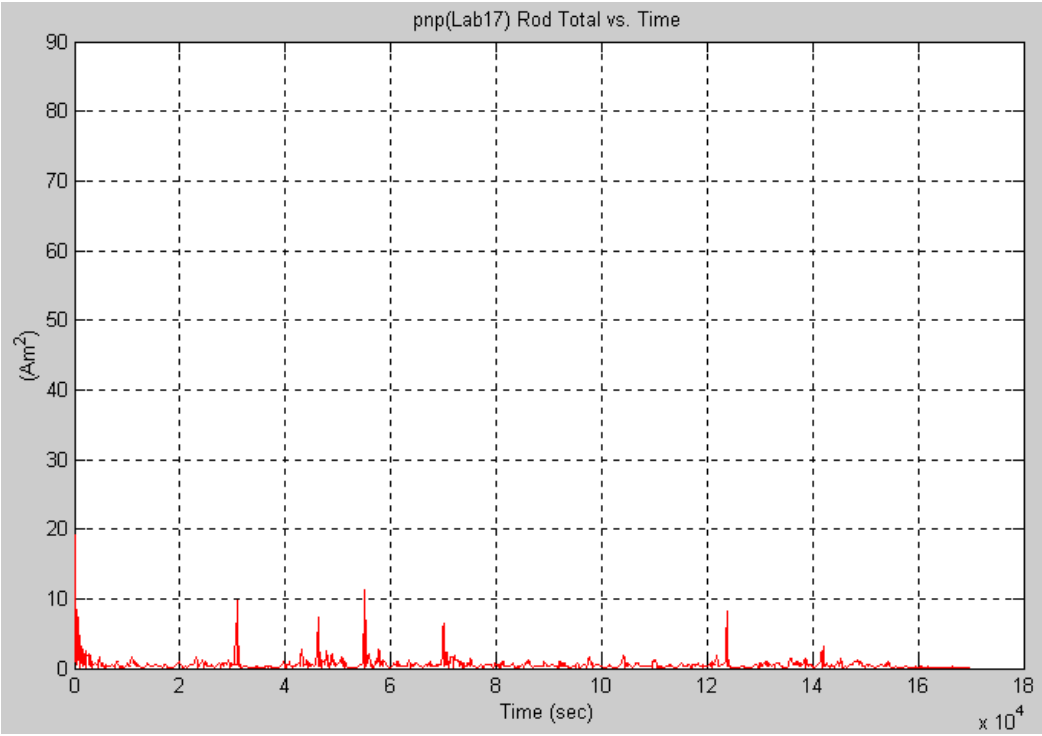

Figure 5.C.14. "pnp" Configuration 1: Instantaneous Rod Total vs. Time

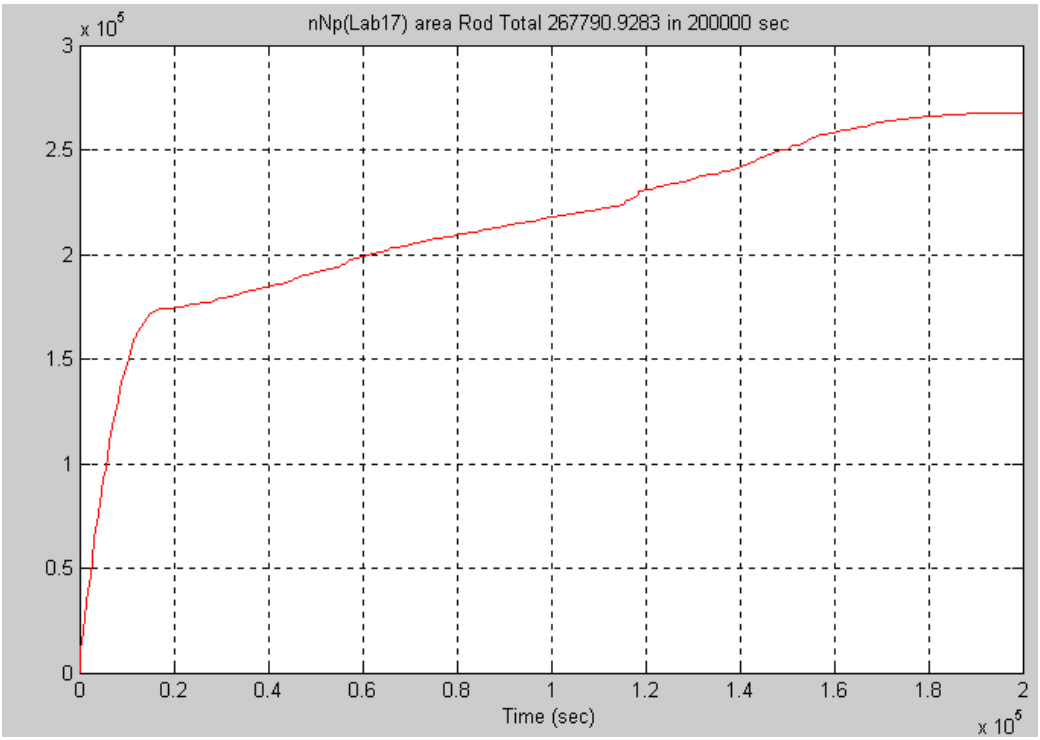

Figure 5.C.15. "nNp" Configuration 1: Cumulative Rod Total vs. Time

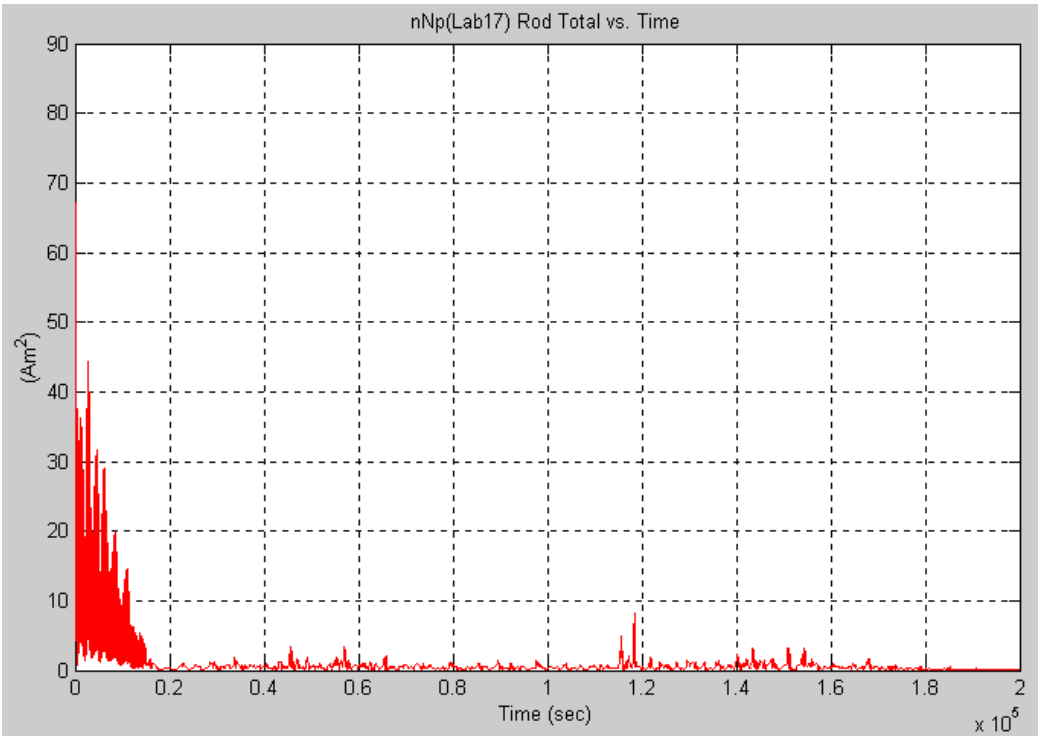

Figure 5.C.16. "nNp" Configuration 1: Instantaneous Rod Total vs. Time

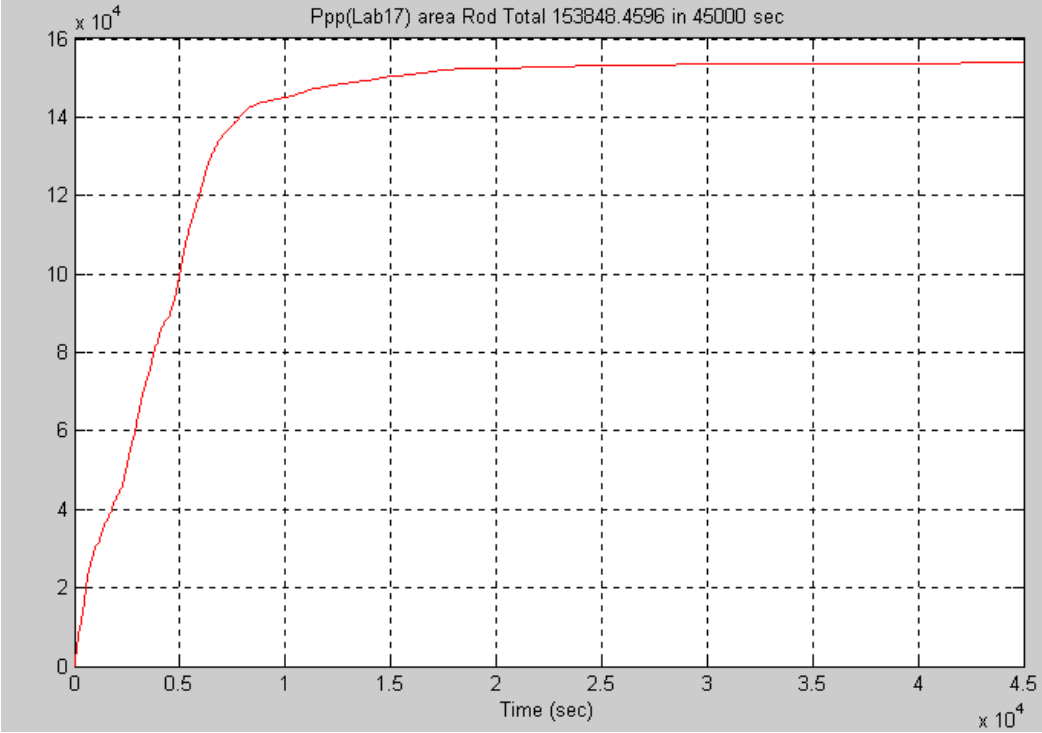

Figure 5.C.17. "Ppp" Configuration 1: Cumulative Rod Total vs. Time

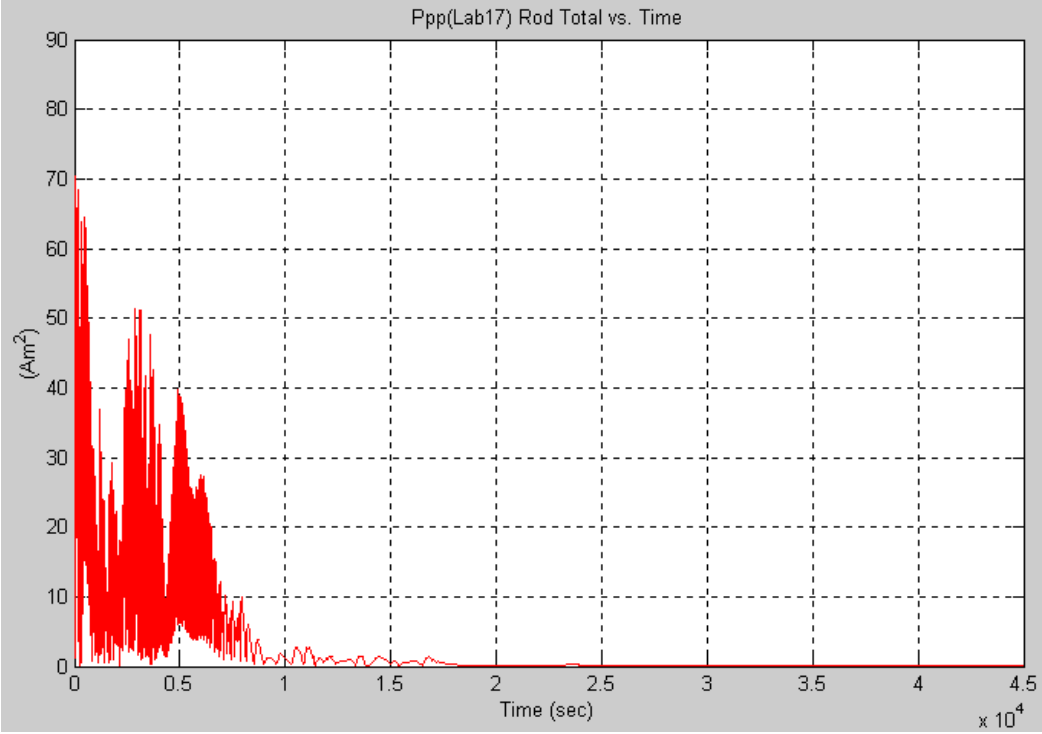

Figure 5.C.18. "Ppp" Configuration 1: Instantaneous Rod Total vs. Time

D. CONFIGURATION 2 RESULTS

The combo model's results became the baseline reference for all data comparison. The power required to achieve steady state was consistently lower than any other model or program, regardless of initial satellite angular rates. The advantage of lower required power levels, however, was somewhat diminished by the apparent trade-off with increased settling times. The majority of the other models and programs consistently performed better than the configuration 2 model with respect to time to achieve steady state. Nevertheless, time to achieve steady state has been considered of less overall importance than power use for the initial acquisition of orbit attitude.

All 32 initial angular rate test cases were analyzed using the combo model. There was, like the results of the Bdot program runs, no apparent correlation between sign or magnitude combinations of the initial angular rates and the resulting time or power consumption required to achieve a steady state condition. There appeared, however, to be some correlation between power consumption and time to achieve steady state. The initial power use for "high" satellite angular rates and "low" satellite angular rates is comparable between test cases, regardless of which angular rate had the highest magnitude. All configuration 2 test cases had comparable power consumption versus time, once the initial higher rates were "knocked down" by the system. Therefore, the test cases that took the longest time to achieve a steady state condition, correspondingly also had the highest power consumption levels. Figures 5.D.1 through 5.D.18 show the instantaneous and cumulative power consumption results for configuration 2.

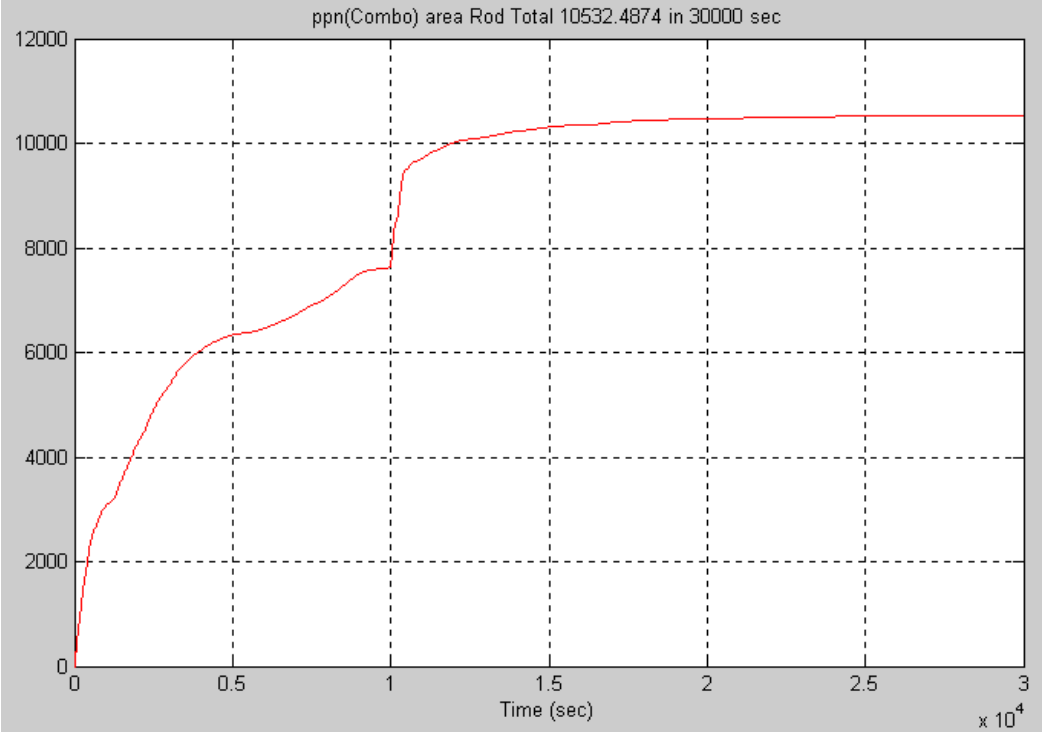

Figure 5.D.1. "ppn" Configuration 2: Cumulative Rod Total vs. Time

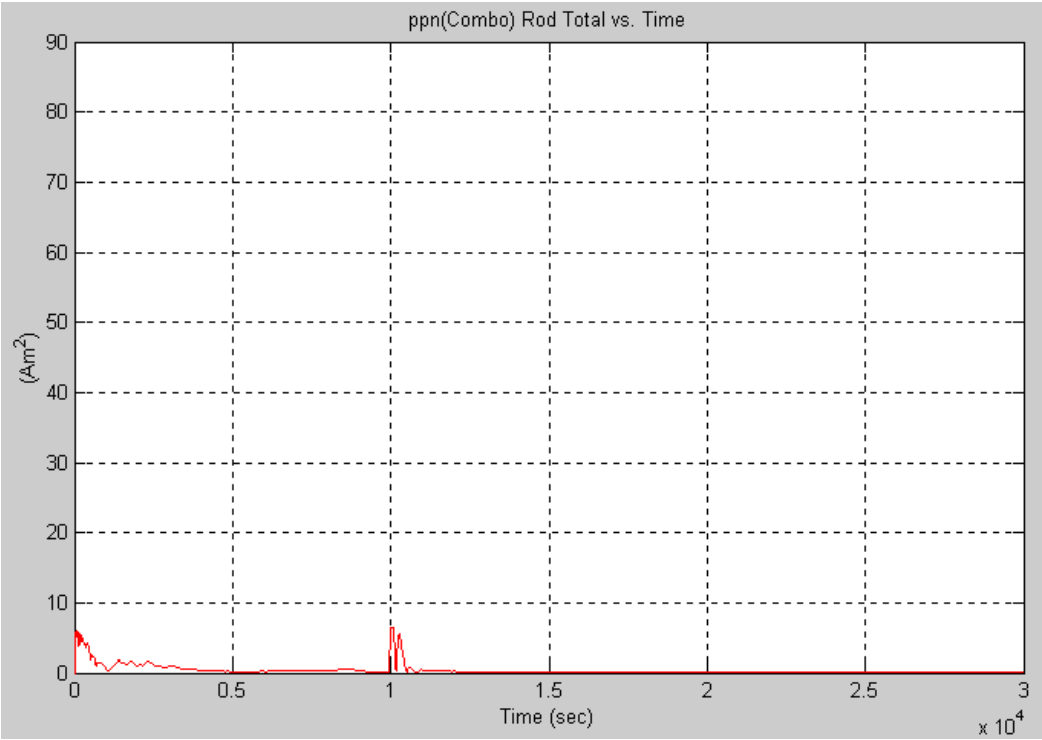

Figure 5.D.2. "ppn" Configuration 2: Instantaneous Rod Total vs. Time

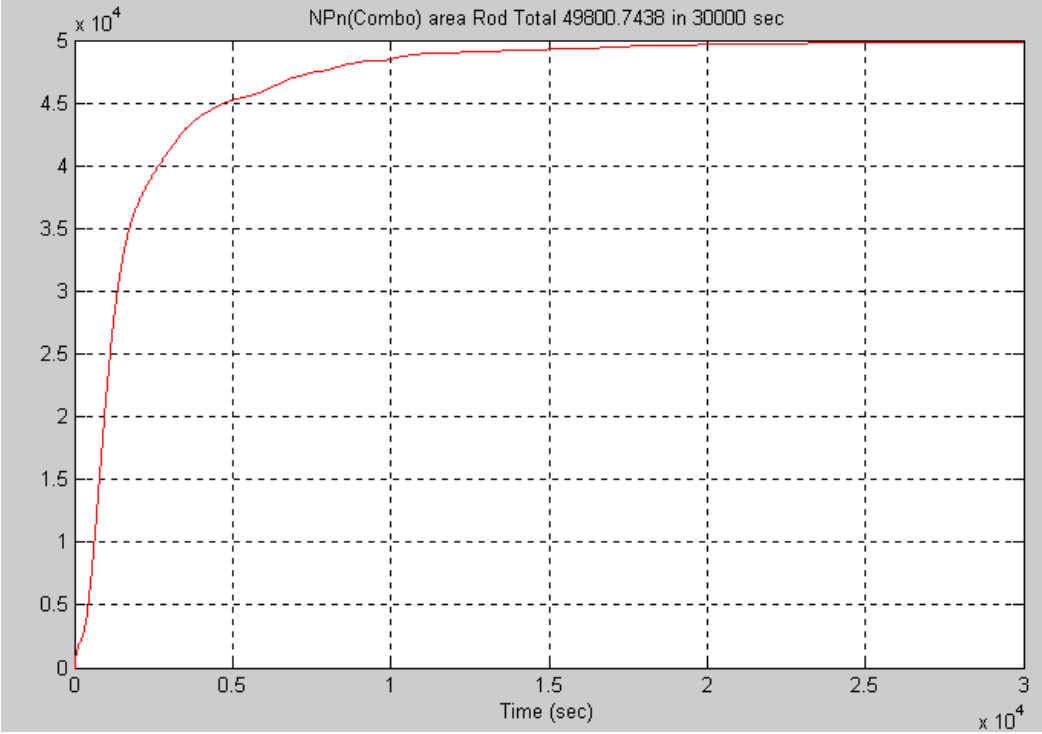

Figure 5.D.3. "NPn" Configuration 2: Cumulative Rod Total vs. Time

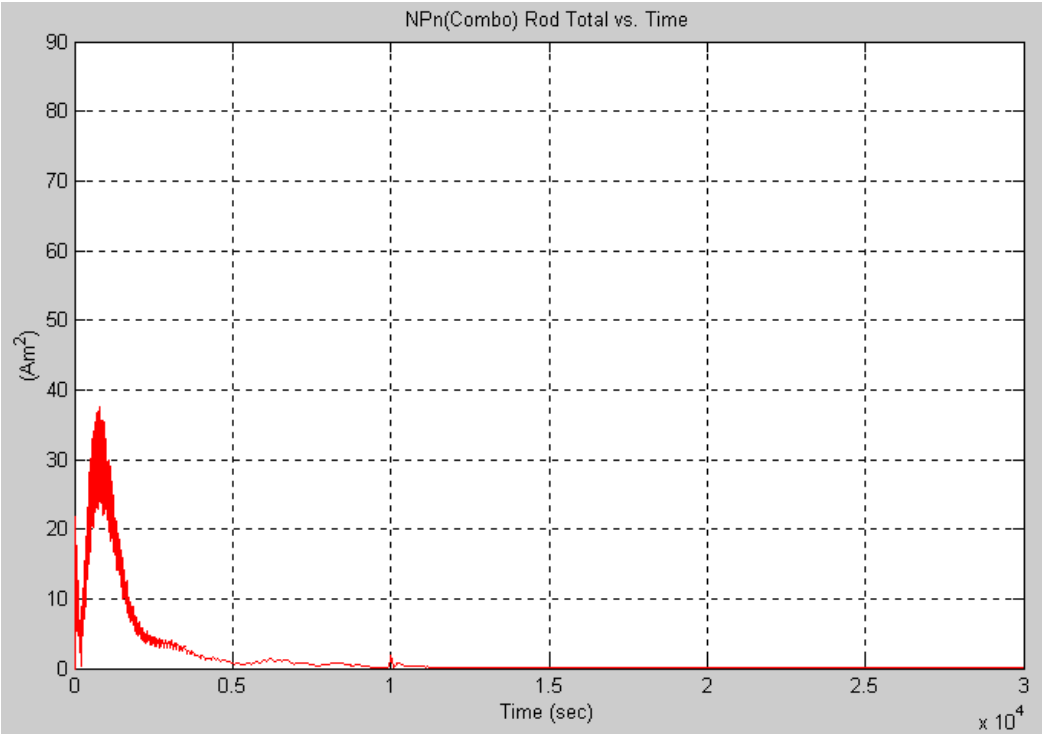

Figure 5.D.4. "NPn" Configuration 2: Instantaneous Rod Total vs. Time

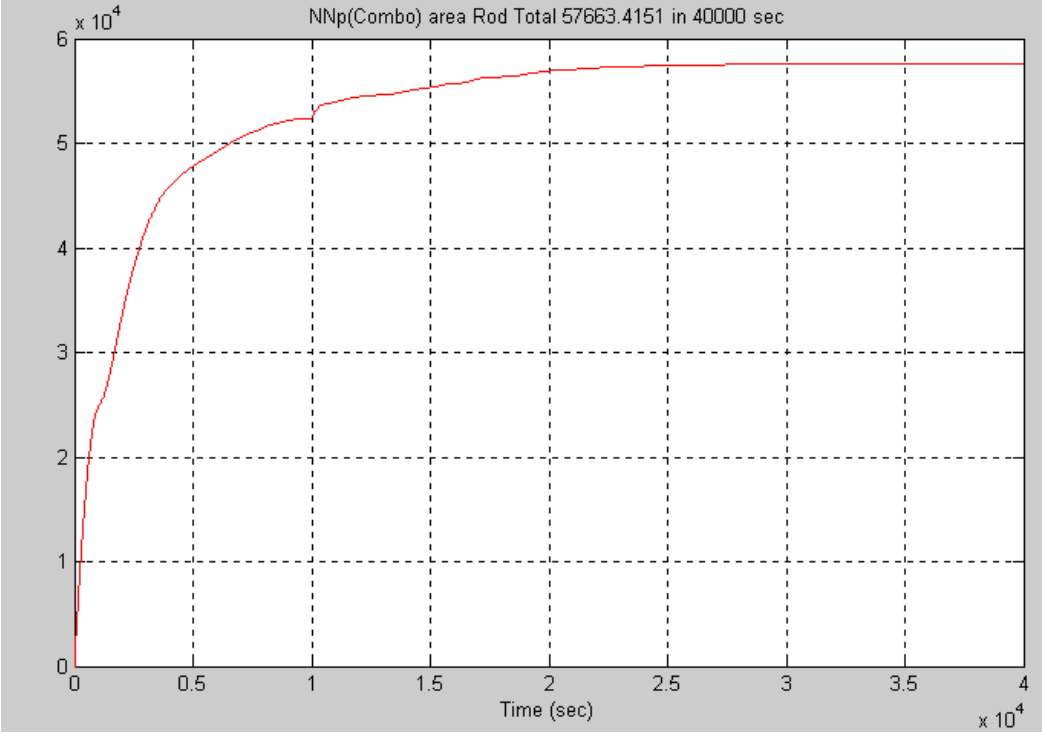

Figure 5.D.5. "NNp" Configuration 2: Cumulative Rod Total vs. Time

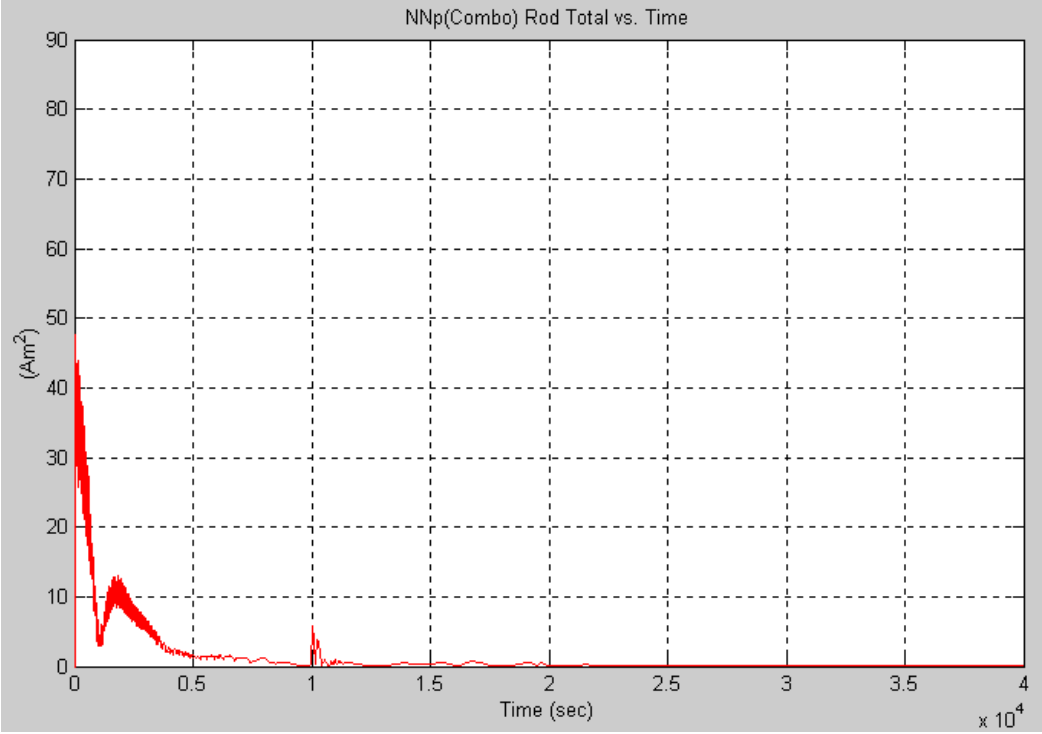

Figure 5.D.6. "NNp" Configuration 2: Instantaneous Rod Total vs. Time

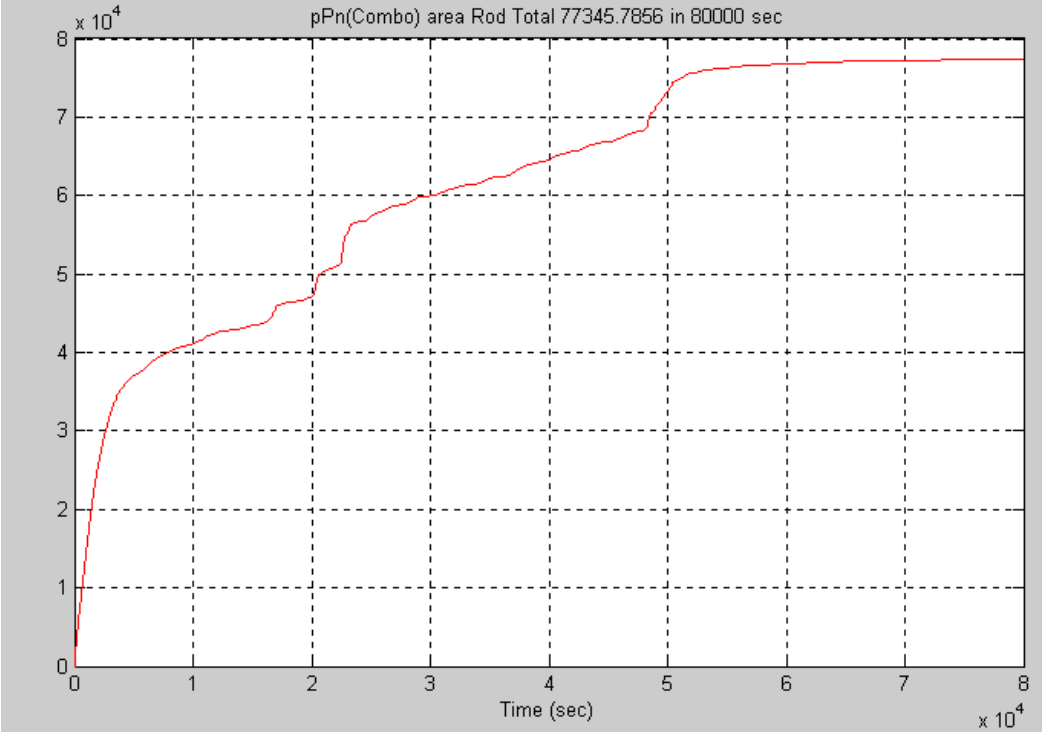

Figure 5.D.7. "pPn" Configuration 2: Cumulative Rod Total vs. Time

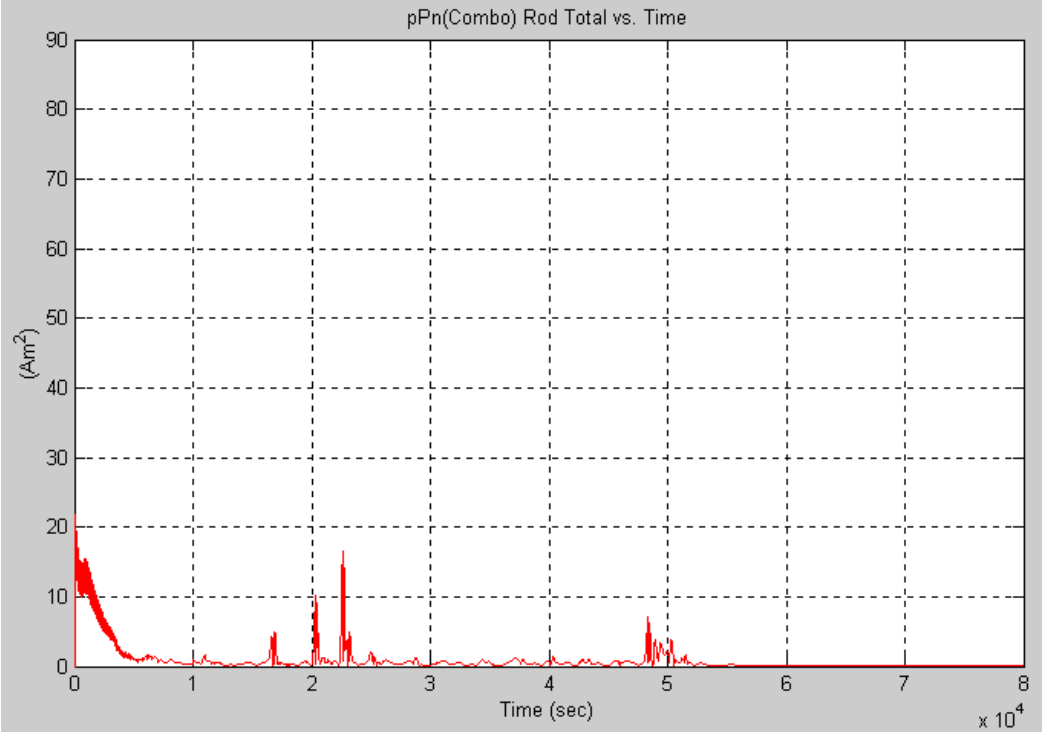

Figure 5.D.8. "pPn" Configuration 2: Instantaneous Rod Total vs. Time

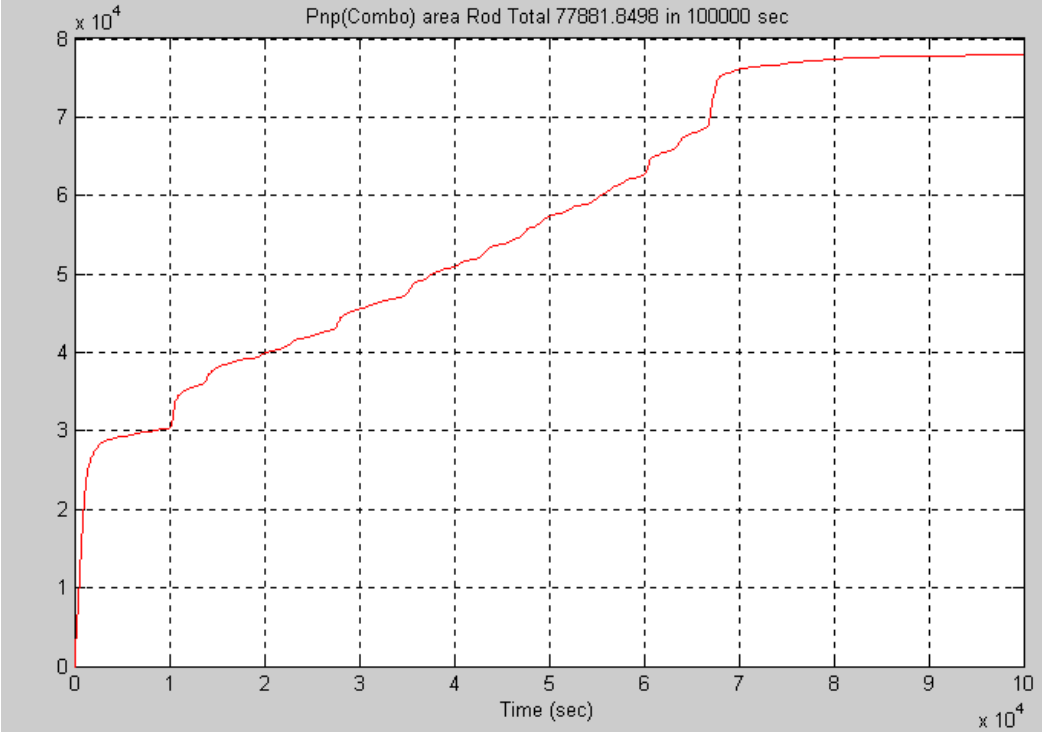

Figure 5.D.9. "Pnp" Configuration 2: Cumulative Rod Total vs. Time

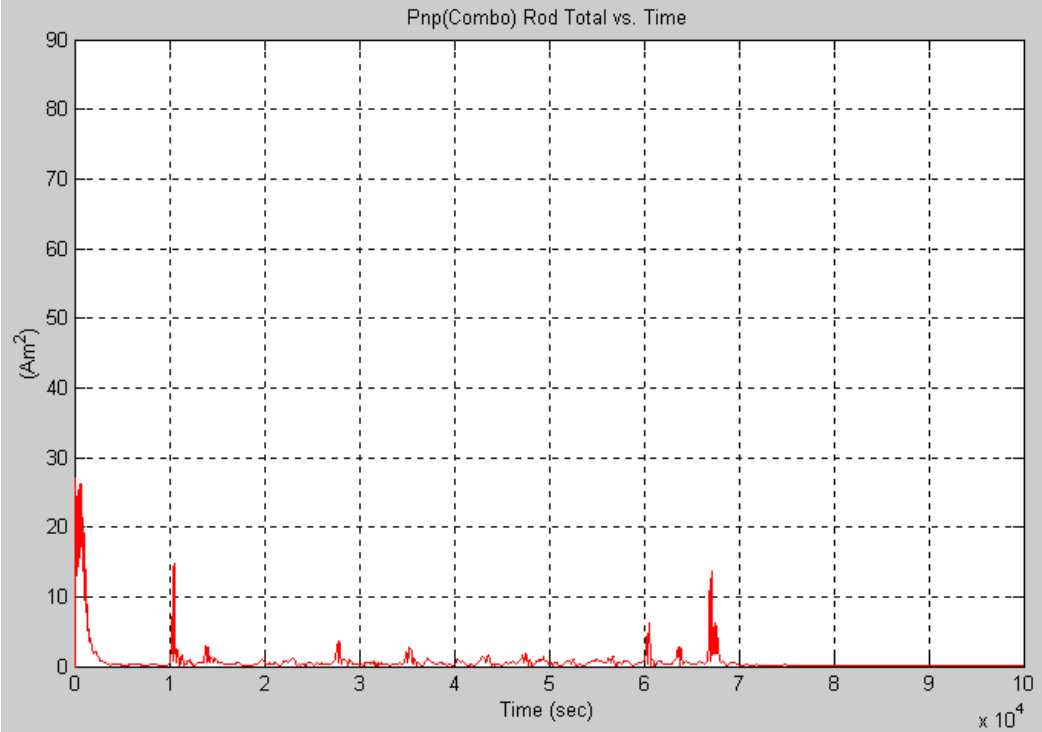

Figure 5.D.10. "Pnp" Configuration 2: Instantaneous Rod Total vs. Time

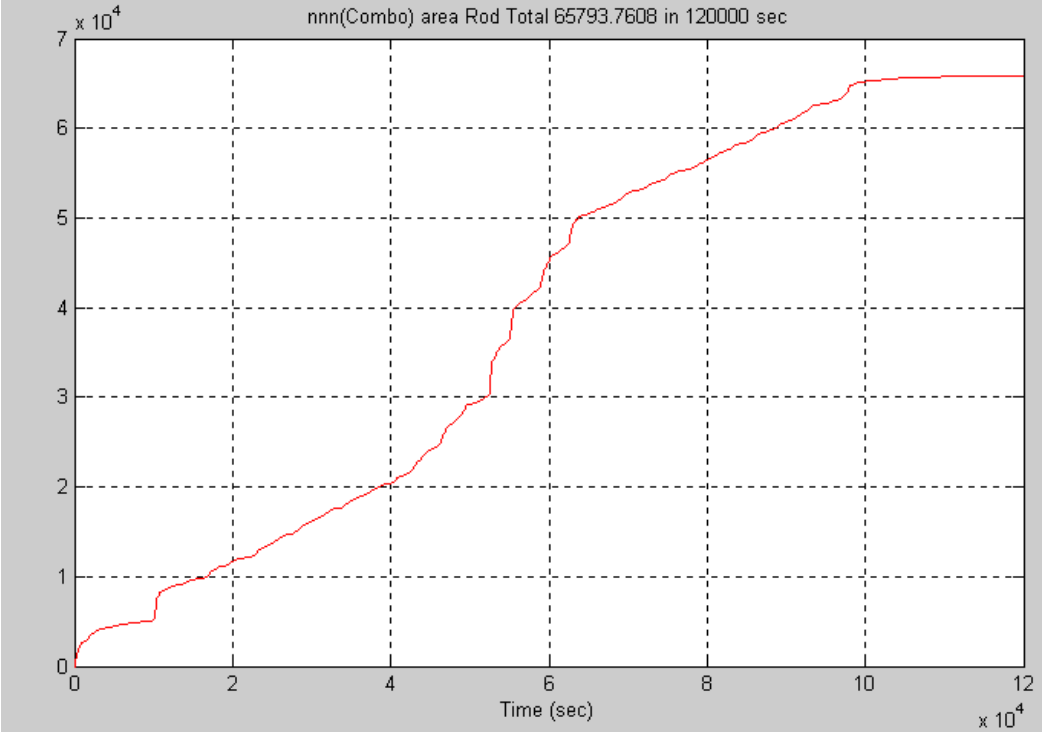

Figure 5.D.11. "nnn" Configuration 2: Cumulative Rod Total vs. Time

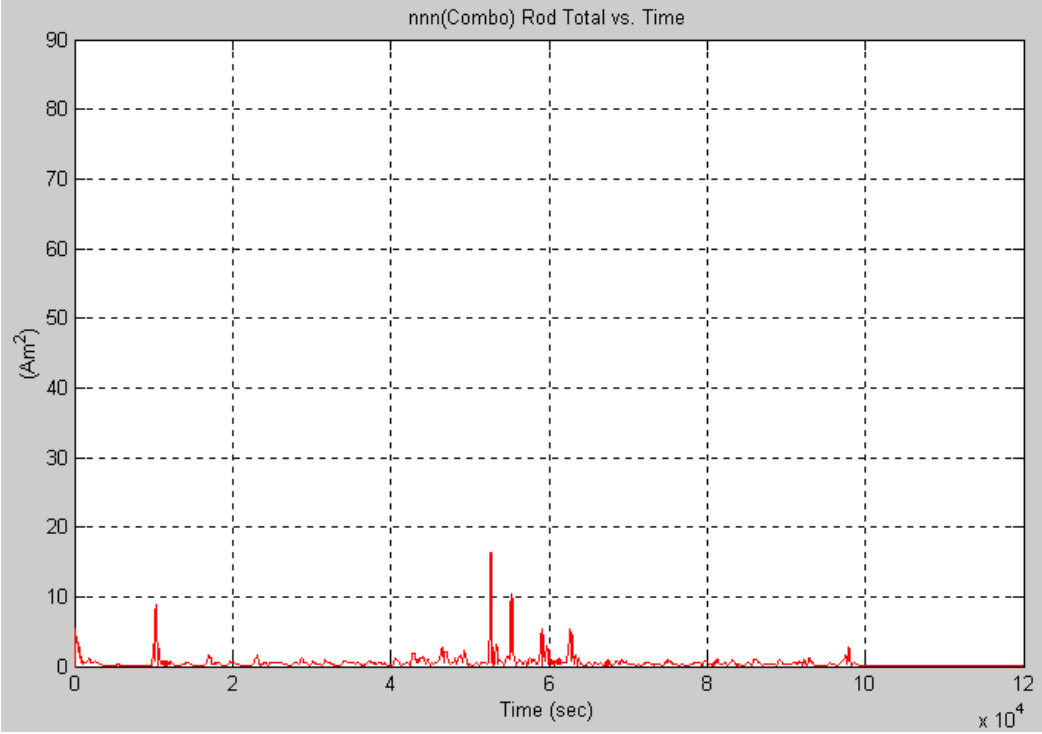

Figure 5.D.12. "nnn" Configuration 2: Instantaneous Rod Total vs. Time

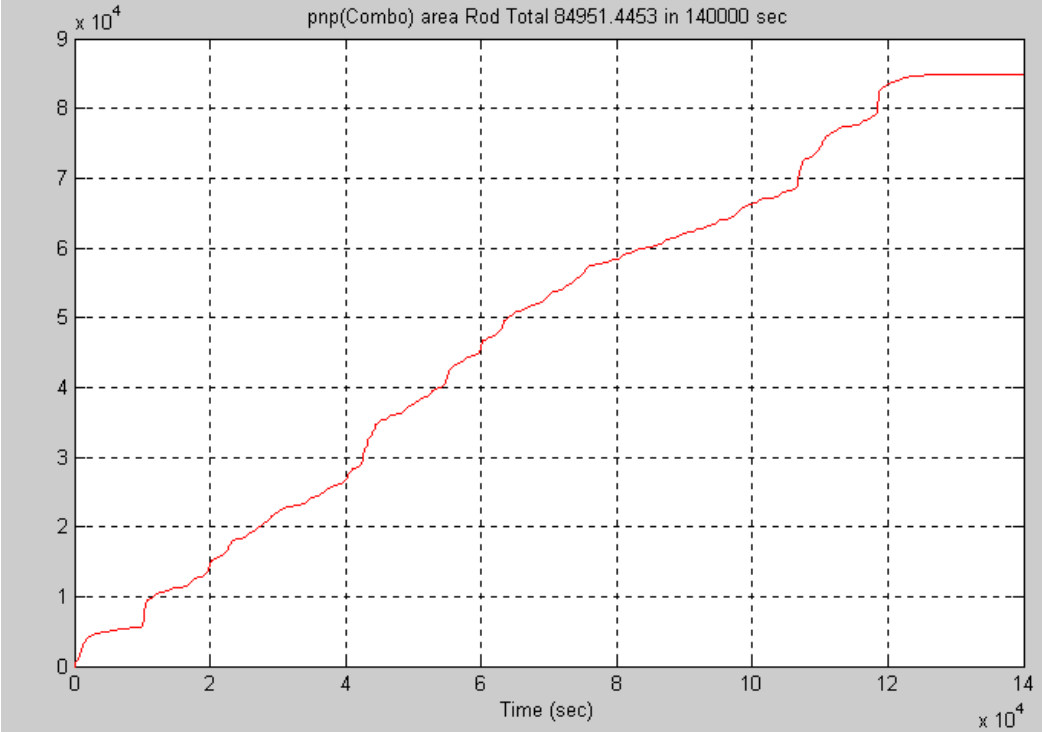

Figure 5.D.13. "pnp" Configuration 2: Cumulative Rod Total vs. Time

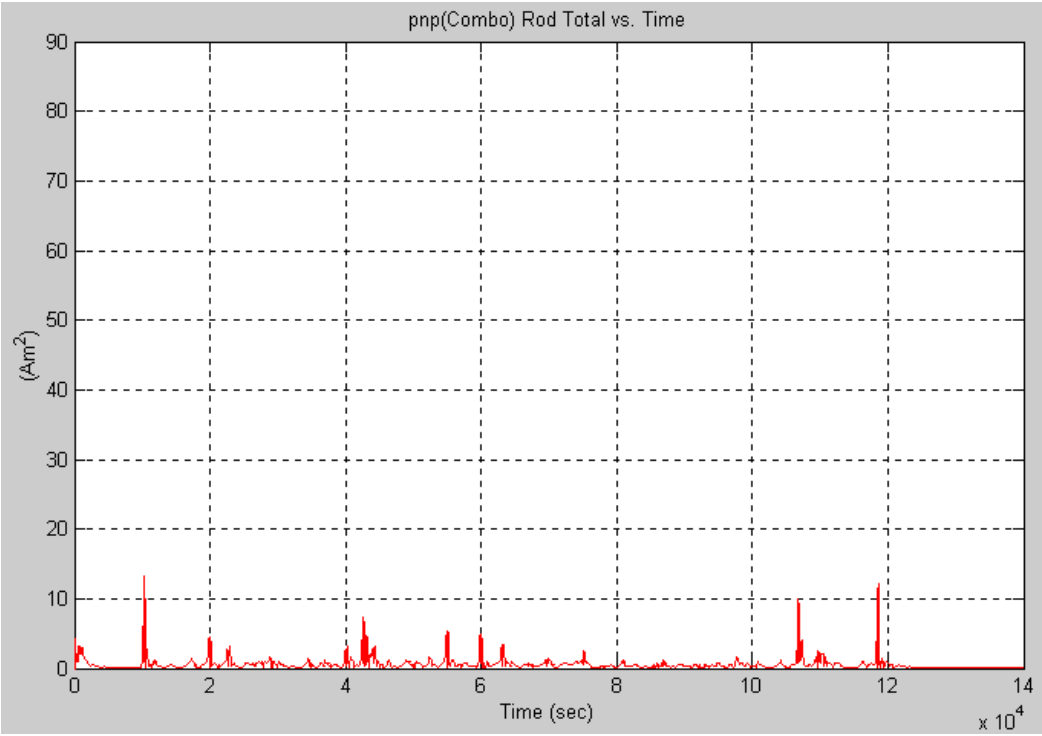

Figure 5.D.14. "pnp" Configuration 2: Instantaneous Rod Total vs. Time

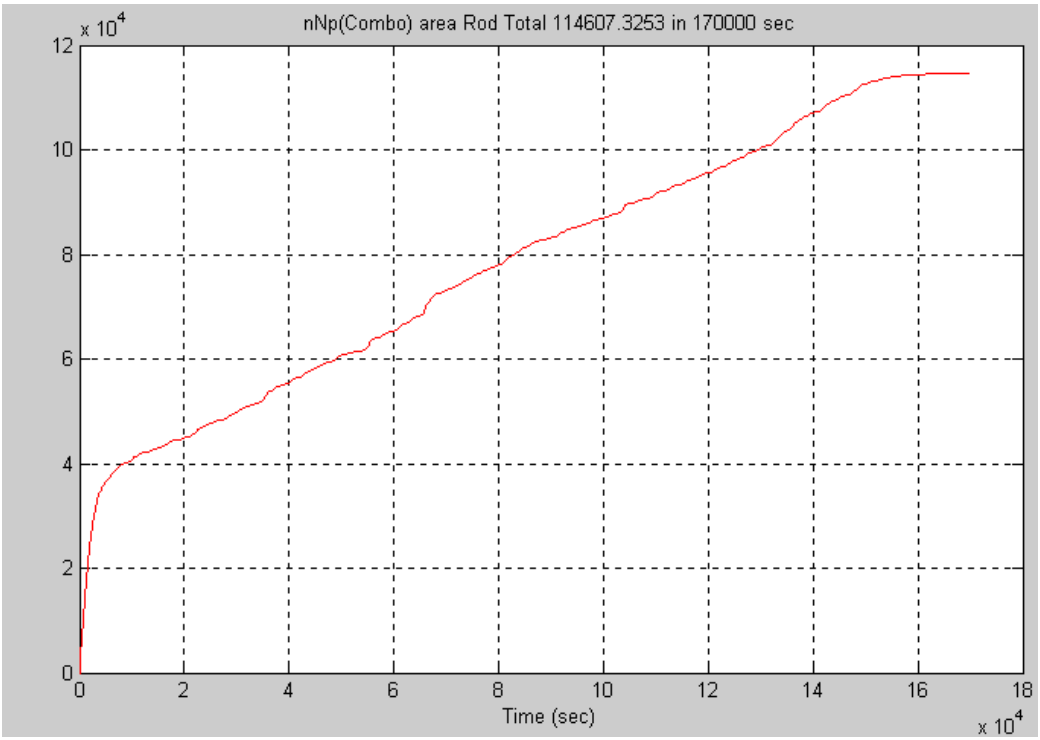

Figure 5.D.15. "nNp" Configuration 2: Cumulative Rod Total vs. Time

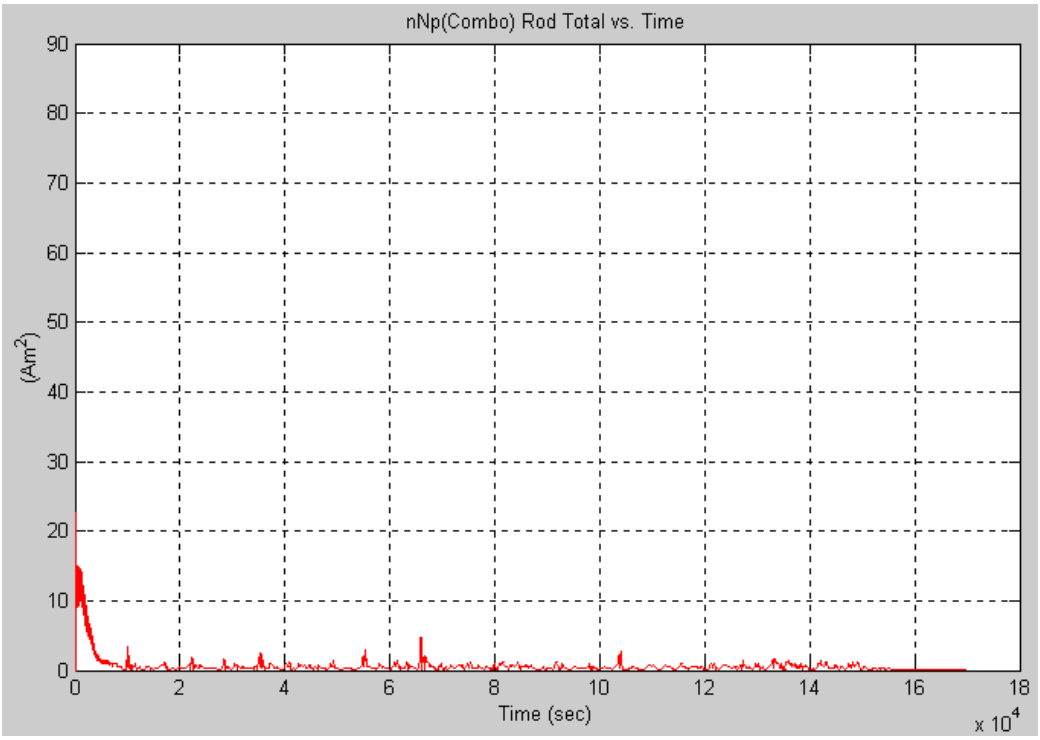

Figure 5.D.16. "nNp" Configuration 2: Instantaneous Rod Total vs. Time

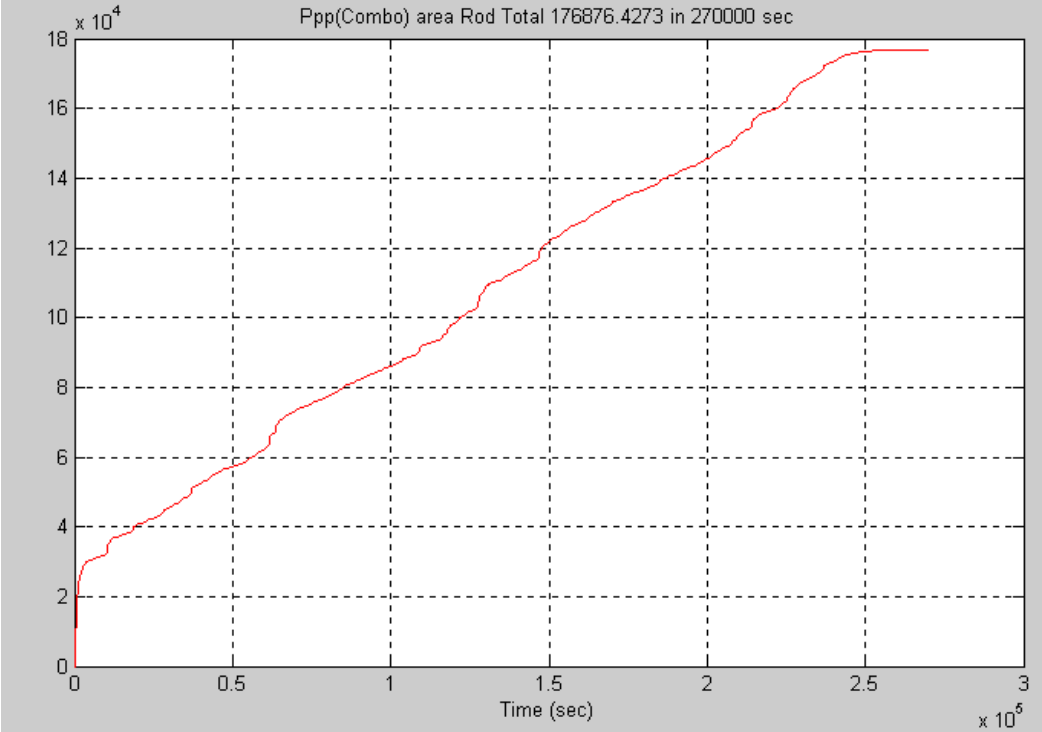

Figure 5.D.17. "Ppp" Configuration 2: Cumulative Rod Total vs. Time

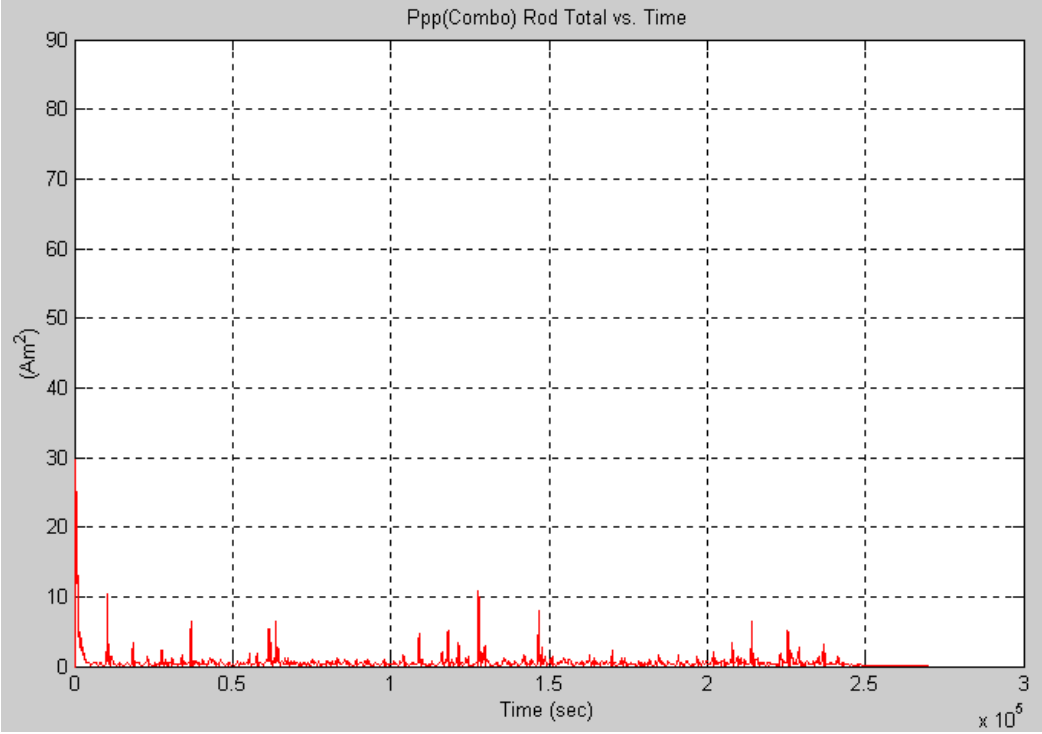

Figure 5.D.18. "Ppp" Configuration 2: Instantaneous Rod Total vs. Time

E. CONFIGURATION 3 RESULTS

When the Bdot program was run independently, then handed-off to the LAB17 model, using the final conditions from the Bdot test case as the initial conditions for the LAB17 test case, the following results occurred: Compared to the nine combo model test cases chosen to represent the full spread of outcome possibilities, the LAB17 hand-off method test cases tended not to perform as well compared to the fastest half of the combo method test cases. It performed better, though, than the slowest half of the combo method test cases. Performance levels, mentioned above, include both power consumption and time response to test case initial conditions. The results also further amplified the finding that there was no apparent correlation between sign or magnitude of the test case initial angular rates and the performance of the system in power consumption or time response. Figures 5.E.1 through 5.E.2 show the instantaneous and cumulative power consumption results for configuration 3.

Cases “NPn,” “NNp,” “pPn,” “nnn,” and “Ppp” clearly illustrate the power spike occurring at the hand-off point between the Bdot and Lab17 models. This is most likely due to the poor initial estimates within the Kalman Filter.

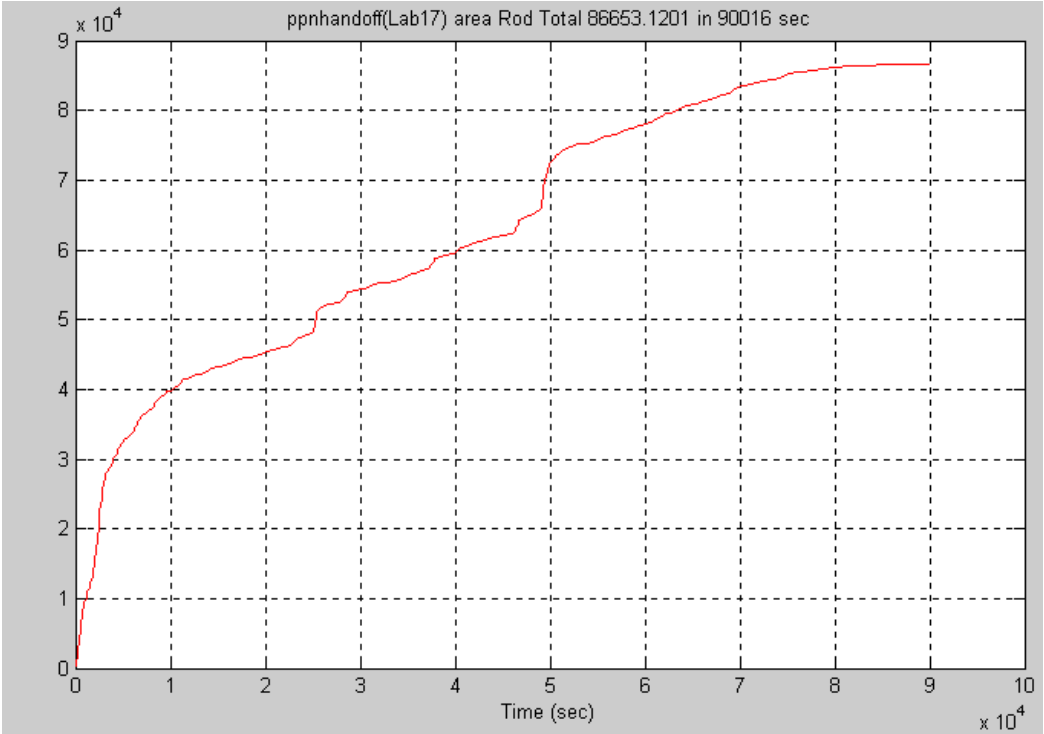

Figure 5.E.1. "ppn" Configuration 3: Cumulative Rod Total vs. Time

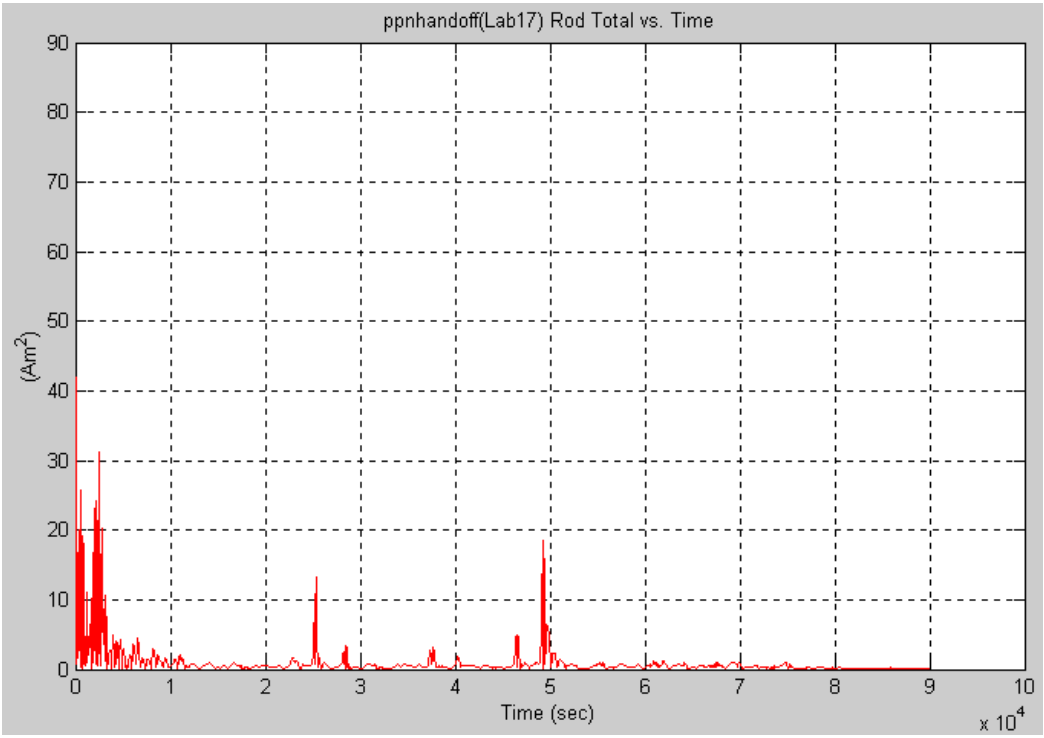

Figure 5.E.2. "ppn" Configuration 3: Instantaneous Rod Total vs. Time

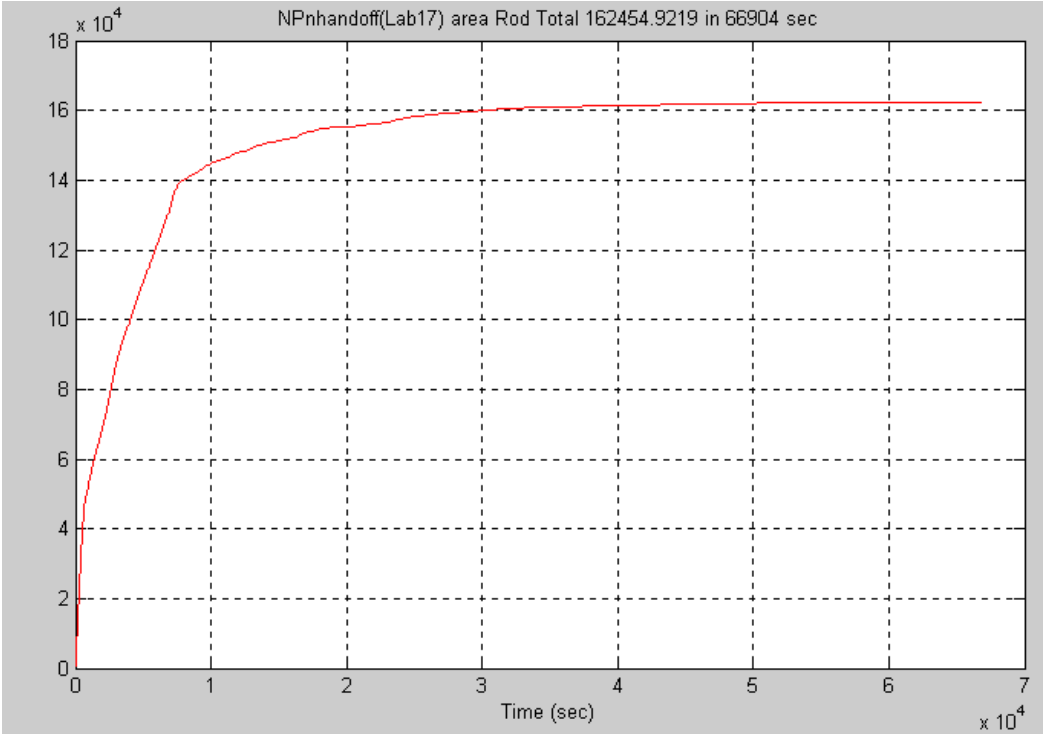

Figure 5.E.3. "NPn" Configuration 3: Cumulative Rod Total vs. Time

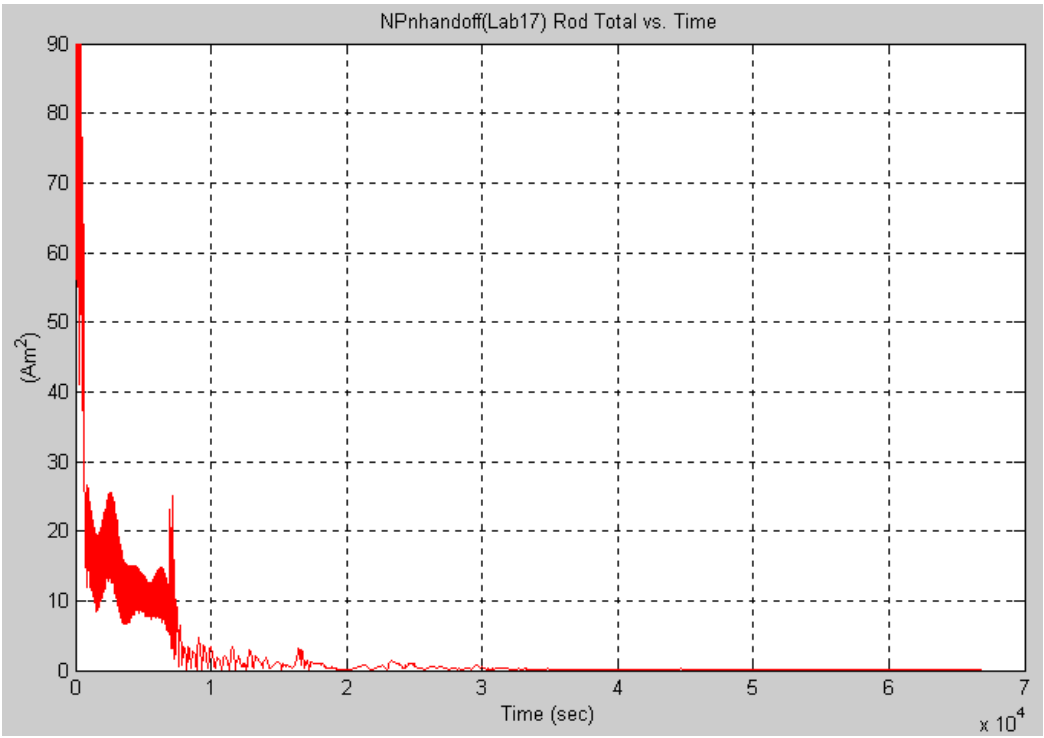

Figure 5.E.4. "NPn" Configuration 3: Instantaneous Rod Total vs. Time

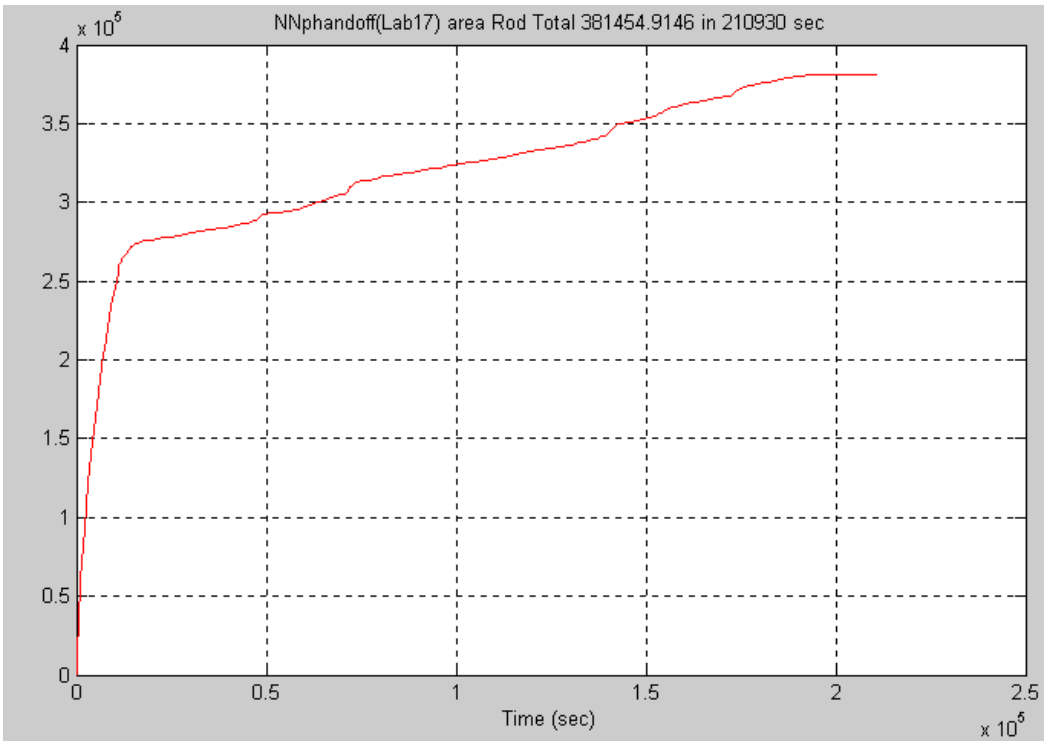

Figure 5.E.5. "NNp" Configuration 3: Cumulative Rod Total vs. Time

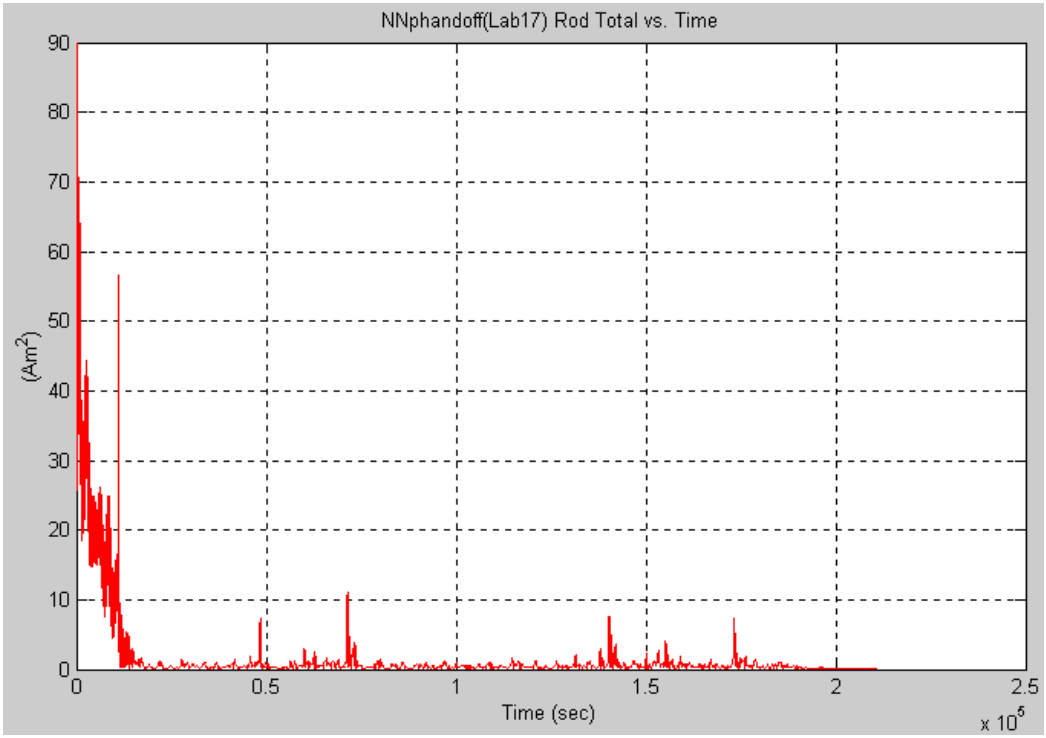

Figure 5.E.6. "NNp" Configuration 3: Instantaneous Rod Total vs. Time

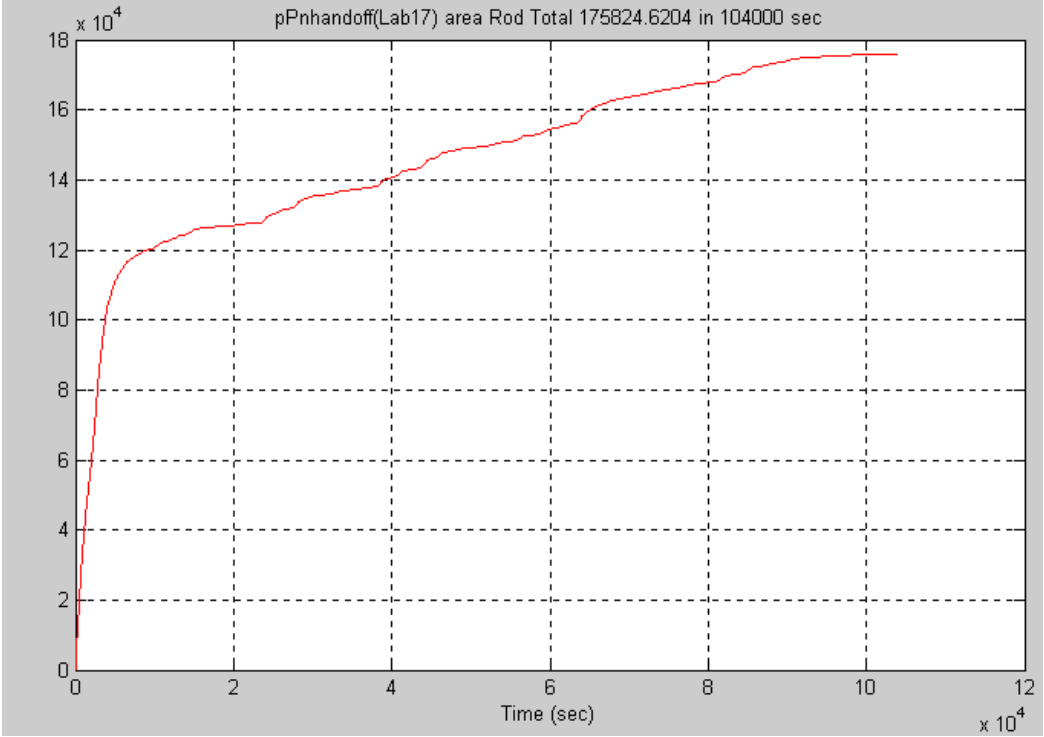

Figure 5.E.7. "pPn" Configuration 3: Cumulative Rod Total vs. Time

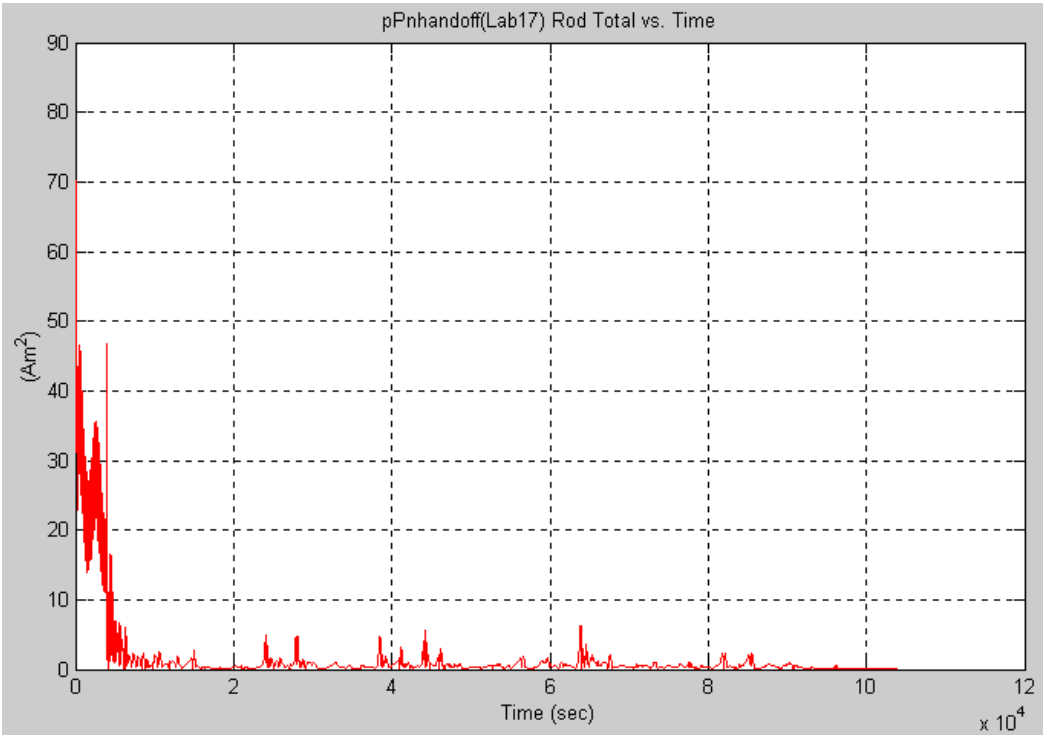

Figure 5.E.8. "pPn" Configuration 3: Instantaneous Rod Total vs. Time

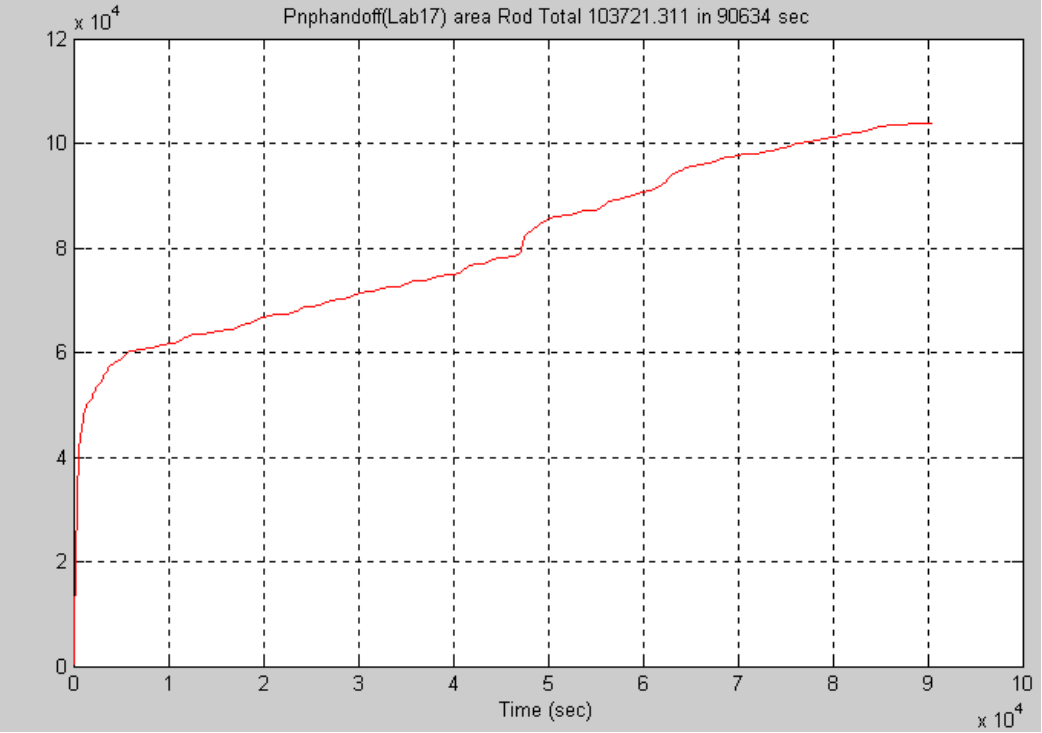

Figure 5.E.9. "Pnp" Configuration 3: Cumulative Rod Total vs. Time

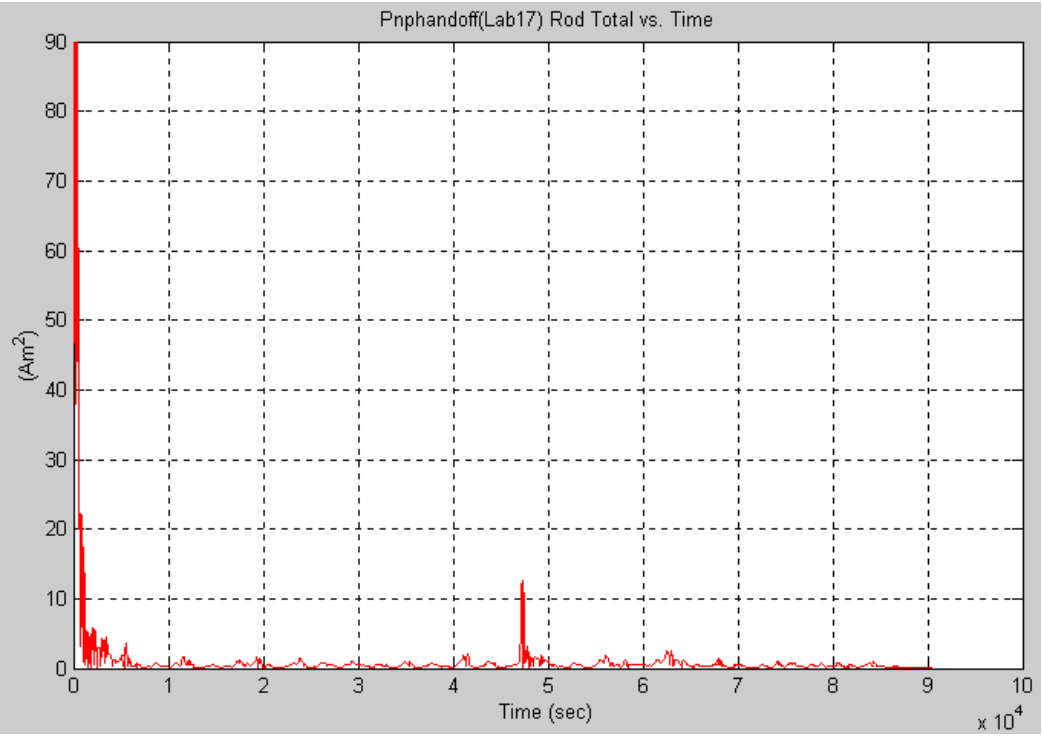

Figure 5.E.10. "Pnp" Configuration 3: Instantaneous Rod Total vs. Time

Figure 5.E.11. "nnn" Configuration 3: Cumulative Rod Total vs. Time

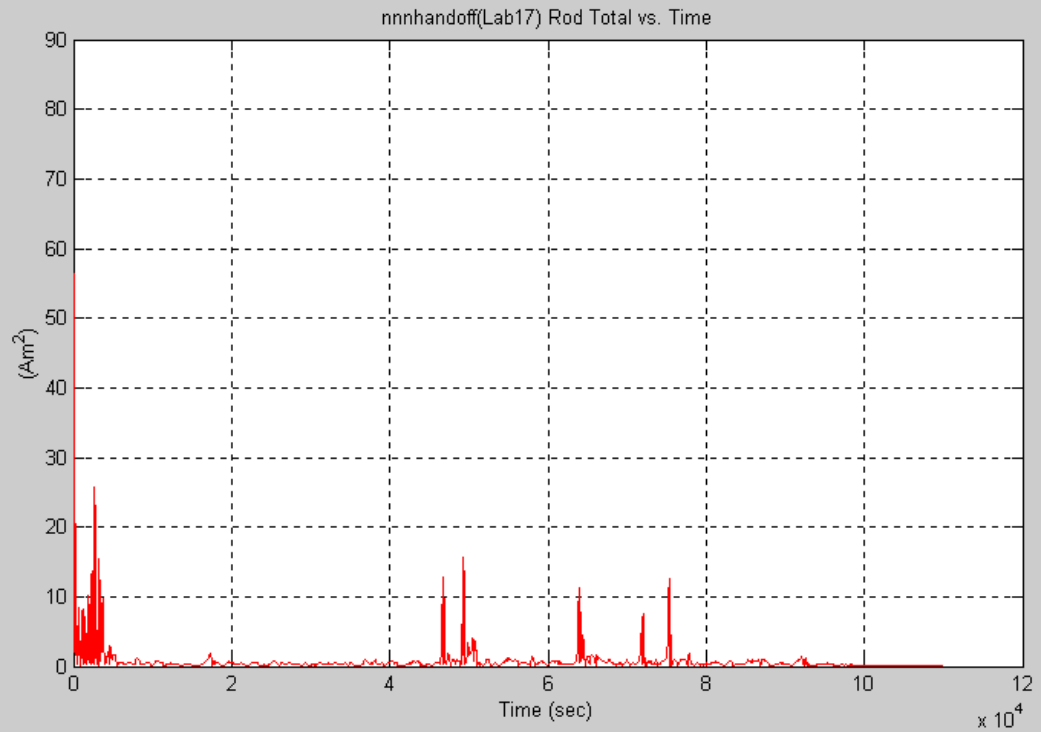

Figure 5.E.12. "nnn" Configuration 3: Instantaneous Rod Total vs. Time

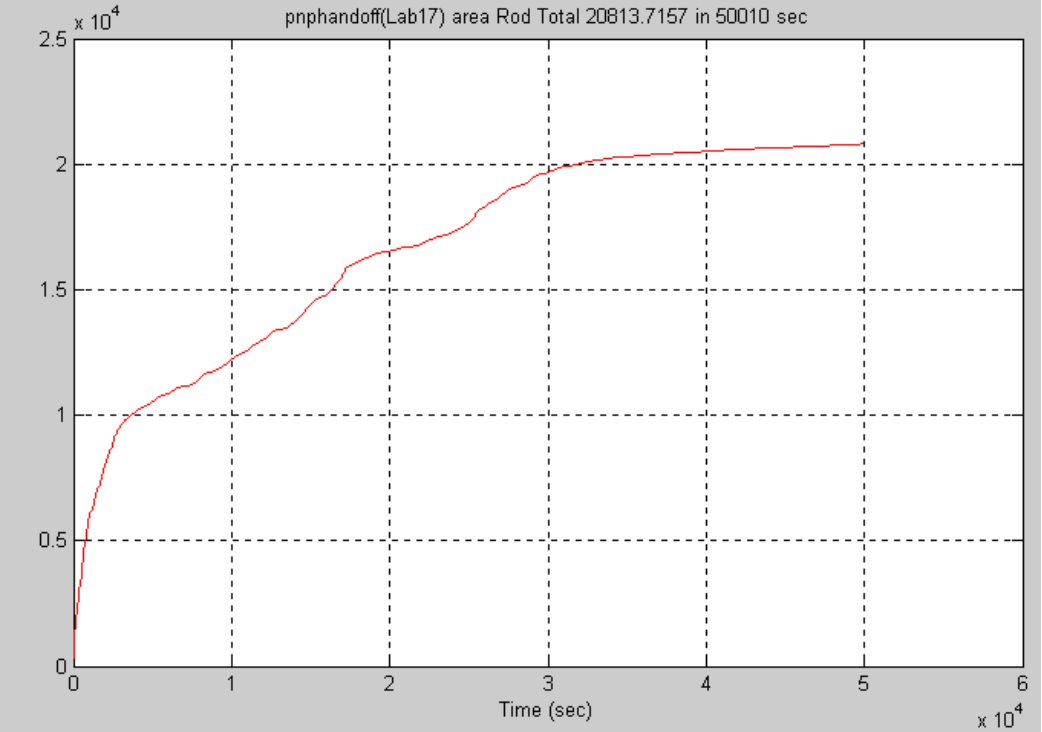

Figure 5.E.13. "pnp" Configuration 3: Cumulative Rod Total vs. Time

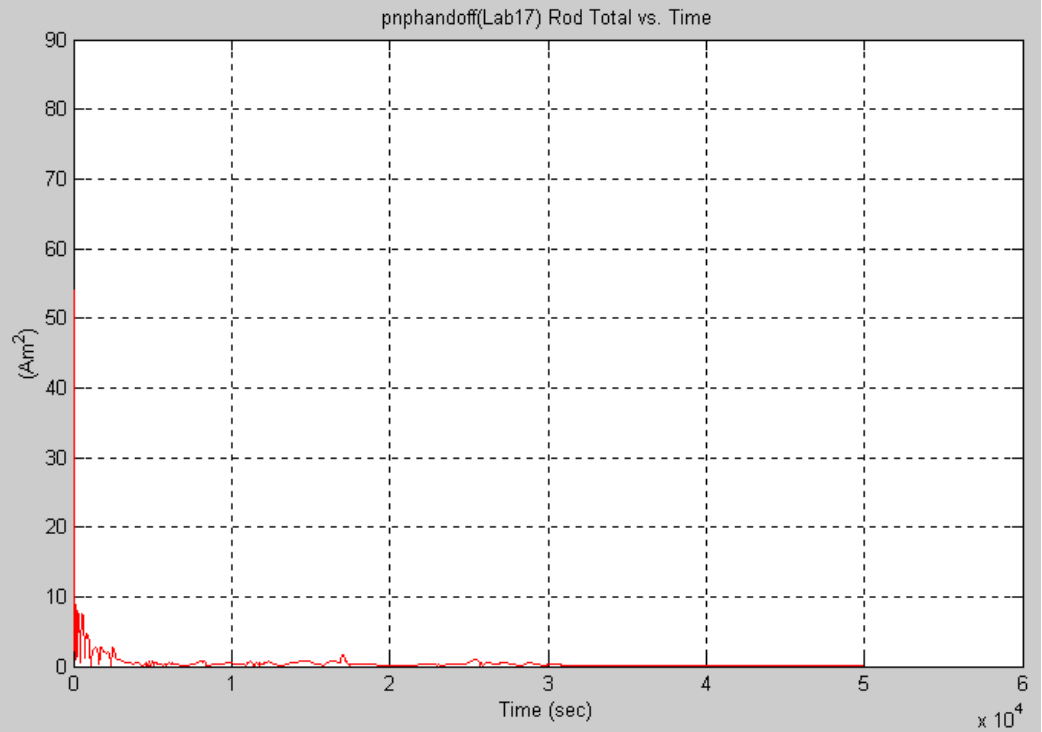

Figure 5.E.14. "pnp" Configuration 3: Instantaneous Rod Total vs. Time

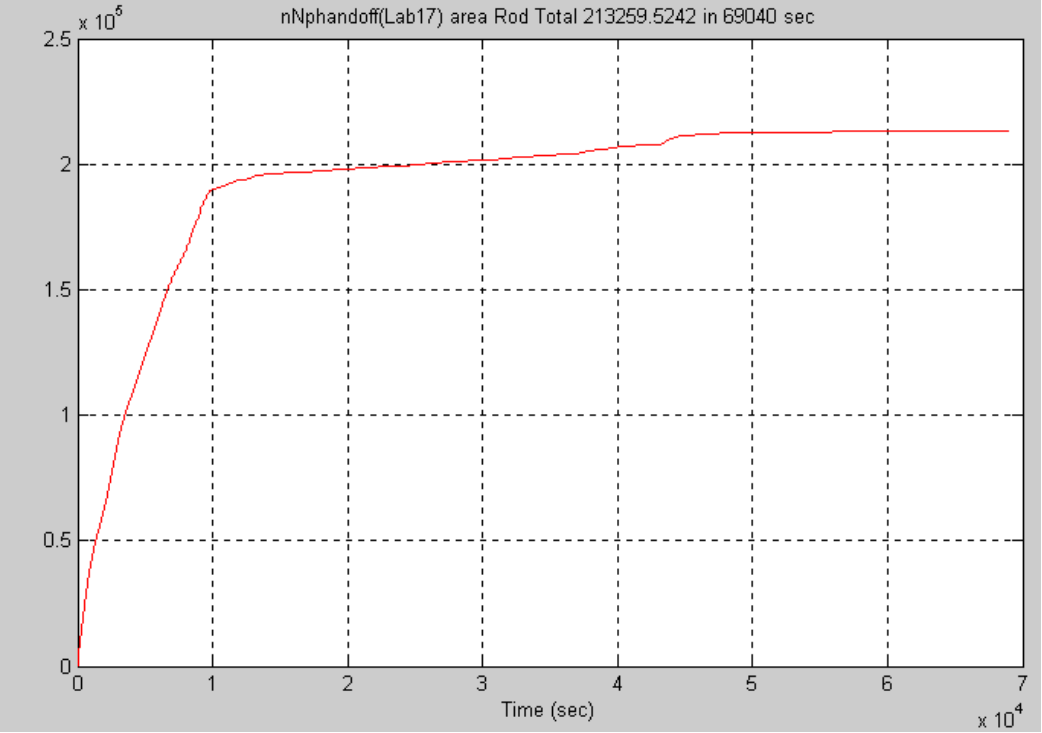

Figure 5.E.15. "nNp" Configuration 3: Cumulative Rod Total vs. Time

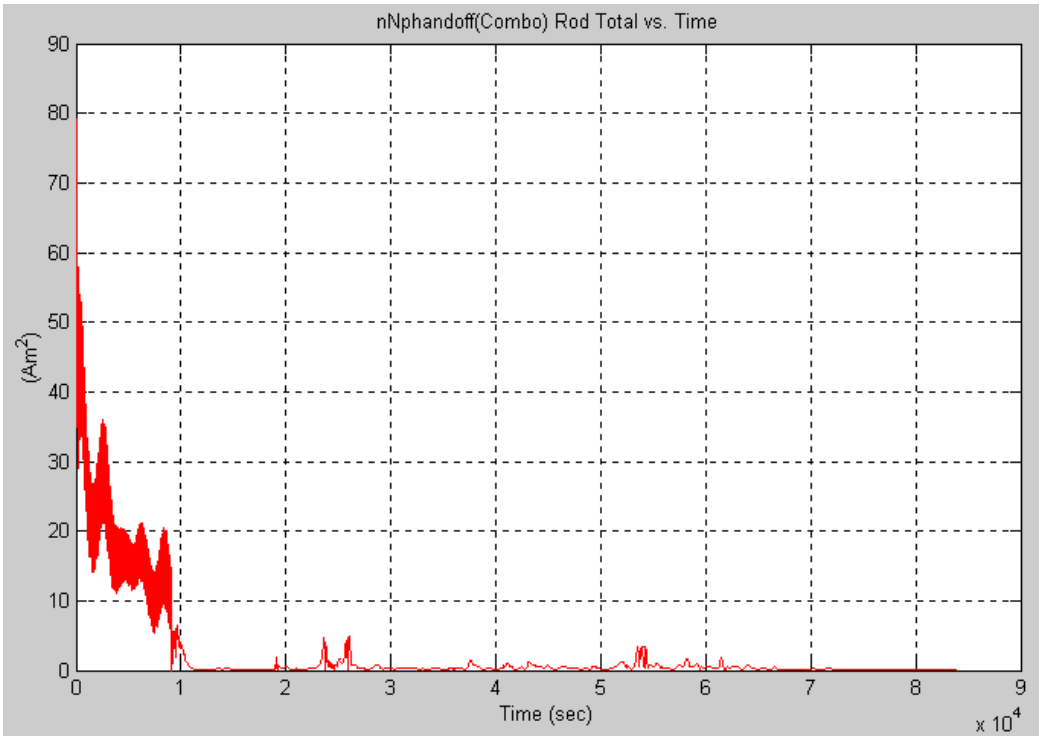

Figure 5.E.16. "nNp" Configuration 3: Instantaneous Rod Total vs. Time

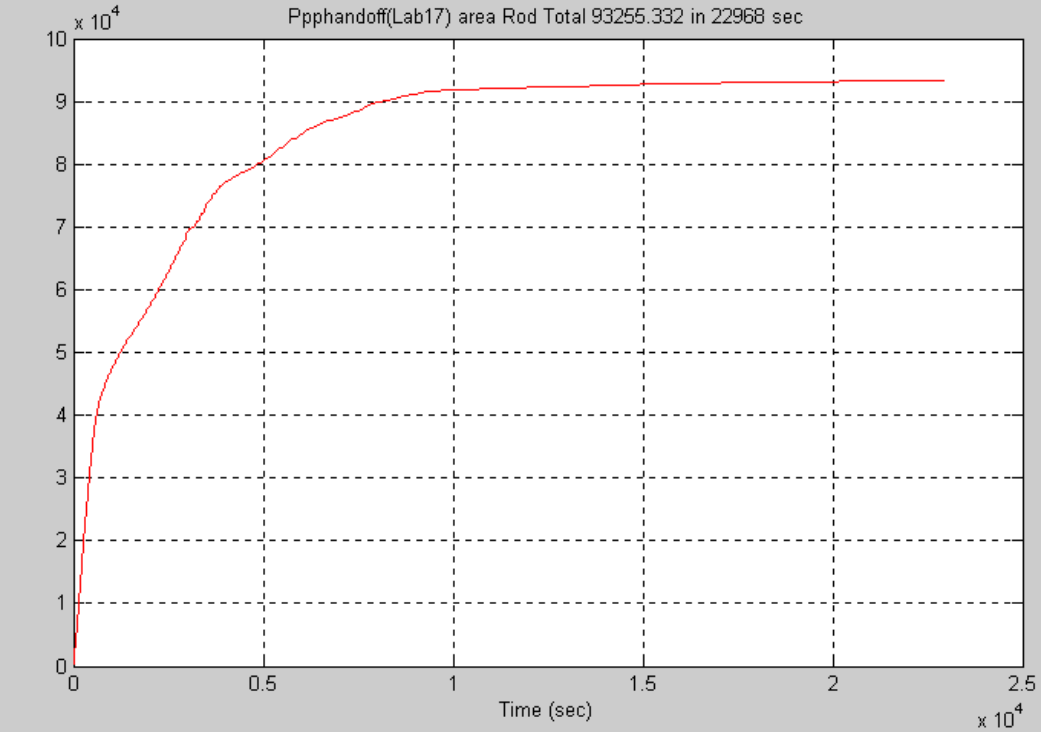

Figure 5.E.17. "Ppp" Configuration 3: Cumulative Rod Total vs. Time

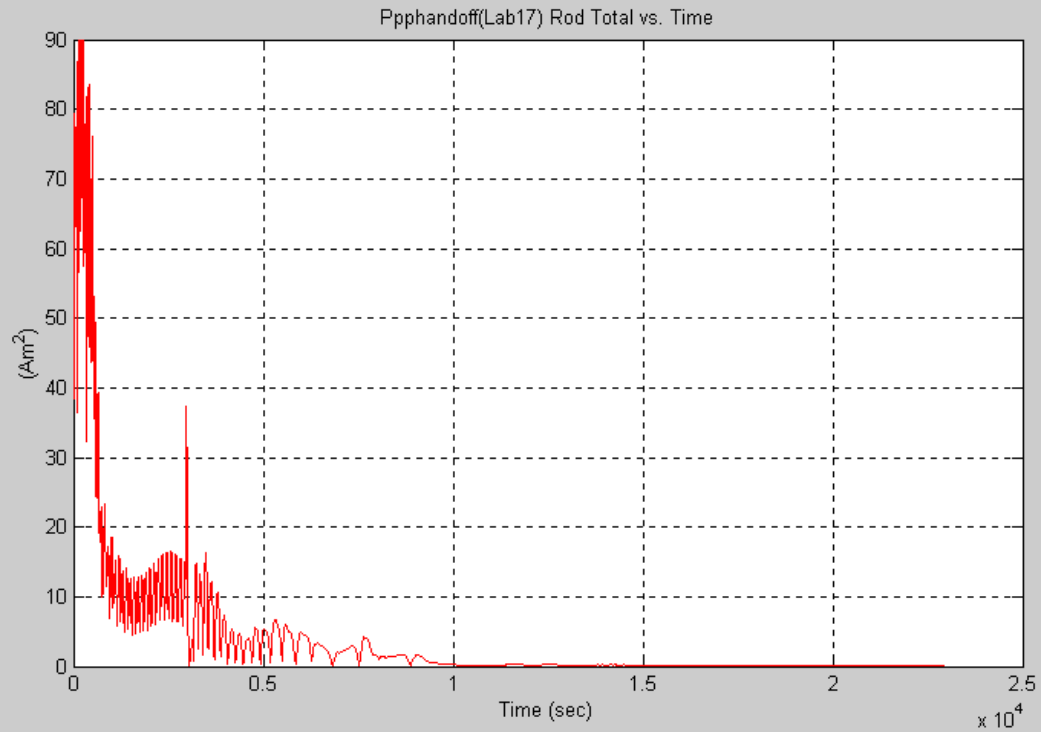

Figure 5.E.18. "Ppp" Configuration 3: Instantaneous Rod Total vs. Time

THIS PAGE INTENTIONALLY LEFT BLANK

VI. CONCLUSIONS AND RECOMMENDATIONS

A. CONCLUSIONS

Table 6.A.1 summarizes the comparative results of each of the three attitude control methods analyzed in this study. The reference combo method was chosen primarily for its relatively superior performance in power consumption required to reach a steady state. The nine comparison test cases were chosen to represent the entire performance range of the combo method test cases.

The most obvious conclusions that can be obtained from the analysis of these control methods and resulting data are as follows: The combo model, configuration 2 generally consumed the lowest power levels of any other method, but required the longest settling times for medium to high initial angular rates. The control methods that included the Bdot control law (configuration 2 and 3) quickly reduced the satellite angular rates to a level that thence required only minimal power consumption to achieve steady state pointing accuracies of less than ten degrees. Time to achieve system steady state was achieved more quickly and with less power consumption for cases with higher initial angular rates when the hand-off from a Bdot control law occurred after a threshold combined angular rate was achieved instead of performing the hand-off after a predetermined time interval. The configuration 2 model used a timed hand-off from its internal Bdot law control loop, and the configuration 3 model handed-off from a separate Bdot program to the various other models after a threshold combined angular rate was achieved.

The first of the three main analysis objectives was to examine sensitivity of the three configurations to initial conditions. All three configurations performed well for all the test case initial conditions and were viable options for an ACS. The second objective was to compare the differences between using Bdot or no Bdot within a configuration. Although there was questionable improvement in system time responses between the configurations, the power consumption results indicated that both configurations 2 and 3, which used a Bdot control loop, required less power to achieve steady state than configuration 1, which did not include Bdot. The third objective was to explore the

difference between using a timed Bdot hand-off or an angular rate based Bdot hand-off. Configuration 2, which used a timed hand-off, had better power consumption performance, but better time response results than configuration 3, which used the angular rate based hand-off.

	Pwr x1e4	Pwr x1e4	Pwr x1e4	Combo	Time req'd	Hndff bdot	Lab17
Init Rates	Lab17	ho Lab17	Combo	Sim sec	Bdot (sec)	to Lab17	Simulink
pPp				20000	9200		
ppn	119278	86653	1	30000	20	90000	200000
nnp				30000	3500		
NPp				30000	6700		
NPn	169540	162455	49801	30000	6900	56000	67000
nPn				30000	8900		
NNp	5585031	3814549	57663	40000	11000	190000	92000
Ppn				50000	3500		
Pnn				60000	1100		
Nnn				70000	3550		
Nnp				70000	3800		
pPn	66757	175825	77346	80000	3500	100000	60000
pNn				80000	8700		
NNn				80000	11000		
pnn				90000	380		
Npn				90000	840		
Pnp	2474116	103721	77882	100000	650	90000	90000
npn				110000	550		
npp				110000	640		
ppp				110000	3700		
Npp				110000	950		
PNn				110000	14000		
nnn	1	87621	65794	120000	32	110000	30000
PNp				120000	6700		
pNp				120000	8700		
PPp				120000	11000		
pnp	98606	20814	84951	140000	12	50000	170000
nPp				150000	8900		
nNp	2677909	2132595	114607	170000	9044	60000	200000
nNn				170000	9000		
PPn				180000	11200		
Ppp	153848	93255	176876	270000	3000	20000	40000

Table 6.A.1. Test Case Table Data.

Figure 6.A.2 shows common system power consumption response characteristics that can be gleaned from the visual comparison of the three configurations. Magnetic torque rod power consumption was lower, and high angular rates were generally arrested faster, when a Bdot control law was used to reduce initial angular rates to a more-manageable “low” level. When the Bdot control law was used to achieve a sufficiently

low threshold combined angular rate, as opposed to a timed hand-off from a Bdot control law, the power spike that often occurs at the hand-off point was eliminated.

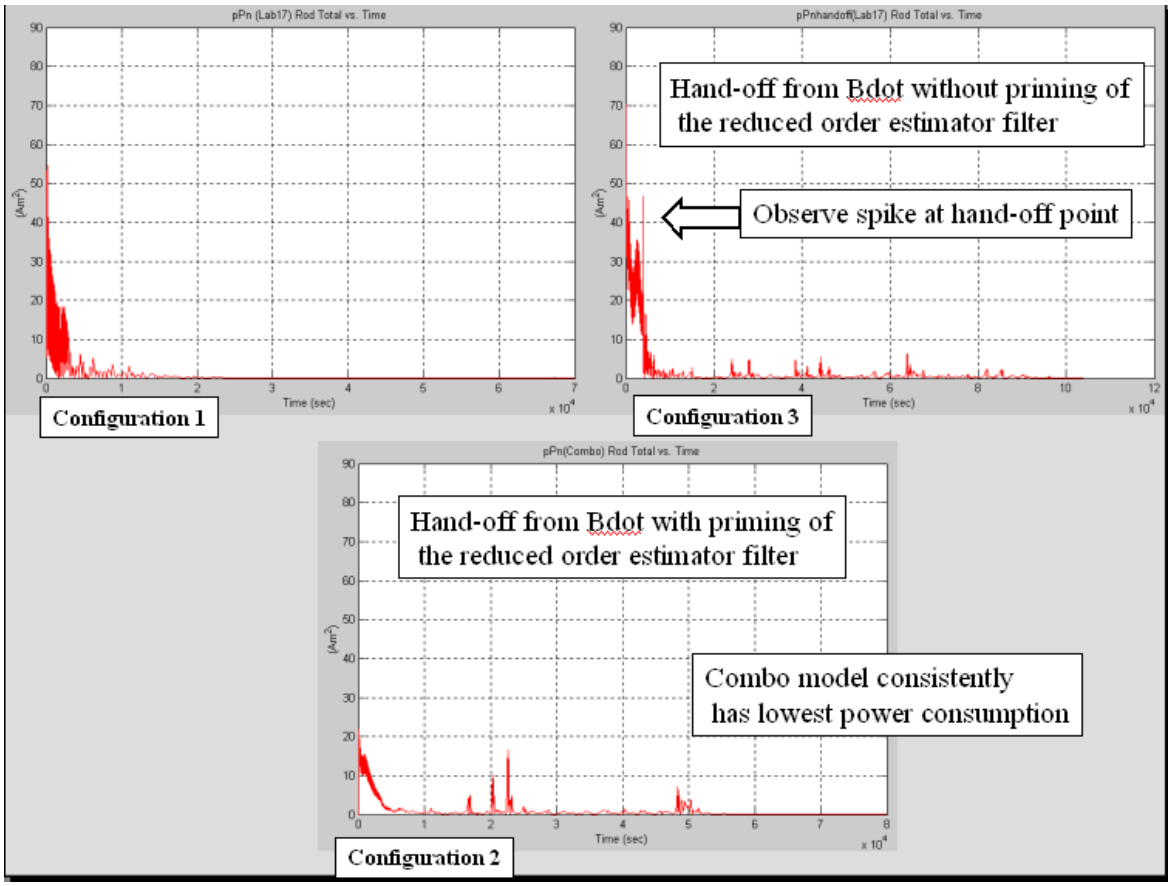

Figure 6.A.2. "pPn" Test Case.

B. RECOMMENDATIONS

The procedure for conducting an analysis of the handoff from 'nps.m,' which was the Bdot control law program to another program was cumbersome and time-consuming. If further analysis is deemed appropriate to determine whether a Bdot control law should be used for NPSAT1, a combined MATLAB program incorporating each of the smaller steps should be developed to more fully automate the data acquisition and analysis.

It appears, howerer, that there is clear evidence that the Bdot control law is a powerful and efficient method to arrest initial angular rates, regardless of their magnitude. Should it be decided to go forward with some implementation of a Bdot control law, it is recommended that the Bdot control law be a selectable control loop

within a combined program or system model. It is recommended that the hand-off that will occur from the Bdot control law loop should be done after a threshold combined angular rate is achieved, and not after a predetermined time interval. The time for the handoff models to begin steady state pointing accuracy acquisition after the initial arresting of the launch vehicle tip-off rates or a loss of attitude control can be minimized by handing off control as soon as the benefit of the Bdot control law ceases. The gains within the control loop that will receive a hand-off from the Bdot control law loop can be optimized for very low angular rates, since the Bdot control law would handle any initially higher angular rates.

All of the control methods analyzed appeared to be valid control methods to achieve three-axis attitude stabilization using only magnetic torquers and magnetometers for active control. The most efficient control method analyzed appeared to be configuration 2. This method was achieved by simply modifying the configuration 1 model to perform the Bdot hand-off based on achievement of a predetermined combined angular rate as opposed to a predetermined run time. This method also appears to eliminate the power spike that seemingly occurs when the angular rates have not been sufficiently arrested prior to hand-off.

LIST OF REFERENCES

1. McClelland, B., *NPSAT1 PDR Follow-up: B-dot Control Law*, pp. 1-7, Naval Center for Space Technology, 19 March, 2001.

2. Leonard, B., *NPSAT1 ACS Internal Review*, pp. 1-20, Naval Postgraduate School, Monterey, CA, 2001.

THIS PAGE INTENTIONALLY LEFT BLANK

APPENDIX A. PROGRAMS

A. NRL BDOT CONTROL LAW (NPS.M)

```
% Matlab simulation files  courtesy of Dr. Glenn Creamer, NRL Code 8231
% Main program (nps.m)

clear time w1 w2 w3 m1 m2 m3 b1 b2 b3
clear ugg1 ugg2 ugg3 umag1 umag2 umag3
clear yaw_angle pitch_angle roll_angle libration
global earth_radius satellite_inertia inv_satellite_inertia dt

% output storage parameters
count=0;
k=0;
store_count=3;

% conversion factors
d2r=pi/180;
sqrt2=sqrt(2);

% Earth parameters
earth_radius=6378.1363;
earth_rate=7.272205217e-05;
earth_gravity_constant=3.986004415e+05;

% orbit parameters
inc=35*d2r;              %*****  UPDATE DATA ITEM
ra=0*d2r;
altitude=600;            %*****  UPDATE DATA ITEM
radius=earth_radius+altitude;

% orbit rate and period
orbit_rate=sqrt(earth_gravity_constant/radius^3);
period=2*pi/orbit_rate;

% DCM relating perifocal PQW frame to Earth-centered ECI frame
eci_from_pqw=[cos(ra) -sin(ra)*cos(inc) sin(ra)*sin(inc)
              sin(ra) cos(ra)*cos(inc) -cos(ra)*sin(inc)
                0 sin(inc) cos(inc)];

% initial Greenwich sidereal time
greenwich_time=0*d2r;

% satellite inertia matrix and its inverse
satellite_inertia=[30 0 0      %*****  UPDATE DATA ITEM
```

```
                    0 31 0
                    0 0 2];
inv_satellite_inertia=inv(satellite_inertia);

% satellite torque coil capability
m_max=30;                              %*****  UPDATE DATA ITEM

dipole_off=input('Disable mag torquers? (1=Yes,0=No)');

% magnetic b-dot control feedback gains
k_mag=100000000;

% initial satellite state
true_anomaly=0*d2r;
%rates=[0.01;0.01;0.01];
rates= [-0.1; 0.1; 0.01];            % NPS PDR sim results used these rates
%rates= [ 0.0; 0.001083; 0.0];   % orbital rate @ 600km altitude on Y axis
%quats=[0;0;0;1];
quats= [0.62721137512625; 0.32650557562198;    % ran routine initquat.m
          0.62721137512625;  0.32650557562198];  %     to get this

state=[rates;quats];
bfield_xyz_old=[0;0;0];

% begin time loop
dt= 2;                                 %*****  UPDATE DATA ITEM
%t_final=3600*.5;
t_final= input('Input sim duration (seconds):   ');  % total sim time

for t=0:dt:t_final
  % DCM relating spacecraft XYZ frame to ECI frame
  xyz_from_eci=quats_to_dcm(quats);

  %   DCM relating rotating orbit frame
  %            (x along velocity, z along zenith) to PQW frame
  orb_from_pqw=[-sin(true_anomaly) cos(true_anomaly) 0
                              0                    0                1
                     cos(true_anomaly) sin(true_anomaly)  0];

  % DCM relating rotating orbit frame to ECI frame
  orb_from_eci=orb_from_pqw*eci_from_pqw';

  % DCM relating spacecraft XYZ frame to rotating orbit frame
  xyz_from_orb=xyz_from_eci*orb_from_eci';

  %  3(yaw)-2(pitch)-1(roll) Euler angle sequence describing
```

```
%  spacecraft frame relative to orbit frame
yaw=atan(xyz_from_orb(1,2)/xyz_from_orb(1,1));
pitch=asin(-xyz_from_orb(1,3));
roll=atan(xyz_from_orb(2,3)/xyz_from_orb(3,3));

% position of satellite in PQW frame
r_pqw=radius*[cos(true_anomaly);sin(true_anomaly);0];

% position of satellite in ECI frame
r_eci=eci_from_pqw*r_pqw;

% position of satellite in ECEF frame
ecef_from_eci=[cos(greenwich_time) sin(greenwich_time) 0
                    -sin(greenwich_time) cos(greenwich_time) 0
                                0                          0                    1];
r_ecef=ecef_from_eci*r_eci;

% gravity gradient torque
r_xyz=xyz_from_eci*r_eci;
r_xyz_unit=r_xyz/sqrt(dot(r_xyz,r_xyz));
u_gg=3*orbit_rate^2*skew(r_xyz_unit)*satellite_inertia*r_xyz_unit;

% angle of spacecraft z-axis relative to local zenith direction (libration angle)
theta=acos(r_xyz_unit(3));

% local magnetic field in ECEF frame
bfield_ecef=bfield(r_ecef,2);

      % local magnetic field in XYZ frame
bfield_xyz=xyz_from_eci*ecef_from_eci'*bfield_ecef;

% time derivative of local magnetic field in XYZ frame
bdot=(bfield_xyz-bfield_xyz_old)/dt;
bfield_xyz_old=bfield_xyz;

% commanded spacecraft dipole

if dipole_off==1,
  dipole(1:3)=0;
else

if t < 3600*30                  % may want to remove this time-out
  dipole(1)=-k_mag*bdot(1);
  dipole(2)=-k_mag*bdot(2);
  dipole(3)=-k_mag*bdot(3);
else
```

```
  dipole(1:3)=0;
end
end

% dipole saturation
for i=1:3
  if abs(dipole(i)) > m_max
    dipole(i)=m_max*sign(dipole(i));
  end
end

% corresponding magnetic torque
u_mag=cross(dipole,bfield_xyz)';

% store critical outputs before updating
count=count+1;
if count == store_count
  k=k+1;
  count=0;
  time(k)=t;
  w1(k)=rates(1);
  w2(k)=rates(2);
  w3(k)=rates(3);
  m1(k)=dipole(1);
  m2(k)=dipole(2);
  m3(k)=dipole(3);
  b1(k)=bfield_xyz(1);
  b2(k)=bfield_xyz(2);
  b3(k)=bfield_xyz(3);
  ugg1(k)=u_gg(1);
  ugg2(k)=u_gg(2);
  ugg3(k)=u_gg(3);
  umag1(k)=u_mag(1);
  umag2(k)=u_mag(2);
  umag3(k)=u_mag(3);
  yaw_angle(k)=yaw;
  pitch_angle(k)=pitch;
  roll_angle(k)=roll;
  libration(k)=theta;
 end

% ***** PROPAGATE ATTITUDE AND ORBIT STATES *****

% updated rotational state of satellite relative to ECI frame
u_ext=u_gg+u_mag;
state=satellite_dynamics(state,t,u_ext);
```

```
  rates=state(1:3);
  quats=state(4:7);
  quats=qnorm(quats);

  % updated greenwich time
  greenwich_time=greenwich_time+earth_rate*dt;

  % updated true anomaly
  true_anomaly=true_anomaly+orbit_rate*dt;
end

plotresult

function state=satellite_dynamics(state_old,t,u_ext)
global satellite_inertia inv_satellite_inertia dt

rates_temp=state_old(1:3);
q_temp=state_old(4:7);
rates_dot=inv_satellite_inertia*
          (u_ext-skew(rates_temp)*satellite_inertia*rates_temp);
qmatrix=[q_temp(4) -q_temp(3)  q_temp(2)  q_temp(1);
             q_temp(3)  q_temp(4) -q_temp(1)  q_temp(2);
            -q_temp(2)  q_temp(1)  q_temp(4)  q_temp(3);
            -q_temp(1) -q_temp(2) -q_temp(3) q_temp(4)];

quats_dot=0.5*qmatrix*[rates_temp;0];
f1=dt*[rates_dot;quats_dot];

rates_temp=state_old(1:3)+f1(1:3)/2;
q_temp=state_old(4:7)+f1(4:7)/2;
rates_dot=inv_satellite_inertia*
    (u_ext-skew(rates_temp)*satellite_inertia*rates_temp);
qmatrix=[q_temp(4) -q_temp(3)   q_temp(2) q_temp(1);
             q_temp(3)   q_temp(4) -q_temp(1) q_temp(2);
            -q_temp(2)   q_temp(1)  q_temp(4) q_temp(3);
            -q_temp(1)  -q_temp(2) -q_temp(3) q_temp(4)];

quats_dot=0.5*qmatrix*[rates_temp;0];
f2=dt*[rates_dot;quats_dot];

rates_temp=state_old(1:3)+f2(1:3)/2;
q_temp=state_old(4:7)+f2(4:7)/2;
rates_dot=inv_satellite_inertia*
              (u_ext-skew(rates_temp)*satellite_inertia*rates_temp);
qmatrix=[q_temp(4) -q_temp(3)  q_temp(2) q_temp(1);
             q_temp(3)  q_temp(4) -q_temp(1) q_temp(2);
```

```
            -q_temp(2)  q_temp(1)  q_temp(4) q_temp(3);
             -q_temp(1) -q_temp(2) -q_temp(3) q_temp(4)];
quats_dot=0.5*qmatrix*[rates_temp;0];
f3=dt*[rates_dot;quats_dot];

rates_temp=state_old(1:3)+f3(1:3);
q_temp=state_old(4:7)+f3(4:7);
rates_dot=inv_satellite_inertia*(u_ext-skew(rates_temp)*
                                    satellite_inertia*rates_temp);
qmatrix=[q_temp(4) -q_temp(3)   q_temp(2) q_temp(1);
             q_temp(3)   q_temp(4) -q_temp(1) q_temp(2);
            -q_temp(2)  q_temp(1)   q_temp(4) q_temp(3);
            -q_temp(1) -q_temp(2) -q_temp(3) q_temp(4)];
quats_dot=0.5*qmatrix*[rates_temp;0];
f4=dt*[rates_dot;quats_dot];

state=state_old+(f1+2*f2+2*f3+f4)/6;

function bfield_ecef=bfield(r_ecef,order)
global earth_radius

if order > 8
  order=8;
  'Desired order exceeds 8 --- model order reset to 8'
end

% current orbit position in Earth-fixed REF frame (up, south, east)
r=sqrt(r_ecef(1)^2+r_ecef(2)^2+r_ecef(3)^2);
delta=asin(r_ecef(3)/r);
cdelta=cos(delta);
sdelta=sin(delta);
theta=pi/2-delta;
stheta=sin(theta);
ctheta=cos(theta);
phi=acos(r_ecef(1)/(r*cdelta));
sphi=r_ecef(2)/(r*cdelta);
cphi=r_ecef(1)/(r*cdelta);
if sphi<0
  phi=-phi;
end

ref_from_ecef=[cdelta*cphi cdelta*sphi  sdelta
                    sdelta*cphi sdelta*sphi  -cdelta
                    -sphi             cphi            0];

% S factors
```

```
s0(1)=1;
s(1,1)=1;
if order > 1
  for n=2:order
    s0(n)=s0(n-1)*(2*n-1)/n;
    s(n,1)=s0(n)*sqrt(2*n/(n+1));
    for m=2:n
      s(n,m)=s(n,m-1)*sqrt((n-m+1)/(n+m));
    end
  end
end

% Legendre functions and their derivatives wrt theta
p0(1)=ctheta;
p(1,1)=stheta;
dp0(1)=-stheta;
dp(1,1)=ctheta;
if order > 1
  for n=2:order
    if n==2
      p0(2)=ctheta^2-1/3;
      dp0(2)=-2*stheta*ctheta;
    else
      p0(n)=p0(n-1)*ctheta-(n-1)^2/((2*n-1)*(2*n-3))*p0(n-2);
      dp0(n)=dp0(n-1)*ctheta-p0(n-1)*
                        stheta-(n-1)^2/((2*n-1)*(2*n-3))*dp0(n-2);
    end
    p(n,n)=p(n-1,n-1)*stheta;
    dp(n,n)=dp(n-1,n-1)*stheta+p(n-1,n-1)*ctheta;
    for m=1:(n-1)
      if m==(n-1)
        p(n,m)=p(n-1,m)*ctheta;
        dp(n,m)=dp(n-1,m)*ctheta-p(n-1,m)*stheta;
      else
        p(n,m)=p(n-1,m)*ctheta-((n-1)^2-m^2)/((2*n-1)*(2*n-3))*p(n-2,m);
        dp(n,m)=dp(n-1,m)*ctheta-p(n-1,m)*
                          stheta-((n-1)^2-m^2)/((2*n-1)*(2*n-3))*dp(n-2,m);
      end
    end
  end
end

% look-up table for Gaussian coefficients
coeffs=gauss_coeffs;
g=coeffs(1:44);
h=coeffs(45:88);
```

```
% first order, zeroth degree field components
br=2*(earth_radius/r)^3*s0(1)*g(1)*p0(1);
bt=-(earth_radius/r)^3*s0(1)*g(1)*dp0(1);
bp=0;

% higher orders, zeroth degree field components
if order > 1
  j=1;
  for n=2:order
    j=j+n;
    br=br+(n+1)*(earth_radius/r)^(n+2)*s0(n)*g(j)*p0(n);
    bt=bt-(earth_radius/r)^(n+2)*s0(n)*g(j)*dp0(n);
  end
end

% all orders, higher degree field components
j=1;
for n=1:order
  j=j+1;
  for m=1:n
       br=br+(n+1)*(earth_radius/r)^(n+2)*s(n,m)*(g(j)*
                                  cos(m*phi)+h(j)*sin(m*phi))*p(n,m);
    bt=bt-(earth_radius/r)^(n+2)*s(n,m)*(g(j)*cos(m*phi)+h(j)*
                                   sin(m*phi))*dp(n,m);
    bp=bp-(1/stheta)*(earth_radius/r)^(n+2)*m*
                         s(n,m)*(-g(j)*sin(m*phi)+h(j)*cos(m*phi))*p(n,m);
    j=j+1;
  end
end

% B-field in REF frame
bfield_ref=[br;bt;bp];
% B-field in ECEF frame
bfield_ecef=ref_from_ecef'*bfield_ref;

function coeffs=gauss_coeffs

g=[-29682 -1789 -2197 3074 1685 1329 -2268 1249 769 941 782 291 –421
      116 -210 352 237 -122 -167 -26 66 64 65 -172 2 17 -94 78 –67
        1 29 4 8 10 -2 24 4 -1 -9 -14 4 5 0 -7]*1.0e-09;
h=[0 5318 0 -2356 -425 0 -263 302 -406 0 262 -232 98 -301 0 44 157 –152
     -64 99 0 -16 77 67 -57 4 28 0 -77 -25 3 22 16 -23 -3 0 12 -20 7 –21
      12 10 -17 -10]*1.0e-09;

coeffs=[g h];
```

```
function qn=qnorm(q)

mag=sqrt(dot(q,q));
qn=[q(1);q(2);q(3);q(4)]/mag;

function dcm=quats_to_dcm(q)
dcm=[q(4)^2+q(1)^2-q(2)^2-q(3)^2        2*(q(1)*q(2)+q(3)*q(4))
                                        2*(q(1)*q(3)-q(2)*q(4));
      2*(q(1)*q(2)-q(3)*q(4))           q(4)^2-q(1)^2+q(2)^2-q(3)^2
                                        2*(q(2)*q(3)+q(1)*q(4));
      2*(q(1)*q(3)+q(2)*q(4))           2*(q(2)*q(3)-q(1)*q(4))
                                        q(4)^2-q(1)^2-q(2)^2+q(3)^2];

function skew_matrix=skew(vector)
skew_matrix=[0          -vector(3)    vector(2);
              vector(3)      0        -vector(1);
             -vector(2)  vector(1)          0];

%plotresult.m

r2d= 180/pi;

figure
subplot(311),plot(time,roll_angle*r2d),title('Attitude Error')
ylabel('Roll(deg)'),grid
subplot(312),plot(time,pitch_angle*r2d),ylabel('Pitch(deg)'),grid
subplot(313),plot(time,yaw_angle*r2d),ylabel('Yaw(deg)'),grid
xlabel('time(sec)')

figure
subplot(311),plot(time,w1*r2d),title('Body Rates'), ylabel('wx(deg/sec)'),grid
subplot(312),plot(time,w2*r2d),ylabel('wy(deg/sec)'),ylabel('wy(deg/sec)'),grid
subplot(313),plot(time,w3*r2d),ylabel('wz(deg/sec)'),ylabel('wz(deg/sec)'),grid
xlabel('time(sec)')
```

B. NPS (LAB15MOIDATA.M)

```
%  Lab 15MOIdata.m   written by Prof Barry Leonard

Ix=5;Iy=5.1;Iz=2;kax=.028;kay=.015;kaz=.032*4;   %  save for b8
                                                 %  steady state mag act
Ixy=0;Ixz=0;Iyz=0;
beta=0*pi/180;
Imoi=[Ix -Ixy -Ixz;-Ixy Iy -Iyz;-Ixz -Iyz Iz];
Iinv=inv(Imoi);
```

```
pho=-.1;tho=.1;pso=-.1;
phdo=-0.1;thdo=0.1;psdo=0.01;
  s1=sin(pho/2);s2=sin(tho/2);s3=sin(pso/2);
  c1=cos(pho/2);c2=cos(tho/2);c3=cos(pso/2);
  e1o=s1*c2*c3-c1*s2*s3;e2o=c1*s2*c3+s1*c2*s3;   %Wie pg.321
  e3o=c1*c2*s3-s1*s2*c3;e4o=c1*c2*c3+s1*s2*s3;
  S1=sin(pho);S2=sin(tho);S3=sin(pso);
  C1=cos(pho);C2=cos(tho);C3=cos(pso);

  wxo=phdo-psdo*S2-wo*S3*C2;
  wyo=thdo*C1+psdo*C2*S1-wo*(C3*C1+S3*S2*S1);
  wzo=psdo*C2*C1-thdo*S1-wo*(S3*S2*C1-C3*S1);
eo=[e1o e2o e3o e4o];qo=eo;
Ho=Imoi*[wxo wyo wzo]';

sat=30;
g1=0.75;g2=0.82;g3=0.43;   %  varies with inclination
                           %  (from torque ave. with high sat.)
ao=Ix-Iy+Iz;a1=Iy-Iz;a2=Ix-Iz;a3=Iy-Ix;

A=[0 0 0 1 0 0;0 0 0 0 1 0;0 0 0 0 0 1;
    -4*wo^2*a1/Ix 0 0 0 0 wo*ao/Ix;
      0 -3*wo^2*a2/Iy 0 0 0 0;
      0 0 -wo^2*a3/Iz -wo*ao/Iz 0 0];
B=Kme*[0 0 0;0 0 0;0 0 0;kax/Ix 0 0;0 kay/Iy 0;0 0 kaz/Iz];

Qx=110*eye(6); Ru=1*[.1 0 0;0 .095 0;0 0 .008];%for 5 5.1 2 with b8
[K,S,e]=lqr(A,B,Qx,Ru);

Aaa=A(1:3,1:3);Aab=A(1:3,4:6);Aba=A(4:6,1:3);Abb=A(4:6,4:6);
Ba=B(1:3,1:3);Bb=B(4:6,1:3);Ka=K(1:3,1:3);Kb=K(1:3,4:6);
Ga=G(1:3,1:3);Gb=G(4:6,1:3);
Lr=1*diag([1 .5 .6]);              %for 5 5.1 2 with b8
Lr=0.09*diag([1 .5 .6]);

Ar=Abb-Lr*Aab-(Bb-Lr*Ba)*Kb;
Br=Ar*Lr+Aba-Lr*Aaa-(Bb-Lr*Ba)*Ka;
Cr=-Kb;Dr=-Ka-Kb*Lr;
Kp=Ka; Kd=Kb;

  s1=sin(pho/2);s2=sin(tho/2);s3=sin(pso/2);
  c1=cos(pho/2);c2=cos(tho/2);c3=cos(pso/2);
  e1o=s1*c2*c3-c1*s2*s3;e2o=c1*s2*c3+s1*c2*s3;%Wie pg.321
  e3o=c1*c2*s3-s1*s2*c3;e4o=c1*c2*c3+s1*s2*s3;
  S1=sin(pho);S2=sin(tho);S3=sin(pso);
```

```
  C1=cos(pho);C2=cos(tho);C3=cos(pso);

  wxo=phdo-psdo*S2-wo*S3*C2;
  wyo=thdo*C1+psdo*C2*S1-wo*(C3*C1+S3*S2*S1);
  wzo=psdo*C2*C1-thdo*S1-wo*(S3*S2*C1-C3*S1);
eo=[e1o e2o e3o e4o];qo=eo;
Ho=Imoi*[wxo wyo wzo]';
```

C. NPS (LAB16DATA.M)

```
%Lab16Data                written by Prof Barry Leonard

clear

Re=6371.2e3;mu=398601.2e9;we=7.2921e-5;epsilon=11.398*pi/180;
Altitude=[450 500 550 600 650 700 750 800]*1e3;  %look up table data for aero
Density=[36.1 18 9.25 4.89 2.64 1.47 .837 .439]*1e-13; %  look up table
                                                        %  data for aero
h=600e3;                  % spacecraft altitude (km)
incln=(35)*pi/180;        % inclination (radians)
beta=0*pi/180;            % angle between outward normal vector and sun vector
nuo=-115*pi/180;
alphao=0*pi/180;
Lm=-70.454;Lgo=0;uo=(Lgo+Lm+90)*pi/180;
wn=0;wo=sqrt(mu/(Re+h)^3);
V=wo*(Re+h);rho=asin(Re/(h+Re));Kme=7.9638e15/(Re+h)^3;
Cd=2.5;Kaero=0.5*Cd*V^2;                % Cd = drag coefficient
psun=4.5e-6;Psolar=2*psun;
Area=[0.2674 0.2674 .1927]; dL=[.002 .002 .008];

Ixy=0;Ixz=0;Iyz=0;
Ix=5;Iy=5.1;Iz=2;kax=1;kay=0.1*kax;kaz=kax*1;
Imoi=[Ix -Ixy -Ixz;       % The Inertia tensor or Inertia Matrix
      -Ixy Iy -Iyz;
      -Ixz -Iyz Iz];
Iinv=inv(Imoi);                         % Inertia Matrix Inverse

sat=30;
g1=0.75;g2=0.82;g3=0.43;   %   varies with inclination
                           %   (from torque ave. with high sat.)

ao=Ix-Iy+Iz;a1=Iy-Iz;a2=Ix-Iz;a3=Iy-Ix;
A=[0 0 0 1 0 0;0 0 0 0 1 0;0 0 0 0 0 1;-4*wo^2*a1/Ix 0 0 0 0 wo*ao/Ix;...
      0 -3*wo^2*a2/Iy 0 0 0 0;0 0 -wo^2*a3/Iz -wo*ao/Iz 0 0];
B=Kme*[0 0 0;0 0 0;0 0 0;kax/Ix 0 0;0 kay/Iy 0;0 0 kaz/Iz];
G=[0 0 0;0 0 0;0 0 0;1/Ix 0 0;0 1/Iy 0;0 0 1/Iz];
Qx=10*eye(6); Ru=[.1 0 0;0 .1 0;0 0 .01];
```

```
[K,S,e]=lqr(A,B,Qx,Ru);

Aaa=A(1:3,1:3);Aab=A(1:3,4:6);Aba=A(4:6,1:3);Abb=A(4:6,4:6);
Ba=B(1:3,1:3);Bb=B(4:6,1:3);Ka=K(1:3,1:3);Kb=K(1:3,4:6);
Ga=G(1:3,1:3);Gb=G(4:6,1:3);
Lr=0.2*eye(3);Ar=Abb-Lr*Aab-(Bb-Lr*Ba)*Kb;
Br=Ar*Lr+Aba-Lr*Aaa-(Bb-Lr*Ba)*Ka;
Cr=-Kb;Dr=-Ka-Kb*Lr;
Kp=Ka; Kd=Kb;
pho=-.1;tho=.1;pso=-.01;                % Euler angles
phdo=.1;thdo=-0.01;psdo=0.01;           % Euler rates

 s1=sin(pho/2);s2=sin(tho/2);s3=sin(pso/2);
 c1=cos(pho/2);c2=cos(tho/2);c3=cos(pso/2);

 e1o=s1*c2*c3-c1*s2*s3;e2o=c1*s2*c3+s1*c2*s3;    % Wie pg.321
 e3o=c1*c2*s3-s1*s2*c3;e4o=c1*c2*c3+s1*s2*s3;

 S1=sin(pho);S2=sin(tho);S3=sin(pso);
 C1=cos(pho);C2=cos(tho);C3=cos(pso);

 wxo=phdo-psdo*S2-wo*S3*C2;                          % wx
 wyo=thdo*C1+psdo*C2*S1-wo*(C3*C1+S3*S2*S1);         % wy
 wzo=psdo*C2*C1-thdo*S1-wo*(S3*S2*C1-C3*S1);         % wz

eo=[e1o e2o e3o e4o];
qo=eo;
Ho=Imoi*[wxo wyo wzo]';             % [Ho] = Angular Momentum [3x1]

%SphericalHarmMag3

r=Re+h;a=Re;                        % r = radius from sat to center of earth
                                    % Re = a = Earth radius = 6371.2e3 km
kme=Kme*1e9;                        %conversion from nT.m^3 to T.m^3
dth=5;tmin=0;tmax=180;Jmax=(tmax-tmin)/dth;
dphi=10;phimin=-180;phimax=180;Imax=(phimax-phimin)/dphi;

ggg=[-30186 -2036 0 0 0 0 0 0 0;-1898 2997 1551 0 0 0 0 0 0;...
      1299 -2144 1296 805 0 0 0 0 0;951 807 462 -393 235 0 0 0 0;...
     -204 368 275 -20 -161 -38 0 0 0;46 57 15 -210 -1 -8 -114 0 0;...
      66 -57 -7 7 -22 -9 11 -8 0;11 13 3 -12 -4 6 -2 9 1];

hhh=[0 5735 0 0 0 0 0 0 0;0 -2124 -37 0 0 0 0 0 0;...
      0 -361 249 -253 0 0 0 0 0;0 148 -264 37 -307 0 0 0 0;...
      0 39 142 -147 -99 74 0 0 0;0 -23 102 88 -43 -9 -4 0 0;...
      0 -68 -24 -4 11 27 -17 -14 0;0 4 -15 2 -19 1 18 -6 -19];
```

```
gg=[-29615 -1728 0 0 0 0 0 0 0;-2267 3072 1672 0 0 0 0 0 0;...
       1341 -2290 1253 715 0 0 0 0 0;935 787 251 -405 110 0 0 0 0;...
       -217 351 222 -131 -169 -12 0 0 0;72 68 74 -161 -5 17 -91 0 0;...
        79 -74 0 33 9 7 8 -2 0;25 6 -9 -8 -17 9 7 -8 -7];

hh=[0 5186 0 0 0 0 0 0 0;0 -2478 -458 0 0 0 0 0 0;...
       0 -227 296 -492 0 0 0 0 0;0 272 -232 119 -304 0 0 0 0;...
       0 44 172 -134 -40 107 0 0 0;0 -17 64 65 -61 1 44 0 0;...
       0 -65 -24 6 24 15 -25 -6 0;0 12 -22 8 -21 15 9 -16 -3];

for J=1:Jmax+1;
 t=(J-1)*dth*pi/180;  th(J)=(J-1)*dth;
 Ct=cos(t);St=sin(t);

for I=1:Imax+1;
 p=(phimin+(I-1)*dphi)*pi/180;  phi(I)=phimin+(I-1)*dphi;
 Cp=cos(p);Sp=sin(p);

 for i=1:8
  for j=1:i+1
   Km(i,j)=((i-1)^2-(j-1)^2)/(2*i-1)/(2*i-3);
   if i==1; Km=0;end
  end
 end

Km=tril(Km,1);
 for i=1:8
  for j=1:i+1
   P(1,1)=Ct;

   if i==1 & j==2;P(i,j)=St*1;end
   if i>1 & j==i+1;P(i,j)=St*P(i-1,j-1);end
   if i==2;Pk=1;end;
   if i>2;Pk=P(i-2,j);end
   if i>1 & j~=i+1;P(i,j)=Ct*P(i-1,j)-Km(i,j)*Pk;end
  end
 end

P=tril(P,1);
 for i=1:8
  for j=1:i+1
   dp(1,1)=-St;
   if i==1 & j==2;dp(i,j)=St*0+Ct*1;end
   if i>1 & j==i+1;dp(i,j)=St*dp(i-1,j-1)+Ct*P(i-1,j-1);end
   if i==2;dpk=0;end;
```

```
    if i>2;dpk=dp(i-2,j);end
    if i>1 & j~=i+1;dp(i,j)=Ct*dp(i-1,j)-St*P(i-1,j)-Km(i,j)*dpk;end
   end
  end

 dp=tril(dp,1);
 for i=1:8
  for j=1:9
    dm=0;if j==2;dm=1;end
    if j==1 & i==1; S=1;end
    if j==1 & i~=1;S(i,j)=S(i-1,j)*(2*i-1)/i;end
    if j>1;S(i,j)=S(i,j-1)*sqrt((i-(j-1)+1)*(dm+1)/(i+(j-1)));end
  end
 end

S=tril(S,1);
G=S.*gg;
H=S.*hh;
 for i=1:8
  j=1:i+1;m=j-1;
  F(i,j)=G(i,j).*cos(m*p)+H(i,j).*sin(m*p);
 end

 for i=1:8
  j=1:i+1;m=j-1;
  f(i,j)=m.*(-G(i,j).*sin(m*p)+H(i,j).*cos(m*p));
 end

 if St==0; St=0.001; ;end
 for i=1:8
  aa1(i)=(i+1)*(a/r)^(i+2);
  aa2(i)=-aa1(i)/(i+1);
  aa3(i)=aa2(i)/St;
 end

 FPS=sum((F.*P)')' ;  B1=aa1'.*FPS;  Br8=sum(B1);  Br1=B1(1);
 FdpS=sum((F.*dp)')';  B2=aa2'.*FdpS;  Bt8=sum(B2);  Bt2=B2(1);
 fPS=sum((f.*P)')' ;  B3=aa3'.*fPS;  Bp8=sum(B3);  Bp3=B3(1);

 br8(I,J)=Br8/kme;  br1(I,J)=Br1/kme;
 bt8(I,J)=Bt8/kme;  bt1(I,J)=Bt2/kme;
 bp8(I,J)=Bp8/kme;  bp1(I,J)=Bp3/kme;
 b1(I,J)=(Br1.^2+Bt2.^2+Bp3.^2).^0.5/kme;
 b8(I,J)=(Br8.^2+Bt8.^2+Bp8.^2).^0.5/kme;
end
end
```

```
Inclination=[0.01 10 20 30 40 50 60 70 80 90 100 110 120]*pi/180;
gx=[.967 .955 .922 .876 .826 .78 .739 .709 .691 .686 .691 .709 .739];
gy=[0.0001 .0678 .256 .46 .632 .762 .857 .923 .965 .981 .965 .923 .857];
gz=[.804 .781 .711 .614 .522 .446 .39 .353 .335 .333 .335 .353 .39];
```

D. NPS (LAB17.MDL)

See Figure A1.

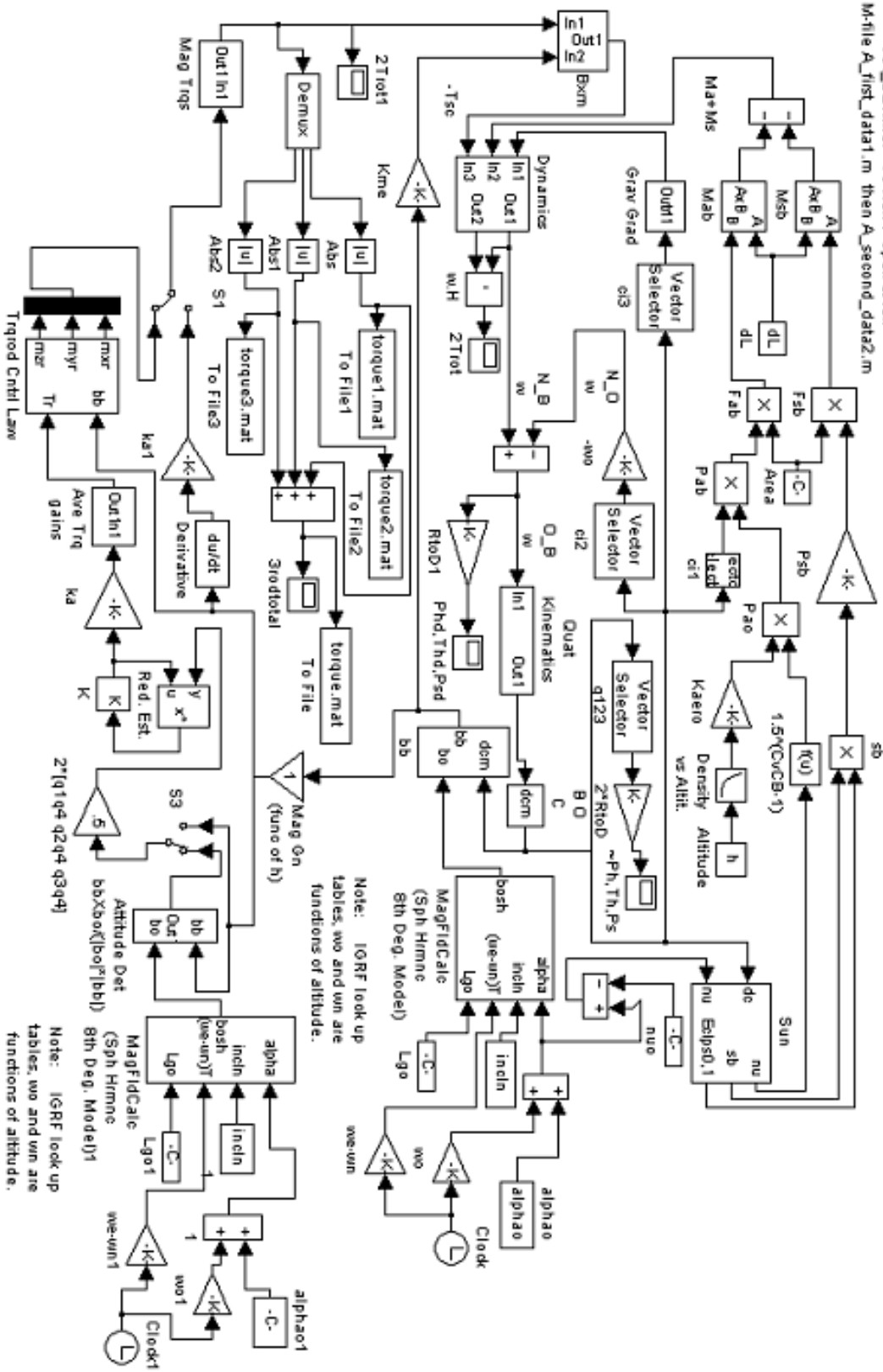

Figure A1. Lab17.mdl.

E. NPS (NPSAT1ACSDATA.M)

```
%NPSAT1ACSData          written by Prof Barry Leonard

clear
tic
Re=6371.2e3;mu=398601.2e9;we=7.2921e-5;%earth radius, gravity and spin rate
Altitude=[450 500 550 600 650 700 750 800]*1e3;%look up table data for aero
Density=[36.1 18 9.25 4.89 2.64 1.47 .837 .439]*1e-13;%density table data

h=600e3;incln=(35)*pi/180;beta=15*pi/180;%altitude,inclination, solar angle
nuo=-115*pi/180;alphao=0*pi/180;%initial subsolar point and true anomaly
Lgo=0;%initial position of Greenwich Meridian WRT RAAN
kpre=0; %nodal precession constant assumed to be zero here
wn=kpre*(Re/(Re+h))^3.5*cos(incln);%nodal precession (zero eccentricity)
wo=sqrt(mu/(Re+h)^3);V=wo*(Re+h); %orbital angular and linear velocity
rho=asin(Re/(h+Re)); %earth angular radius

Cd=2.5;psun=4.5e-6;%drag coefficient and solar pressure constant~N/m^2
Kaero=0.5*Cd*V^2;Psolar=2*psun; % constants for aero and solar torque calc.

Area=[0.2674 0.2674 .1927]; %projected area~m^2 in body x,y,z directions
dL=[.002 .002 .008]; %predicted (cp-cm)~m  in body x,y,z directions

Ix=5;Iy=5.1;Iz=2;Ixy=0;Ixz=0;Iyz=0; % moments of inertia (MOI)~kg.m^2
Imoi=[Ix -Ixy -Ixz;-Ixy Iy -Iyz;-Ixz -Iyz Iz]; %MOI matrix
Iinv=inv(Imoi); %MOI matrix inverse
ao=Ix-Iy+Iz;a1=Iy-Iz;a2=Ix-Iz;a3=Iy-Ix;%MOI combination constants

pho=-.1;tho=.1;pso=-0.1; %initial Euler angles (phi,theta,psi) ~r
phdo=-0.1;thdo=0.1;psdo=0.01;  % initial Euler angle rates ~r/s

%calculation of initial quaternion (qo) and angular momentum (Ho):
  s1=sin(pho/2);s2=sin(tho/2);s3=sin(pso/2);c1=cos(pho/2);c2=cos(tho/2);
  c3=cos(pso/2); q1o=s1*c2*c3-c1*s2*s3;q2o=c1*s2*c3+s1*c2*s3;%Wie pg.321
  q3o=c1*c2*s3-s1*s2*c3;q4o=c1*c2*c3+s1*s2*s3;
  S1=sin(pho);S2=sin(tho);S3=sin(pso);C1=cos(pho);C2=cos(tho);C3=cos(pso);
  wxo=phdo-psdo*S2-wo*S3*C2;
  wyo=thdo*C1+psdo*C2*S1-wo*(C3*C1+S3*S2*S1);
  wzo=psdo*C2*C1-thdo*S1-wo*(S3*S2*C1-C3*S1);
qo=[q1o q2o q3o q4o];
Ho=Imoi*[wxo wyo wzo]';

%Calculation of spherical harmonic magnetic field model (Wertz pp779-783)
r=Re+h;a=Re; %definitions to match Wertz pg 780
```

```
% IGRF Epoch 2000 Guassian coefficients ~ n.T   :
gg=[-29615 -1728 0 0 0 0 0 0 0;-2267 3072 1672 0 0 0 0 0 0;...
    1341 -2290 1253 715 0 0 0 0 0;935 787 251 -405 110 0 0 0 0;...
    -217 351 222 -131 -169 -12 0 0 0;72 68 74 -161 -5 17 -91 0 0;...
    79 -74 0 33 9 7 8 -2 0;25 6 -9 -8 -17 9 7 -8 -7];
hh=[0 5186 0 0 0 0 0 0 0;0 -2478 -458 0 0 0 0 0 0;...
     0 -227 296 -492 0 0 0 0 0;0 272 -232 119 -304 0 0 0 0;...
     0 44 172 -134 -40 107 0 0 0;0 -17 64 65 -61 1 44 0 0;...
     0 -65 -24 6 24 15 -25 -6 0;0 12 -22 8 -21 15 9 -16 -3];
Kme=(a/r)^3*sqrt(gg(1,1)^2+gg(1,2)^2+hh(1,2)^2)*1e-9;%dipole strength~Tesla

ka=[.02863  .01534  .1309];sat=30;%actuator gains and saturation
%ka=[.03  .015  .13];
%Calc of state space A,B,G matrices follows (xdot=Ax+Bu+Gw,w=disturbance)
A=[0 0 0 1 0 0;0 0 0 0 1 0;0 0 0 0 0 1;-4*wo^2*a1/Ix 0 0 0 0 wo*ao/Ix;...
  0 -3*wo^2*a2/Iy 0 0 0 0;0 0 -wo^2*a3/Iz -wo*ao/Iz 0 0];
B=Kme*[0 0 0;0 0 0;0 0 0;ka(1)/Ix 0 0;0 ka(2)/Iy 0;0 0 ka(3)/Iz];
G=[0 0 0;0 0 0;0 0 0;1/Ix 0 0;0 1/Iy 0;0 0 1/Iz];

Qx=110*eye(6); Ru=1*[.1 0 0;0 .095 0;0 0 .008]; %LQR weighting matrices
[K,S,e]=lqr(A,B,Qx,Ru); %LQR gain calculation

%partitioning of A,B,G matrices required for reduced order estimator:
Aaa=A(1:3,1:3);Aab=A(1:3,4:6);Aba=A(4:6,1:3);Abb=A(4:6,4:6);
Ba=B(1:3,1:3);Bb=B(4:6,1:3);Ka=K(1:3,1:3);Kb=K(1:3,4:6);
Ga=G(1:3,1:3);Gb=G(4:6,1:3);
Lr=0.09*diag([1 .5 .6]); %Estimator gain found by simulation

del_t=5;tmin=0;tmax=180;%colatitude increment, min, max (theta)
Jmax=(tmax-tmin)/del_t; % max value of J index
del_p=10;pmin=-180;pmax=180; %longitude increment, min, max (phi)
Imax=(pmax-pmin)/del_p;  %max value of I index

for J=1:Jmax+1;
  t=(J-1)*del_t*pi/180;Ct=cos(t);St=sin(t); %sine & cosine of theta
  th(J)=(J-1)*del_t; %theta vector (look up tables Mag Fld Model)
for I=1:Imax+1;
  p=(pmin+(I-1)*del_p)*pi/180;Cp=cos(p);Sp=sin(p);%sin & cos phi
  phi(I)=pmin+(I-1)*del_p;%phi vector (look up tables Mag Fld Model)
 % Calculation of Legendre function constant (Km) follows
  for i=1:8
    for j=1:i+1
      Km(i,j)=((i-1)^2-(j-1)^2)/(2*i-1)/(2*i-3);
      if i==1; Km=0;end
    end
```

```
 end
Km=tril(Km,1);

%Calculation of Legendre function (P) follows
 for i=1:8
   for j=1:i+1
     P(1,1)=Ct;
     if i==1 & j==2;P(i,j)=St*1;end
     if i>1 & j==i+1;P(i,j)=St*P(i-1,j-1);end

     if i==2;Pk=1;end;
     if i>2;Pk=P(i-2,j);end
     if i>1 & j~=i+1;P(i,j)=Ct*P(i-1,j)-Km(i,j)*Pk;end
   end
 end
P=tril(P,1);

% Calculation of partial of Legendre function WRT theta (dp) follows
 for i=1:8
   for j=1:i+1
     dp(1,1)=-St;
     if i==1 & j==2;dp(i,j)=St*0+Ct*1;end
     if i>1 & j==i+1;dp(i,j)=St*dp(i-1,j-1)+Ct*P(i-1,j-1);end
     if i==2;dpk=0;end;
     if i>2;dpk=dp(i-2,j);end
     if i>1 & j~=i+1;dp(i,j)=Ct*dp(i-1,j)-St*P(i-1,j)-Km(i,j)*dpk;end
    end
  end
 dp=tril(dp,1);

 % Calculation of Gausian coefficient norm. factor (S) follows
 for i=1:8
   for j=1:9
     dm=0;if j==2;dm=1;end
     if j==1 & i==1; S=1;end
     if j==1 & i~=1;S(i,j)=S(i-1,j)*(2*i-1)/i;end
     if j>1;S(i,j)=S(i,j-1)*sqrt((i-(j-1)+1)*(dm+1)/(i+(j-1)));end
   end
 end
S=tril(S,1);

%Calculation of normalized Gaussian coefficients ~ n.T  :
Gg=S.*gg; Hh=S.*hh;

 for i=1:8
   j=1:i+1;m=j-1;
```

```
  F(i,j)=Gg(i,j).*cos(m*p)+Hh(i,j).*sin(m*p); %definition
 end
 for i=1:8
  j=1:i+1;m=j-1;
  f(i,j)=m.*(-Gg(i,j).*sin(m*p)+Hh(i,j).*cos(m*p));% definition
 end

 if St==0; St=0.001; ;end %singularity avoidance in following loop
 %Calculation of altitude dependent coefficients follows
 for i=1:8
  aa1(i)=(i+1)*(a/r)^(i+2); aa2(i)=-aa1(i)/(i+1); aa3(i)=aa2(i)/St;
 end

%Calculation of radial,theta and phi magnetic field components ~Tesla
FPS=sum((F.*P)')'  ;   B1=aa1'.*FPS;   Br8=sum(B1)*1e-9;
FdpS=sum((F.*dp)')';   B2=aa2'.*FdpS;  Bt8=sum(B2)*1e-9;
fPS=sum((f.*P)')'  ;   B3=aa3'.*fPS;   Bp8=sum(B3)*1e-9;

%Calculation of normalized field components (input to lookup tables)
br8(I,J)=Br8/Kme;
bt8(I,J)=Bt8/Kme;
bp8(I,J)=Bp8/Kme;

%Calculation of field vector normalized magnitude:
b8(I,J)=(Br8.^2+Bt8.^2+Bp8.^2).^0.5/Kme;

end  %end I loop
end  %end J loop

% Table inputs for average actuator gains vs inclination follows:
Inclination=[0.01 10 20 30 40 50 60 70 80 90 100 110 120]*pi/180;
gx=[.967 .955 .922 .876 .826 .78 .739 .709 .691 .686 .691 .709 .739];
gy=[0.0001 .0678 .256 .46 .632 .762 .857 .923 .965 .981 .965 .923 .857];
gz=[.804 .781 .711 .614 .522 .446 .39 .353 .335 .333 .335 .353 .39];
toc
```

F. NPS (NPSATACSINTRVW.MDL)

See Figure A2.

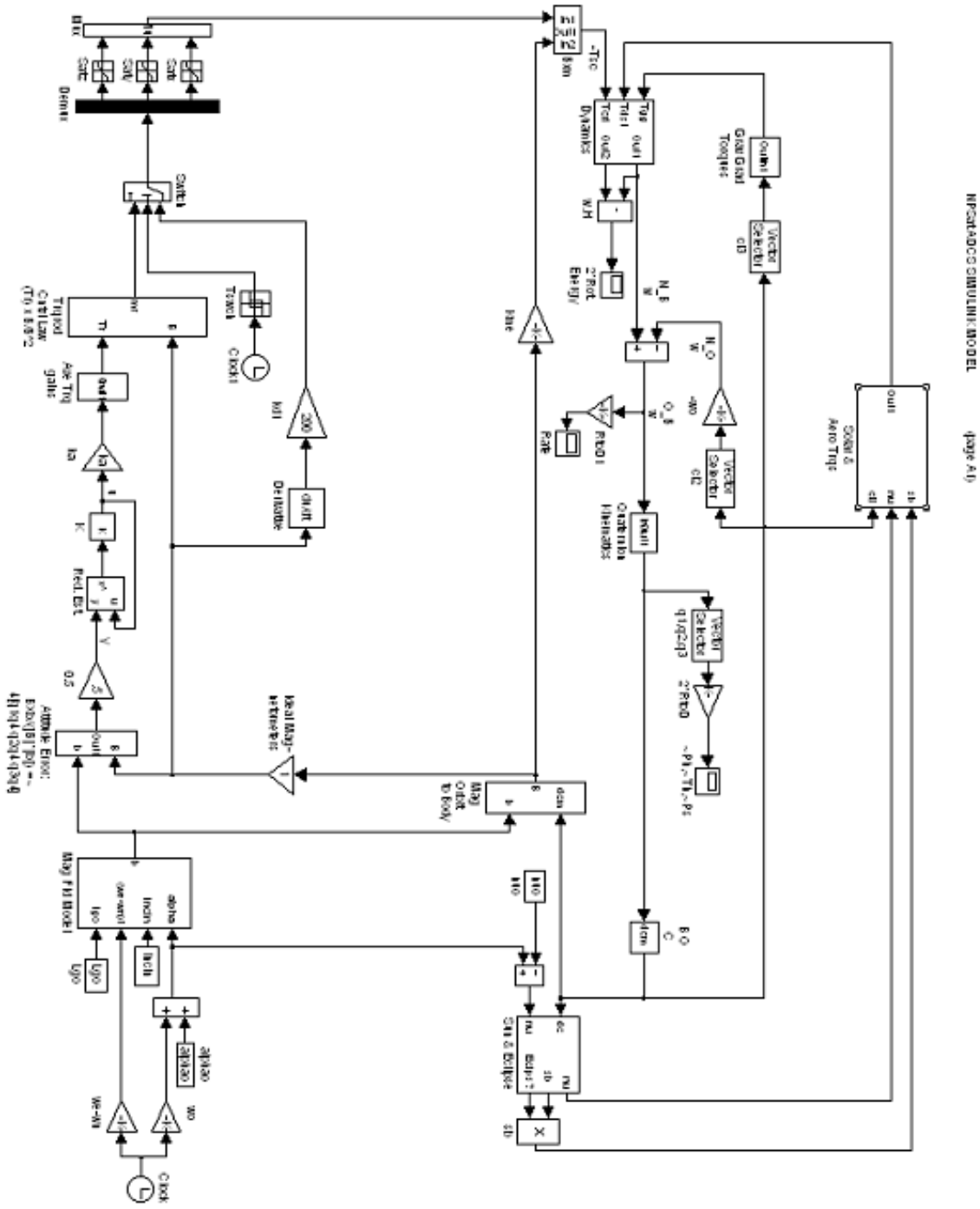

Figure A2. NPSATACSIntRvw.mdl.

G. NPS (GRABDATASET.M)

```
%grabdataset.m      written by Lt Todd Zirkle for manipulating data captured from
%                   a SIMULINK run during analysis for NPSSAT1 NPS Monterey
%
%   This program measures and plots the instantaneous and cumulative total of
%    commanded rod torques and the time required to achieve a 3-axis steady
%    state pointing accuracy of less than 10 degrees.
%   This program also solves and plots the area under the instantaneous rod
%    total curve to produce an energy index for comparison with other runs
%    using different initial conditions.
%
%   Eleven variables are recorded in a matrix as a '.mat file' from
%    a simulation using one of two modified SIMULINK simulations originally
%    written by Prof Barry Leonard.
%   'Lab17.mdl' 05/18/01 and 'NPSATACSIntRvw.mdl' 07/16/01
%
%  This program picks off some of the desired variables.
%   The desired torque rod outputs in Am^2 are recorded as
%   'rod1', 'rod2', and 'rod3'
%   The total commanded torque from the three rods combined is 'rodtot'
%
%    After loading the desired '.mat' file containing the data matrix
%    into the MATLAB workspace, the matrix size is used to edit this
%    program's array sizes.

clear ans xacksis DataArray rodone rod1 rod2 rod3 rodtot
clear rodtwo rodthree rodtotal
clear PhdT ThdT PsdT PhT ThT PsT
clear Phd Thd Psd Ph Th Ps lasttime
clear Timegap RulerTime miniarea areatot areaCumPlot

DataArray = NPn7600';              %  matrix name from workspace containing data
xacksis = DataArray(1:11370,1); %  array size must be updated to
                                   %  match matrix size
xaxiss=xacksis';
rod1= DataArray(1:11370,2); rodone = rod1';
rod2= DataArray(1:11370,3); rodtwo = rod2';
rod3= DataArray(1:11370,4); rodthree = rod3';
rodtot= DataArray(1:11370,5); rodtotal = rodtot';
PhdT= DataArray(1:11370,6); Phd = PhdT';
ThdT= DataArray(1:11370,7); Thd = ThdT';
PsdT= DataArray(1:11370,8); Psd = PsdT';
PhT= DataArray(1:11370,9); Ph = PhT';
ThT= DataArray(1:11370,10); Th = ThT';
PsT= DataArray(1:11370,11); Ps = PsT';
```

```
areatot=0;          % essentially starts the areatot at the origin which is zero

for k = 1:11369  % will be one less than the size of the matrix dataset
  Timegap(k)= xacksis(k+1)-xacksis(k); % delta t for integrating area under curve
  holdtotal=areatot;
  miniarea(k)=rodtot(k)*Timegap(k);  %   represents area under curve
                                     %   from (t+n) to (t+n+timegap)
  areatot=holdtotal+miniarea(k);   %   cumulative area up til this point
  areaCumPlot(k)=areatot;            % records cumulative area at each time interval
end

areaCumPlot(11370)=areaCumPlot(11369);   %  the last delta t is reused for
                                         %  the last miniarea calculation
lasttime=xacksis(11370);   % last time of simulation recorded for plot label use

 figure                                % plots rod total commanded torques vs. time
 plot(xaxiss,rodtot,'r'),title('NPn (Lab17) Rod Total vs. Time'),
         ylabel('(Am^2)'),grid
         xlabel('Time (sec)')

 figure           % plots cum area under curve vs. time [energy index (Am^2 * sec)]
 plot(xaxiss,areaCumPlot,'r'),
title(['NPn(Lab17) area Rod Total ',num2str(areatot),' in ',num2str(lasttime),' sec'])
 ylabel(' '),grid
 xlabel('Time (sec)')
```

H. NPS (CREATE_VARIABLES.M)

```
%create variables      written by Lt Todd Zirkle for capturing data from
%                      NRL program written by Dr. Glenn Creamer, NRL Code 8231
%                         (nps.m)
%  This program captures 11 variables for analysis and plotting purposes
%    Before running this program, run 'nps.m' after ensuring the initial conditions
%    have been set to the desired values.
%  This program will capture the variables by assigning them
%    to new variable names.
%  After renaming the 11 variables, the program clears all 'nps.m' variables.
%  The resulting data is saved by saving the MATLAB workspace
%    to a data folder.
%  It is recommended that the '.mat' file's name in some way reflects
%    the initial conditions used to produce the data, since the only other
%    way to ascertain the initial conditions is to pick out the first row of
%    data from the six variables assigned to rates and angles.
%  EXAMPLE FILE NAME:  'bdot_pNp_testcase1.mat'
%   In this example, pNp stands for
%                'phidot' =.01 rad/s, 'thdot' =-.1 rad/s, 'psidot' =.01 rad/s
```

```
clear brod1 brod2 brod3 brodtot bww1 bww2 bww3 bpitt brole byeaw

brod1=[m1];          % command to torque rod 1 (phi)   ((from 0 to 30 Am^2))
brod2=[m2];          % command to torque rod 2 (theta) ((from 0 to 30 Am^2))
brod3=[m3];          % command to torque rod 3 (psi)    ((from 0 to 30 Am^2))
brodtot=[rod3tot];   % rod3tot = the sum of  [abs(rod1)+abs(rod2)+abs(rod3)]
bww1=[w1];
bww2=[w2];
bww3=[w3];
bpitt=[pitch_angle];
brole=[roll_angle];
byeaw=[yaw_angle];
btime=[time];

clear yaw xyz_from_orb xyz_from_eci u_ext u_gg u_mag
clear watt_hrs_total t t_final theta true_anomaly
clear store_count state sqrt2 satellite_inertia inv_satellite_inertia
clear ra radius rates roll r_eci r_pqw r_xyz r_xyz_unit
clear pitch quats r2d r_ecef orb_from_eci orb_from_pqw
clear orbit_rate period inv_satellite k k_mag m_max
clear eci_from_pqw greenwich_time i inc earth_gravity_constant
clear earth_radius earth_rate ecef_from eci d2r dipole
clear dipole_off dt count bdot bfield_ecef bfield_xyz
clear bfield_xyz_old ans ampsec_total altitude
clear ecef_from_eci
clear time w1 w2 w3 w4 m1 m2 m3 b1 b2 b3
clear rate_goal rg time_counter pwr1 pwr2 pwr3 pwr4  pwrSS
clear pwr6 pwr7 pwr8 percent_pwr rod_current rod3tot
clear pwr_u ugg1 ugg2 ugg3 umag1 umag2 umag3
clear yaw_angle pitch_angle roll_angle libration
```

I. NPS (NPSSAT1TESTCASE.M)

```
%NPSsat1 Test case data manipulator
%
%   Written by Lt Todd Zirkle for manipulating data captured from
%      MATLAB programs and SIMULINK runs during analysis
%      for NPSSAT1  NPS Monterey
%
%    This program computes and plots the results of combining
%     two different simulations' data.  A Bdot control law simulation is
%     used to arrest rotation rates up to a predetermined rate goal, then the
%     final states of that simulation are used for the initial conditions of the
%     second program, which further arrests the rotation rates and then
%     achieves a predetermined three-axis pointing accuracy.
```

```
%
%  Uses an NRL program written by Dr. Glenn Creamer, NRL  (nps.m)
%     Uses two modified SIMULINK simulations originally written
%     by Prof Barry Leonard.  'Lab17.mdl'                  05/18/01
%                             'NPSATACSIntRvw.mdl'  07/16/01
%
%   This program essentially combines two other programs written by Lt Zirkle:
%     'grabdataset.m' and 'create_variables.m'
%     As the original programs gathered rodtotal and energy index vs. time plots
%     for the Dr. Creamer program and the Prof Leonard programs, this program
%     does the same for the case of both programs being run in a handoff fashion
%     as described above.
%
%   This program captures torque rod total and time variables for analysis and
%     plotting purposes
%   Before running this program, run 'nps.m' after ensuring the initial conditions
%     have been set to the desired values.
%   This program will capture the variables by assigning them to new variable
%     names.  After renaming the variables, the program clears all non-essential
%     variables.
%
%    This program measures and plots the instantaneous and cumulative total of
%     commanded rod torques and the time required to achieve a 3-axis steady
%     state pointing accuracy of less than 10 degrees.
%    This program also solves and plots the area under the instantaneous rod total
%     curve to produce an energy index for comparison with other runs using
%     different initial conditions.
%
%    After loading the desired '.mat' files containing data matrices into the
%     MATLAB workspace, the matrix sizes are used to edit this program's array
%     sizes.
%    The data are saved as a '.mat' file. One of the two Prof Leonard programs
%     is run after initially running the Bdot program.  This data is stored as
%     "handoff data"

%    first import handoff data, then bdot data
%    ensure handoff variable name appears on the
%    line that creates the HDataArray matrix
%    then ensure the matrix sizes are updated

clear Hxacksis HDataArray Hrodone Hrod1 Hrod2 Hrod3 Hrodtot
clear Hrodtwo Hrodthree Hrodtotal
clear HPhdT HThdT HPsdT HPhT HThT HPsT
clear HPhd HThd HPsd HPh HTh HPs
clear HTimegap HRulerTime Hminiarea Hareatot HareaCumPlot
clear newtime Composite_Rodtotal Composite_Time bdottime
```

```
HDataArray = NPnhandoff6600';  % input name of handoff matrix
Hxaxis = HDataArray(1:8135,1);  % input size of handoff matrix
                                % Hxaxis will be the (time (x axis))
Hxacksis = Hxaxis';
bdottime = btime';              % time (x-axis) before handoff
Hrodtot= HDataArray(1:8135,5); Hrodtotal = Hrodtot';
HTimegap(1)= Hxacksis(2)-Hxacksis(1);
 newtime(1)=6908;               % final bdot time must be entered here

 for k=1:1151                   % input matrix size of bdot matrix
  Composite_Rodtotal(k)=brodtot(k);
  Composite_Time(k)=bdottime(k);
 end

Composite_Rodtotal(1152)=Hrodtot(1);
Composite_Time(1152)=newtime(1);

 for k = 2:8134                 % will be one less than handoff matrix size
  HTimegap(k)= Hxacksis(k+1)-Hxacksis(k);
  newtime(k)=newtime(k-1)+HTimegap(k);
  Composite_Rodtotal(1151+k)=Hrodtot(k);   % input one less than bdot size
  Composite_Time(1151+k)=newtime(k);       % input one less than bdot size
 end

 HTimegap(8135)= Hxacksis(8135)-Hxacksis(8134);  % h-off x2, h-off less one
 newtime(8135)=newtime(8134)+HTimegap(8135);  % h-off, h-off less one, h-off
 Composite_Rodtotal(1151+8135)=Hrodtot(8135);     % bdot plus h-off size, h-off
 Composite_Time(1151+8135)=newtime(8135);         % bdot plus h-off size, h-off

 figure                                          % plots composite rod total vs. time
  plot(Comp_Time,Comp_Rodtotal,'r'),title('Handoff Rod Total vs Time'),
  ylabel(' Am^2 '),grid
  xlabel('Time (sec)')
```

J. NPS (RODTOTAL_VS_TIME.M)

```
%Rodtotal_vs_Time    written by Lt Todd Zirkle to plot simulated torque rod data
%                    for analysis of simulations supporting NPSSAT1  NPS Monterey
%
%  This program captures a row of data from a saved 11 row matrix
%  The matrix was produced from a simulation using one of two modified
%   SIMULINK simulations originally written by Prof Barry Leonard.
%          'Lab17.mdl' 05/18/01 and 'NPSATACSIntRvw.mdl' 07/16/01
%  This program could be used to capture any row for plotting purposes
%  This program grabs torque rod totals and plots them vs. time
```

```
clear ans HDataArray Hxaxis Hxacksis Hrodtot

HDataArray = NPnCombo6908';   % input matrix name from '.mat' file
                              % loaded into workspace prior to run
Hxaxis = HDataArray(1:1720,1);   % input array size here from matrix size
Hxacksis = Hxaxis';              %  time axis
Hrodtot= HDataArray(1:1720,5); Hrodtotal = Hrodtot';

figure              % plots torque rod total (sum of absolute values of 3 rods) vs time
  plot(Hxaxis,Hrodtot,'r'),title('B.Leonard Combo with Bdot Rod Total vs Time'),
  ylabel(' Am^2 '),grid
  xlabel('Time (sec)')
```

K. NPS (PLOTRESULT2.M)

```
%plotresult2.m     written by Todd A. Zirkle for graphical analysis
%                  of NPSSAT1 data       NPS Monterey

figure
subplot(411),plot(time,w1),
title(['w_t_o_t_a_l < ',num2str(rate_goal),' degrees (',num2str(rg),' rad) in
 ',num2str(time_counter),' sec']),
 ylabel('w_x(rad/sec)'),grid
subplot(412),plot(time,w2),ylabel('w_y(rad/sec)'),ylabel('w_y(rad/sec)'),grid
subplot(413),plot(time,w3),ylabel('w_z(rad/sec)'),ylabel('w_z(rad/sec)'),grid
subplot(414),plot(time,w4),ylabel('w_t_o_t_a_l'),ylabel('w_t_o_t_a_l'),grid
xlabel('time(sec)')

figure
subplot(511),plot(time,pwr_u),title(['Total Power = ',num2str(pwr3),'
W-hrs']),ylabel(' W-hrs'),grid
subplot(512),plot(time,watt_hrs_total),ylabel(' W-hrs'),ylabel(' W-hrs'),grid
subplot(513),plot(time,m1,'r'),ylabel('Am^2'), ylabel('Am^2'),grid
subplot(514),plot(time,m2,'g'),ylabel('Am^2'), ylabel('Am^2'),grid
subplot(515),plot(time,m3,'b'),ylabel('Am^2'), ylabel('Am^2'),grid
xlabel('time(sec)')

figure
subplot(511),plot(time,pwrSS),title(['SS Power = ',num2str(pwr6),'
W-hrs']),ylabel(' W-hrs'),grid
subplot(512),plot(time,pwr6),ylabel(' W-hrs'),ylabel(' W-hrs'),grid
subplot(513),plot(time,m1,'r'),ylabel('Am^2'), ylabel('Am^2'),grid
subplot(514),plot(time,m2,'g'),ylabel('Am^2'), ylabel('Am^2'),grid
subplot(515),plot(time,m3,'b'),ylabel('Am^2'), ylabel('Am^2'),grid
xlabel('time(sec)')
```

```
figure
subplot(411),plot(time,rod3tot),title(['3 Rod torque = ',num2str(rod3tot),' Am^2']),
ylabel(' Am^2'),grid
subplot(412),plot(time,m1,'r'),ylabel('Am^2'), ylabel('Am^2'),grid
subplot(413),plot(time,m2,'g'),ylabel('Am^2'), ylabel('Am^2'),grid
subplot(414),plot(time,m3,'b'),ylabel('Am^2'), ylabel('Am^2'),grid
xlabel('time(sec)')

figure
plot(time,rod3tot),title(['3 Rod torque = ',num2str(rod3tot),' Am^2']),
                                    ylabel(' Am^2'),grid
```

BIBLIOGRAPHY

Franklin, G. F., Powell, J. D., Emami-Naeini, A., "Feedback Control Of Dynamic Systems." Addison Wesley, 1988.

Martel, F., Pal, P. K., and Psiaki, M., "Active Magnetic Control System for Gravity Gradient Stabilized Spacecraft." Second Annual AIAA/USU Conference on Small Satellites, (26-28 September 1988, Logan, UT). Washington, DC: AIAA. pg 7, 13

"MATLAB Control System User's Guide." The Math Works, Natick, MA. 1996.

Psiaki, M. L., Martel, F., and Pal, K. P., "Three- Axis Attitude Determination via Kalman Filtering of Magnetometer Data", Journal of Guidance, Control and Dynamics, Vol. 23, No. 3, 1990.pp 506-514.

Riley, F. E., Sailor, J. D., "Space Systems Engineering", McGraw-Hill Book Company, Inc., 1962.pp 133-151.

Sidi, M. J., "Spacecraft Dynamics and Control." Cambridge University Press. 1997.

Wertz, J. R. "Spacecraft Attitude Determination and Control." Kluwer Academic Publishers. Boston, MA. 1994.

Wertz, J. R., Larson, W. J., "Space Mission Analysis and Design." 3rd Edition, Microcosm Press. 1999.

THIS PAGE INTENTIONALLY LEFT BLANK

INITIAL DISTRIBUTION LIST

1. Defense Technical Information Center 2
   8725 John J. Kingman Road, Suite 0944
   Ft. Belvoir, VA 22060-6218

2. Dudley Knox Library 2
   Naval Postgraduate School
   411 Dyer Road
   Monterey, CA 93943-5101